

**National Nuclear Security Administration**  
Los Alamos Site Office, MS A316  
Environmental Restoration Program  
Los Alamos, New Mexico 87544  
(505) 667-4255/FAX (505) 606-2132

Date: SEP 27 2011  
Refer To: EP2011-0274

John Kieling, Acting Bureau Chief  
Hazardous Waste Bureau  
New Mexico Environment Department  
2905 Rodeo Park Drive East, Building 1  
Santa Fe, NM 87505-6303

**Subject: Submittal of the Completion Report for Regional Aquifer Well R-61**

Dear Mr. Kieling:

Enclosed please find two hard copies with electronic files of the Completion Report for Regional Aquifer Well R-61.

If you have any questions, please contact Ted Ball at (505) 665-3996 ([tedball@lanl.gov](mailto:tedball@lanl.gov)) or Woody Woodworth at (505) 665-5820 ([lance.woodworth@nnsa.doe.gov](mailto:lance.woodworth@nnsa.doe.gov)).

Sincerely,

Sincerely,

B-6 Schappell

Michael J. Graham, Associate Director  
Environmental Programs  
Los Alamos National Laboratory

Daniel S. Clark

George J. Rael, Manager  
Environmental Projects Office  
Los Alamos Site Office



MG/GR/CD/TB/ME:sm

Enclosures: Two hard copies with electronic files – Completion Report for Regional Aquifer  
Well R-61 (LA-UR-11-5091)

Cy: (w/enc.)  
Neil Weber, San Ildefonso Pueblo  
Hai Shen, DOE-LASO, MS A316  
Woody Woodworth, DOE-LASO, MS A316  
Ted Ball, EP-CAP, MS M996  
RPF, MS M707 (electronic copy)  
Public Reading Room, MS M992 (hard copy)

Cy: (Letter and CD and/or DVD)  
Laurie King, EPA Region 6, Dallas, TX  
Steve Yanicak, NMED-DOE-OB, MS M894  
Steve White, TerranearPMC, Los Alamos, NM (w/ MS Word files on CD)  
William Alexander, EP-BPS, MS M992

Cy: (w/o enc.)  
Tom Skibitski, NMED-OB, Santa Fe, NM (date-stamped letter emailed)  
Annette Russell, DOE-LASO (date-stamped letter emailed)  
Craig Douglass, EP-CAP, MS M992 (date-stamped letter emailed)  
Michael J. Graham, ADEP, MS M991 (date-stamped letter emailed)

LA-UR-11-5091  
September 2011  
EP2011-0274

# **Completion Report for Regional Aquifer Well R-61**



Prepared by the Environmental Programs Directorate


Los Alamos National Laboratory, operated by Los Alamos National Security, LLC, for the U.S. Department of Energy under Contract No. DE-AC52-06NA25396, has prepared this document pursuant to the Compliance Order on Consent, signed March 1, 2005. The Compliance Order on Consent contains requirements for the investigation and cleanup, including corrective action, of contamination at Los Alamos National Laboratory. The U.S. government has rights to use, reproduce, and distribute this document. The public may copy and use this document without charge, provided that this notice and any statement of authorship are reproduced on all copies.




# Completion Report for Regional Aquifer Well R-61

September 2011

Responsible project manager:

Ted Ball		Project Manager	Environmental Programs	9-27-11
Printed Name	Signature	Title	Organization	Date

Responsible LANS representative:

Michael Graham		Associate Director	Environmental Programs	27 Sept 11
Printed Name	Signature	Title	Organization	Date

Responsible DOE representative:

George J. Rael		Project Director	DOE-LASO	9-27-2011
Printed Name	Signature	Title	Organization	Date

## EXECUTIVE SUMMARY

This well completion report describes the drilling, well construction, development, aquifer testing, and dedicated sampling system installation for regional aquifer well R-61, located on the mesa top to the south of Mortandad Canyon in Technical Area 05 at Los Alamos National Laboratory (the Laboratory) in Los Alamos County, New Mexico. The R-61 monitoring well is intended to provide hydrogeologic and groundwater quality data to achieve specific data quality objectives consistent with the Groundwater Protection Program for the Laboratory, the Compliance Order on Consent (March 2005, revised 2008), and the New Mexico Environment Department– (NMED-) approved work plan.

The R-61 monitoring well borehole was drilled using dual-rotary air-drilling methods. Fluid additives included potable water and foam. Foam-assisted drilling was used only to a depth of 992 ft below ground surface (bgs), approximately 100 ft above the top of the regional aquifer.

The following geologic formations were encountered at R-61: Tshirege Member of the Bandelier Tuff, Otowi Member of the Bandelier Tuff, Guaje Pumice Bed of the Otowi Member, a thin upper section of Puye Formation sediments, Cerros del Rio volcanic series, a section of Puye Formation fanglomerates, and Miocene pumiceous sediments. R-61 was drilled to a total depth of 1265 ft bgs.

Well R-61 was completed as a dual-screen well, allowing evaluation of water quality and water levels within the regional aquifer. The screened intervals are set between 1125 and 1135 ft bgs within Puye Formation sediments and between 1220.4 and 1241 ft bgs within Miocene pumiceous sediments. A composite depth to water of 1101.3 ft bgs was recorded on May 4, 2011, after well installation.

The well was completed in accordance with an NMED-approved well design. The well was developed, and the regional aquifer groundwater met target water quality parameters for both screened intervals. Aquifer testing indicates that both screened intervals at R-61 are productive and will perform effectively to meet the planned objectives. The sampling system and transducers have been placed in the screened intervals, and groundwater sampling at R-61 will be performed as part of the annual Interim Facility-Wide Groundwater Monitoring Plan.

## CONTENTS

<b>1.0</b>	<b>INTRODUCTION .....</b>	<b>1</b>
<b>2.0</b>	<b>ADMINISTRATIVE PLANNING .....</b>	<b>1</b>
<b>3.0</b>	<b>DRILLING ACTIVITIES.....</b>	<b>2</b>
3.1	Drilling Approach .....	2
3.2	Chronological Drilling Activities for the R-61 Well .....	2
<b>4.0</b>	<b>SAMPLING ACTIVITIES.....</b>	<b>3</b>
4.1	Cuttings Sampling.....	3
4.2	Water Sampling .....	3
<b>5.0</b>	<b>GEOLOGY AND HYDROGEOLOGY .....</b>	<b>4</b>
5.1	Stratigraphy .....	4
5.2	Groundwater .....	5
5.2.1	Regional Aquifer Groundwater Elevation .....	6
<b>6.0</b>	<b>BOREHOLE LOGGING .....</b>	<b>6</b>
<b>7.0</b>	<b>INSTALLATION OF THE R-61 MONITORING WELL .....</b>	<b>6</b>
7.1	Well Design.....	6
7.2	Well Construction.....	6
<b>8.0</b>	<b>POSTINSTALLATION ACTIVITIES .....</b>	<b>7</b>
8.1	Well Development.....	7
8.1.1	Well Development Field Parameters.....	8
8.2	Aquifer Testing.....	9
8.3	Dedicated Sampling System Installation .....	9
8.4	Wellhead Completion.....	9
8.5	Geodetic Survey .....	9
8.6	Waste Management and Site Restoration.....	10
<b>9.0</b>	<b>DEVIATIONS FROM PLANNED ACTIVITIES .....</b>	<b>10</b>
<b>10.0</b>	<b>ACKNOWLEDGMENTS .....</b>	<b>10</b>
<b>11.0</b>	<b>REFERENCES AND MAP DATA SOURCES .....</b>	<b>11</b>
11.1	References .....	11
11.2	Map Data Sources.....	11

## Figures

Figure 1.0-1	Location of monitoring well R-61.....	13
Figure 5.1-1	Monitoring well R-61 borehole stratigraphy .....	14
Figure 5.2-1	Regional aquifer groundwater elevations in the vicinity of R-61 .....	15
Figure 7.2-1	Monitoring well R-61 as-built well construction diagram.....	16
Figure 8.3-1a	Monitoring well R-61 as-built diagram with borehole lithology and technical well completion details .....	17
Figure 8.3-1b	As-built technical notes for monitoring well R-61	
Figure 8.3-1c	Dedicated pump performance curve for monitoring well R-61 .....	18

## Tables

Table 3.1-1	Fluid Quantities Used during R-61 Drilling and Well Construction .....	19
Table 4.2-1	Summary of Groundwater Screening Samples Collected during Well Development and Aquifer Testing of Well R-61 .....	20
Table 7.2-1	R-61 Monitoring Well Annular Fill Materials.....	21
Table 8.5-1	R-61 Survey Coordinates.....	21
Table 8.6-1	Summary of Waste Samples Collected during Drilling, Construction, and Development of R-61 .....	21

## Appendixes

Appendix A	Borehole R-61 Lithologic Log
Appendix B	Screening Groundwater Analytical Results
Appendix C	Aquifer Testing Report
Appendix D	Borehole Video Logging (on DVD included with this document)
Appendix E	Geophysical Logging (on CD included with this document)
Appendix F	R-61 Final Well Design and New Mexico Environment Department Approval

## Acronyms and Abbreviations

amsl	above mean sea level
ASTM	American Society for Testing and Materials
bgs	below ground surface
Consent Order	Compliance Order on Consent
DO	dissolved oxygen
DTW	depth to water
EES-14	Earth and Environmental Sciences Group 14
Eh	oxidation-reduction potential
EP	Environmental Programs
EPA	Environmental Protection Agency (U.S.)
F	filtered
FD	field duplicate
FTB	field trip blank
gpd	gallons per day
gpm	gallons per minute
hp	horsepower

I.D.	inside diameter
LANL	Los Alamos National Laboratory
NAD	North American Datum
NMED	New Mexico Environment Department
NTU	nephelometric turbidity unit
O.D.	outside diameter
ORP	oxidation-reduction potential
PVC	polyvinyl chloride
Qbo	Otowi Member of the Bandelier Tuff
Qbog	Guaje Pumice Bed of the Otowi Member of the Bandelier Tuff
Qbt	Tshirege Member of the Bandelier Tuff
RPF	Records Processing Facility
TA	technical area
Tb 4	Cerros del Rio volcanic series
TD	total depth
Tjfp	Jemez fanglomerate pumiceous (called Miocene pumiceous sediments in this report)
TOC	total organic carbon
Tpf	Puye Formation
UF	unfiltered
VOC	volatile organic compound
WCSF	waste characterization strategy form
WES-EDA	Waste and Environmental Services Division–Environmental Data and Analysis (Group)
WR	whole rock

## 1.0 INTRODUCTION

This completion report summarizes borehole drilling, well construction, well development, aquifer testing, and dedicated sampling system installation for regional aquifer monitoring well R-61. The report is written in accordance with the requirements in Section IV.A.3.e.iv of the March 1, 2005 (revised 2008), Compliance Order on Consent (the Consent Order). The R-61 monitoring well borehole was drilled from March 12 to April 4, 2011, and completed from April 9 to May 4, 2011, at Los Alamos National Laboratory (LANL or the Laboratory) for the Environmental Programs (EP) Directorate.

Well R-61 is located on the mesa top to the south of Mortandad Canyon within the Laboratory's Technical Area 05 (TA-05) in Los Alamos County, New Mexico (Figure 1.0-1). The primary purpose for drilling and installing the R-61 well was to further define the vertical and lateral extent of chromium contamination in the regional aquifer. Specifically, R-61 was located to help delineate the western edge of a southerly flow path of chromium identified in wells R-42 and R-28. Secondary objectives were to establish water levels in the regional aquifer, identify any perched zones, and to collect drill-cutting samples.

The R-61 borehole was drilled to a total depth (TD) of 1265 ft below ground surface (bgs). During drilling, cuttings samples were collected at 5-ft intervals in the borehole from ground surface to TD. A monitoring well was installed with an upper screened interval between 1125 and 1135 ft bgs within Puye Formation sediments and a lower screened interval between 1220.4 and 1241 ft bgs within Miocene pumiceous sediments. A composite depth to water (DTW) of 1101.3 ft bgs was recorded on May 4, 2011, after well installation.

Postinstallation activities included well development, aquifer testing, surface completion, geodetic surveying, and sampling system installation. Future activities will include site restoration and waste management.

The information presented in this report was compiled from field reports and daily activity summaries. Records, including field reports, field logs, and survey information, are on file at the Laboratory's Records Processing Facility (RPF). This report contains brief descriptions of activities and supporting figures, tables, and appendixes associated with the R-61 project.

## 2.0 ADMINISTRATIVE PLANNING

The following LANL documents were prepared to guide activities associated with the drilling, installation, and development of regional aquifer well R-61:

- "Drilling Work Plan for Well R-61" (LANL 2010, 110998),
- "Drilling Plan for Regional Aquifer Well R-61" (TerranearPMC 2011, 201256),
- "Integrated Work Document for Regional and Intermediate Aquifer Well Drilling" (LANL 2007, 100972),
- "Storm Water Pollution Prevention Plan for SWMUs and AOCs (Sites) and Storm Water Monitoring Plan" (LANL 2006, 092600), and
- "Waste Characterization Strategy Form for Installation of Regional Aquifer Well R-61" (LANL 2011, 204885).

### **3.0 DRILLING ACTIVITIES**

This section describes the drilling approach and provides a chronological summary of field activities conducted at monitoring well R-61.

#### **3.1 Drilling Approach**

The drilling methodology, equipment, and sizes of drill casing used for the R-61 monitoring well were selected to retain the ability to investigate and case off any perched groundwater encountered above the regional aquifer. Further, the drilling approach ensured that a sufficiently sized drill casing was used to meet the required 2-in. minimum annular thickness of the filter pack around a 5.56-in.-outside diameter (O.D.) well casing.

Dual-rotary air-drilling methods using a Foremost DR-24HD drill rig were employed to drill the R-61 borehole. Dual-rotary drilling has the advantage of simultaneously advancing and casing the borehole. The Foremost DR-24HD drill rig was equipped with conventional drilling rods, tricone bits, downhole hammer bits, a deck-mounted air compressor, and general drilling equipment. Auxiliary equipment included two Ingersoll Rand trailer-mounted air compressors. Three sizes of A53 grade B flush-welded mild carbon-steel casing (18-in., 16-in., and 12-in. inside diameter [I.D.]) were used for the R-61 project.

The dual-rotary technique at R-61 used filtered compressed air and fluid-assisted air to evacuate cuttings from the borehole during drilling. Drilling fluids, other than air, used in the borehole (all within the vadose zone) included potable water and a mixture of potable water with Baroid AQF-2 foaming agent. The fluids were used to cool the bit and help lift cuttings from the borehole. Use of the foaming agent was terminated at 992 ft bgs, roughly 100 ft above the expected top of the regional aquifer. No additives other than potable water were used for drilling below 992 ft bgs. Total amounts of drilling fluids introduced into the borehole are presented in Table 3.1-1.

#### **3.2 Chronological Drilling Activities for the R-61 Well**

Mobilization of drilling equipment and supplies to the R-61 drill site occurred on March 10 and 11, 2011. Decontamination of the equipment and tooling was performed before mobilization to the site. On March 12, following on-site equipment inspections, the monitoring well borehole was initiated at 0715 h using dual-rotary methods with 18-in. drill casing and a 17-in. tricone bit.

Drilling and advancing of 18-in. casing proceeded through construction fill/alluvium and the Tshirege Member of the Bandelier Tuff to a depth of 145 ft bgs. No indications of groundwater were observed while advancing the 18-in. casing.

On March 14, open-hole drilling commenced using a 14.75-in. tricone bit. Drilling proceeded through the Tshirege and Otowi Members of the Bandelier Tuff to 612 ft bgs at the top of the Cerros del Rio volcanic series. The open borehole was then reamed to a diameter of 20 in. from approximately 150 to 610 ft bgs.

Starting March 18, 2011, a 16-in. casing string was installed in the open borehole to a depth of 612 ft at the top of the Cerros del Rio volcanic series. On March 22, a 15-in. hammer bit was used to advance an open borehole through basaltic and dacitic rocks to 896 ft bgs.

Open-hole drilling was suspended on March 24 because of loss of circulation at 896 ft bgs, and a 12-in. casing string was installed in the borehole. On March 30, a 12-in. underreaming hammer bit was used to advance the borehole and 12-in. casing string through the remaining portion of the Cerros del Rio volcanic

series, the Puye Formation, and Miocene pumiceous sediments. Water was encountered at approximately 1105 ft bgs on April 1, 2011. Casing advance drilling proceeded to TD at 1265 ft bgs on April 4, 2011.

The 16-in. casing shoe was cut on March 25 at 600 ft bgs before installation of the 12-in. casing string. The 12-in. casing shoe was cut on April 6 at 1258.8 ft bgs.

During drilling, field crews worked 12-h shifts, 7 d/wk. All associated activities proceeded normally without incident or delay.

## **4.0 SAMPLING ACTIVITIES**

This section describes the cuttings and groundwater sampling activities for monitoring well R-61. All sampling activities were conducted in accordance with applicable quality procedures.

### **4.1 Cuttings Sampling**

Cuttings samples were collected from the R-61 monitoring well borehole at 5-ft intervals from ground surface to the TD of 1265 ft bgs. At each interval, approximately 500 mL of bulk cuttings were collected by the site geologist from the drilling discharge cyclone, placed in resealable plastic bags, labeled, and archived in core boxes. Whole rock, +35 and +10 sieve-size fractions were also processed, placed in chip trays, and archived for each 5-ft interval. Radiation control technicians screened the cuttings before removal from the site. All screening measurements were within the range of background values. The core boxes were delivered to the Laboratory's archive at the conclusion of drilling activities.

R-61 stratigraphy is summarized in section 5.1, and a detailed lithologic log is presented in Appendix A.

### **4.2 Water Sampling**

Thirteen groundwater samples were collected during well development and aquifer testing from the pump's discharge line for total organic carbon (TOC) analysis. Six samples were collected from the upper screened interval during aquifer testing. One sample was collected from the lower screened interval during well development, and six lower screen samples were collected during aquifer testing (Table 4.2-1).

Additionally, one sample was collected from the lower screened interval near the end of aquifer testing for dissolved gas content analysis. The dissolved gas analysis was conducted in an effort to determine the content and origin of effervescence observed in groundwater from the lower screen. The TOC and dissolved gas analytical results are presented in Appendix B.

Groundwater characterization samples will be collected from the completed well in accordance with the Consent Order. For the first year, the samples will be analyzed for the full suite of constituents, including radionuclides; anions/cations; general inorganic chemicals; volatile and semivolatile organic compounds; and stable isotopes of hydrogen, nitrogen, and oxygen. The analytical results will be included in the appropriate periodic monitoring report issued by the Laboratory. After the first year, the analytical suite and sample frequency at R-61 will be evaluated and presented in the annual Interim Facility-Wide Groundwater Monitoring Plan.



## **5.0 GEOLOGY AND HYDROGEOLOGY**

A brief description of the geologic and hydrogeologic features encountered at R-61 is presented below. The Laboratory's geology task leader and project site geologist examined cuttings to determine geologic contacts and hydrogeologic conditions. Drilling observations and water level measurements were used to characterize groundwater occurrences encountered at R-61.

### **5.1 Stratigraphy**

Rock units for the R-61 borehole are presented below in order of youngest to oldest in stratigraphic occurrence. Lithologic descriptions are based on binocular microscope analysis of drill cuttings collected from the discharge hose. Figure 5.1-1 illustrates the stratigraphy at R-61. A detailed lithologic log for R-61 is presented in Appendix A.

#### **Alluvium/Construction Fill (0–5 ft bgs)**

Thin alluvium or soil mixed with base-course gravel from drill pad construction was encountered from 0 to 5 ft bgs. The alluvium consists of unconsolidated, poorly sorted quartzite gravel and sand.

#### **Unit 2, Tshirege Member of the Bandelier Tuff, Qbt 2 (5–45 ft bgs)**

Unit 2 of the Tshirege Member of the Bandelier Tuff was intersected from 5 to 45 ft bgs. Unit 2 represents a moderately welded rhyolitic ash-flow tuff (i.e., ignimbrite) that is composed of abundant (up to 30% by volume) quartz and sanidine crystals, devitrified pumice lapilli, and minor volcanic lithic fragments set in a matrix (up to 60% by volume) of weathered ash. Cuttings typically contain abundant fragments of indurated tuff and numerous free quartz and sanidine crystals.

#### **Unit 1v, Tshirege Member of the Bandelier Tuff, Qbt 1v (45–160 ft bgs)**

Unit 1v of the Tshirege Member of the Bandelier Tuff occurs from 45 to 160 ft bgs. Unit 1v is a poorly to moderately welded rhyolitic ash-flow tuff that is pumiceous, generally lithic-poor, and crystal-bearing to locally crystal-rich. Abundant ash matrix is rarely preserved in cuttings. Cuttings commonly contain numerous fragments of indurated crystal-rich tuff with compressed, strongly devitrified pumice lapilli. Abundant free quartz and sanidine crystals dominate cuttings in many intervals, and minor small (generally less than 10 mm in diameter) volcanic lithic inclusions also occur in cuttings.

#### **Unit 1g, Tshirege Member of the Bandelier Tuff, Qbt 1g (160–270 ft bgs)**

Unit 1g of the Tshirege Member of the Bandelier Tuff was encountered from 160 to 270 ft bgs. Unit 1g is a poorly welded to nonwelded rhyolitic ash-flow tuff that is poorly to moderately indurated, strongly pumiceous, and crystal-bearing. White to pale orange, lustrous, glassy pumice lapilli that are quartz- and sanidine-phyric are characteristic of Unit 1g. Cuttings contain abundant free quartz and sanidine crystals and minor small (up to 10 mm) volcanic (predominantly dacitic) lithic clasts.

#### **Otowi Member of the Bandelier Tuff, Qbo (270–580 ft bgs)**

The Otowi Member ash flows of the Bandelier Tuff were encountered from 270 to 580 ft bgs. The Otowi Member ash-flow deposit is composed of poorly welded pumiceous rhyolitic ash-flow tuffs that are crystal- and lithic-bearing. Abundant pumice lapilli are white, glassy, lustrous, and quartz- and sanidine-phyric. Otowi Member drill cuttings contain white, glassy pumices, volcanic lithic clasts (up to 10 mm), and quartz.

and sanidine crystals. Lithic xenoliths are commonly subangular to subrounded and generally of intermediate volcanic composition, including porphyritic dacites and andesites.

#### **Guaje Pumice Bed of the Otowi Member of the Bandelier Tuff, Qbog (580–605 ft bgs)**

The Guaje Pumice Bed consists of rhyolitic pumice and ash that forms the base of the Otowi Member. The Guaje deposit was encountered from 580 to 605 ft bgs. Drill cuttings in this interval contain abundant (up to 95% by volume), lustrous, vitric pumice lapilli (up to 15 mm in diameter) with trace occurrences of small volcanic lithic fragments. The deposit is nonwelded and unconsolidated.

#### **Puye Formation, Tpf (605–610 ft bgs)**

Puye Formation volcanoclastic sediments were encountered from 605 to 610 ft bgs. The deposits in this interval are white to light orange fine-grained gravels and sandstones, including rounded pumice gravels. Sand-sized pumice and volcanic clasts are typically subangular to subrounded, and fine quartz grains are subrounded.

#### **Cerros del Rio Volcanic Series, Tb 4 (610–915 ft bgs)**

Cerros del Rio volcanic rocks, encountered at R-61 from 610 to 915 ft bgs, form a complex sequence that includes both massive and vesicular basaltic lavas with minor basaltic scoria deposits. The sequence also includes thin (<5 ft) basaltic sediment layers between flows. These basaltic sediments consist of reworked fine gravel, sand, and mud.

#### **Puye Formation, Tpf (915–1155 ft bgs)**

A lower section of the Puye Formation was intersected from 915 to 1155 ft bgs. These volcanoclastic sediments consist of poorly sorted to unsorted, moderately indurated, medium to coarse gravel with silty fine to coarse sand. Subrounded to well-rounded detrital constituents throughout the typical Puye section are predominantly composed of gray biotite- and/or hornblende-phyric dacites and a locally minor occurrence of white pumice or andesite.

#### **Miocene Pumiceous Sediments, Tjfp (1155–1265 ft bgs)**

A pumice-rich volcanoclastic section was intersected from 1155 ft to the bottom of the R-61 borehole at 1265 ft bgs. These sediments are composed of fine to medium gravel with fine to coarse sand that is moderately to poorly sorted, weakly cemented, and contain detrital pumices making up 30% or more (locally as much as 80%) by volume.

### **5.2 Groundwater**

Drilling at R-61 proceeded without any groundwater indications until 1105 ft bgs as noted by the drilling crew. At 1105 ft bgs, water production was estimated at 15 gallons per minute (gpm). The borehole was then advanced to the TD of 1265 ft bgs. The water level stabilized at 1100.7 ft bgs on April 5, 2011, before well installation. The measured composite DTW in the completed well was 1101.3 ft bgs on May 4. The discrete water levels measured on July 29, after sampling system installation, were 1102.52 ft bgs for the upper screened interval and 1102.28 ft bgs for the lower screened interval.

### **5.2.1 Regional Aquifer Groundwater Elevation**

The regional aquifer water level elevation for R-61 is 5837.48 ft above mean sea level (amsl) based on the upper screen water level measurement from July 29. This elevation conforms well with the surrounding regional aquifer water level elevations as shown in Figure 5.2-1. The level at R-61 will continue to be monitored and incorporated into the Laboratory's regional aquifer water level map.

## **6.0 BOREHOLE LOGGING**

On March 25, a video log of the borehole was recorded from 600 ft bgs, the bottom of the 16-in. casing, to 796 ft bgs, where foamy water was encountered (included as Appendix D on DVD). The video log was run to verify the 16-in. casing cut, view the open portion of the borehole, and observe the DTW.

A natural gamma log was recorded on April 5 inside the 12-in. casing after the TD of 1265 ft bgs had been reached. Appendix E (on CD) contains a plot of this geophysical log.

## **7.0 INSTALLATION OF THE R-61 MONITORING WELL**

The R-61 well was installed between April 9 and May 3, 2011.

### **7.1 Well Design**

The R-61 well was designed in accordance with the Consent Order, and NMED approved the final well design before installation (Appendix F). The well was designed with two screened intervals: one between 1125 and 1135 ft bgs and another between approximately 1220 and 1240 ft bgs. These screens were designed to monitor the groundwater quality near the top of the regional aquifer within the Puye Formation and deeper in the regional aquifer within Miocene pumiceous sediments, respectively.

### **7.2 Well Construction**

The R-61 monitoring well was constructed of 5.0-in.-I.D./5.56-in.-O.D., type A304 passivated stainless-steel threaded casing fabricated to American Society for Testing and Materials (ASTM) A312 standards. The screened sections utilized three 10-ft lengths of 5.0-in.-I.D. rod-based 0.020-in. wire-wrapped screens, one for the 10-ft-long upper screened interval and two for the 20-ft-long lower screened interval. Compatible external stainless-steel couplings (also type A304 stainless steel fabricated to ASTM A312 standards) were used to join all individual casing and screen sections. All casing, couplings, and screens were steam and pressure washed on-site before installation. A 2-in.-I.D. steel tremie pipe (decontaminated before use) was utilized for delivery of backfill and annular fill materials downhole during well construction. Short lengths of 16-in. and 12-in. drill casing (12.2-ft-long casing and shoe from 600 to 612.2 ft bgs; 7.5-ft-long casing and shoe from 1258.8 to 1266.4 ft bgs, respectively) remain in the borehole. The casing stubs were encased in the bentonite seals during well completion.

A 10.6-ft-long stainless-steel sump was placed below the bottom of the lower well screen. Stainless-steel centralizers (four sets of four) were welded to the well casing approximately 2 ft above and below the two screened intervals. A Pulstar work-over rig was used for all well construction activities. Figure 7.2-1 presents an as-built schematic showing construction details for the completed well.

Decontamination of the stainless-steel well casing, screens, and tremie pipe, along with mobilization of the Pulstar work-over rig and initial well construction materials to the site, took place from April 6 to 9, 2011. The 5.0-in.-I.D. well casing was started into the borehole on April 9 at 1330 h. The well casing was hung by wireline with the bottom at 1251.6 ft bgs. No isolation packer was used between the screened intervals during the construction and installation of annular fill materials at R-61.

The installation of annular materials began on April 12 after the bottom of the borehole was measured at 1263.7 ft bgs (approximately 1.3 ft of slough was present in the borehole). The lower bentonite seal was installed on April 12 and 13 from 1246.2 to 1263.6 ft bgs using 6.7 ft<sup>3</sup> of 3/8-in. bentonite chips. The lower bentonite seal used 38% of the calculated annular fill material volume, likely due to additional sloughing during installation.

The lower screen filter pack was installed on April 13 through 15 from 1215.5 to 1246.2 ft bgs using 37 ft<sup>3</sup> of 10/20 silica sand. The filter pack was surged to promote compaction. The lower screen fine sand collar was installed above the lower filter pack from 1213.6 to 1215.5 ft bgs using 3 ft<sup>3</sup> of 20/40 silica sand. The filter pack and the fine sand collar required 36% and 76% additional sand, respectively, than had been calculated. These higher volumes are likely due to borehole washouts in the unconsolidated Miocene pumiceous sediments.

From April 16 to 20, the middle bentonite seal was installed from 1140.4 to 1213.6 ft bgs using 60.3 ft<sup>3</sup> of 3/8-in. bentonite chips. The upper screen filter pack was installed on April 21 from 1119.4 to 1140.4 ft bgs using 24 ft<sup>3</sup> of 10/20 silica sand. The filter pack was surged to promote compaction. The upper screen filter pack volume exceeded the calculated volume by 29%, which is likely due to borehole washouts in the unconsolidated Puye Formation sediments. The upper screen fine sand collar was installed above the upper filter pack from 1116.9 to 1119.4 ft bgs using 2 ft<sup>3</sup> of 20/40 silica sand.

From April 22 to May 3, the upper bentonite seal was installed from 59.9 to 1116.9 ft bgs using 1472.7 ft<sup>3</sup> of 3/8-in. bentonite chips. On May 3, a cement seal was installed from 3 to 59.9 ft bgs. The cement seal used 132 ft<sup>3</sup> of Portland Type I/II/V cement. This volume exceeded the calculated volume of 91.2 ft<sup>3</sup> by 45% and is due to cement loss to the near surface formations. A summary of annular fill materials and calculated volumes is listed in Table 7.2-1.

Operationally, well construction proceeded smoothly, 12 h/d, 7 d/wk, from April 9 through May 3, 2011.

## **8.0 POSTINSTALLATION ACTIVITIES**

Following well installation at R-61, both screens were developed and aquifer pumping tests were conducted. The wellhead and surface pad were constructed, a geodetic survey was performed, and a dedicated dual-screen sampling system was installed. Site restoration activities will be completed following the final disposition of contained drill cuttings and groundwater, per the NMED-approved waste-disposal decision trees.

### **8.1 Well Development**

The well was developed between May 4 and 15, 2011. Initially, the well was bailed and swabbed to remove formation fines from the filter packs and the well sump. Bailing continued until water clarity visibly improved. Each screened interval was then developed with a submersible pump.

The swabbing tool employed was a 4.5-in.-O.D., 1-in.-thick nylon disc attached to a weighted steel rod. The wireline-conveyed tool was drawn repeatedly across each screened interval, causing a surging

action across the screen/filter pack. The bailing tool employed was a 4.0-in.-O.D. by 21-ft-long carbon steel bailer with a total capacity of 12 gal. The tool was lowered by wireline, repeatedly filled, withdrawn from the well, and emptied into the cuttings pit. Approximately 1075 gal. of composite groundwater from both screens was removed during bailing activities.

### **Lower Screen**

After bailing, a 10-horsepower (hp), 4-in. Berkeley submersible pump, with an inflatable packer located above the pump, was installed for well development of the lower screen. On May 11, the screened interval was pumped from top to bottom and then from bottom to top in 2-ft increments. On May 12, the pump intake was set at 1215.9 ft bgs for the remainder of purging. Approximately 8308 gal. of groundwater was purged with the submersible pump during well development of the lower screen.

### **Upper Screen**

A 5-hp, 4-in. Berkeley submersible pump, with an inflatable packer located below the pump, was installed for well development of the upper screen. On May 13, the screened interval was pumped from top to bottom and then from bottom to top in 2-ft increments. The pump intake was set at 1130 ft bgs, and the packer was inflated to ensure discrete water quality parameter samples. On May 14 and 15, additional pumping was conducted using a 5-hp Berkeley submersible pump. The pump intake was set at 1142.4 ft bgs, with the packers inflated, for the remainder of purging. Approximately 2922 gal. of groundwater was purged with the submersible pump during well development.

### **Total Volumes of Introduced Water versus Purged Water**

During drilling, approximately 3762 gal. of potable water was added below the surface of the regional aquifer. An additional 20,165 gal. was added during installation of the annular fill materials below the water table. Thus, approximately 23,927 gal. of potable water was introduced below the water table during drilling and construction.

Approximately 12,305 gal. of groundwater was purged at R-61 during well development from both screened intervals. Another 31,870 gal. was purged from both screens during aquifer testing. The total volume of groundwater purged during postinstallation activities from both screened intervals combined was 44,175 gal.

#### **8.1.1 Well Development Field Parameters**

During the pumping stage of well development of both screens, turbidity, temperature, pH, dissolved oxygen (DO), oxidation-reduction potential (ORP), and specific conductance were measured. The required TOC and turbidity values for adequate well development are less than 2 ppm and less than 5 nephelometric turbidity units (NTU), respectively.

Field parameters were measured by collecting aliquots of groundwater from the discharge pipe with the use of a flow-through cell. The final parameters at the end of well development of the lower screen were pH of 8.28, temperature of 21.22°C, specific conductance of 101  $\mu\text{S}/\text{cm}$ , and turbidity of 3.2 NTU. The final parameters at the end of well development of the upper screen were pH of 7.94, temperature of 22.41°C, specific conductance of 101  $\mu\text{S}/\text{cm}$ , and turbidity of 17.4 NTU. (Note that the turbidity for the upper screened interval was 0 NTU at the end of aquifer testing.) Table B-2.3-1 in Appendix B shows field parameters and purge volumes measured during well development. Figures B-2.3-1 and B-2.3-2 show the water quality parameters plotted against well development and aquifer testing purge volumes.

## 8.2 Aquifer Testing

Aquifer pumping tests were conducted at R-61 between May 19 and 24, 2011. Several short-duration tests with short-duration recovery periods were performed on the first day of testing each screen. A 24-h pump test followed by a 24-h recovery period completed the testing of the screened intervals.

A 5-hp pump was used for the aquifer test of the upper screened interval. A total of 1931 gal. of groundwater was purged during aquifer testing of the upper screen.

A 10-hp pump was used for the aquifer test of the lower screened interval. A total of approximately 29,939 gal. of groundwater was purged during aquifer testing of the lower screen.

Turbidity, temperature, pH, DO, ORP, and specific conductance were measured during the 24-h test. Measured parameters are presented in Appendix B. The R-61 aquifer test results and analysis are presented in Appendix C.

A temporary isolation packer was installed between the screens after aquifer testing while the sampling system was manufactured.

## 8.3 Dedicated Sampling System Installation

The dedicated sampling system for R-61 was installed between July 26 and 28, 2011. The system is a Baski, Inc.–manufactured system that utilizes a single 3-hp, 4-in.-O.D. environmentally retrofitted Grundfos submersible pump capable of purging each screened interval discretely via pneumatically actuated access port valves. The system includes a viton-wrapped isolation packer between the screened intervals. The pump column consists of threaded and coupled passivated 1-in.-I.D. stainless steel. A weep valve was installed at the bottom of the uppermost pipe joint to protect the pump column from freezing. To measure water levels in the well, two 1-in.-I.D. schedule 80 polyvinyl chloride (PVC) tubes are banded to the pump riser for dedicated transducers. The upper PVC transducer tube is equipped with a 0.010-in. slotted screen with a threaded end cap at the bottom of the tube. The lower PVC transducer tube is equipped with a flexible nylon tube that extends from a threaded end cap at the bottom of the PVC tube through the isolation packer and measures water levels in the lower screened interval. Two In-Situ, Inc. Level Troll 500 30-psig transducers were installed in the PVC tubes to monitor water levels in each screened interval.

Sampling system details for R-61 are presented in Figure 8.3-1a. Figure 8.3-1b presents technical notes for the well. Figure 8.3-1c presents the environmentally retrofitted Grundfos pump performance curve.

## 8.4 Wellhead Completion

A reinforced concrete surface pad, 10 ft × 10 ft × 6 in. thick, was installed at the R-61 wellhead. The concrete pad was slightly elevated above the ground surface and crowned to promote runoff. The pad will provide long-term structural integrity for the well. A brass survey pin was embedded in the northwest corner of the pad. A 10-in.-I.D. steel protective casing with a locking lid was installed around the stainless-steel well riser. A total of four bollards, painted yellow for visibility, was set at the outside edges of the pad to protect the wellhead from traffic. All four bollards were designed for easy removal to allow access to the well. Details of the wellhead completion are presented in Figure 8.3-1a.

## 8.5 Geodetic Survey

A New Mexico licensed professional land surveyor conducted a geodetic survey on July 11, 2011 (Table 8.5-1). The survey data conform to Laboratory Information Architecture project standards IA-CB02,

“GIS Horizontal Spatial Reference System,” and IA-D802, “Geospatial Positioning Accuracy Standards for A/E/C and Facility Management.” All coordinates are expressed relative to the New Mexico State Plane Coordinate System Central Zone (North American Datum [NAD] 83); elevation is expressed relative to feet above mean sea level using the National Geodetic Vertical Datum of 1929. Survey points include ground-surface elevation near the concrete pad, the top of the brass pin in the concrete pad, the top of the well casing, and the top of the protective casing for the R-61 monitoring well.

## **8.6 Waste Management and Site Restoration**

Waste generated from the R-61 project included drilling fluids, purged groundwater, drill cuttings, decontamination water, and contact waste. A summary of the waste characterization samples collected during drilling, well construction, and development of the R-61 well is presented in Table 8.6-1.

All waste streams produced during drilling and development activities were sampled in accordance with “Waste Characterization Strategy Form for Installation of Regional Aquifer Well R-61” (LANL 2011, 204885).

Fluids produced during drilling, well development, and aquifer testing are expected to be land-applied after a review of associated analytical results per the waste characterization strategy form (WCSF) and ENV-RCRA-QP-010.2, Land Application of Groundwater. If it is determined the drilling fluids are nonhazardous but cannot meet the criteria for land application, they will be evaluated for treatment and disposal at one of the Laboratory’s wastewater treatment facilities. If analytical data indicate that the drilling fluids are hazardous/nonradioactive or mixed low-level waste, the drilling fluids will be disposed of at an authorized facility.

Cuttings produced during drilling are anticipated to be land-applied after a review of associated analytical results per the WCSF and ENV-RCRA-QP-011.2, Land Application of Drill Cuttings. If the drill cuttings do not meet the criteria for land application, they will be disposed of at an authorized facility.

Decontamination fluid used for cleaning equipment was containerized. The fluid waste was sampled and will be disposed of at an authorized facility. Characterization of contact waste will be based upon acceptable knowledge, pending analyses of the waste samples collected from the drill cuttings, purge water, and decontamination fluid.

Site restoration activities will include removing drilling fluids and cuttings from the pit, managing the fluids, and as described above, removing the polyethylene liner, removing the containment area berms, and backfilling and regrading the containment area, as appropriate.

## **9.0 DEVIATIONS FROM PLANNED ACTIVITIES**

Drilling, sampling, and well construction at R-61 were performed as specified in “Drilling Plan for Regional Aquifer Well R-61” (TerranearPMC 2011, 201256).

## **10.0 ACKNOWLEDGMENTS**

Boart Longyear drilled and installed the R-61 monitoring well.

David C. Schafer designed, implemented and analyzed the aquifer tests.

TerranearPMC provided oversight on all preparatory and field-related activities.

## 11.0 REFERENCES AND MAP DATA SOURCES

### 11.1 References

*The following list includes all documents cited in this report. Parenthetical information following each reference provides the author(s), publication date, and ER ID. This information is also included in text citations. ER IDs are assigned by the Environmental Programs Directorate's Records Processing Facility (RPF) and are used to locate the document at the RPF and, where applicable, in the master reference set.*

*Copies of the master reference set are maintained at the NMED Hazardous Waste Bureau and the Directorate. The set was developed to ensure that the administrative authority has all material needed to review this document, and it is updated with every document submitted to the administrative authority. Documents previously submitted to the administrative authority are not included.*

LANL (Los Alamos National Laboratory), March 2006. "Storm Water Pollution Prevention Plan for SWMUs and AOCs (Sites) and Storm Water Monitoring Plan," Los Alamos National Laboratory document LA-UR-06-1840, Los Alamos, New Mexico. (LANL 2006, 092600)

LANL (Los Alamos National Laboratory), October 4, 2007. "Integrated Work Document for Regional and Intermediate Aquifer Well Drilling (Mobilization, Site Preparation and Setup Stages)," Los Alamos National Laboratory, Los Alamos, New Mexico. (LANL 2007, 100972)

LANL (Los Alamos National Laboratory), October 2010. "Drilling Work Plan for Regional Aquifer Well R-61," Los Alamos National Laboratory document LA-UR-10-6970, Los Alamos, New Mexico. (LANL 2010, 110998)

LANL (Los Alamos National Laboratory), March 8, 2011. "Waste Characterization Strategy Form for Installation of Regional Aquifer Well R-61," EP2011-0083, Los Alamos National Laboratory, Los Alamos, New Mexico. (LANL 2011, 204885)

TerranearPMC, March 2011. "Drilling Plan for Regional Aquifer Well R-61," plan prepared for Los Alamos National Laboratory, Los Alamos, New Mexico. (TerranearPMC 2011, 201256)

### 11.2 Map Data Sources

Point Feature Locations of the Environmental Restoration Project Database; Los Alamos National Laboratory, Waste and Environmental Services Division, EP2008-0109; 12 April 2010.

Hypsography, 100 and 20 Foot Contour Interval; Los Alamos National Laboratory, ENV Environmental Remediation and Surveillance Program; 1991.

Surface Drainages, 1991; Los Alamos National Laboratory, ENV Environmental Remediation and Surveillance Program, ER2002-0591; 1:24,000 Scale Data; Unknown publication date.

Paved Road Arcs; Los Alamos National Laboratory, KSL Site Support Services, Planning, Locating and Mapping Section; 06 January 2004; as published 28 May 2009.

Dirt Road Arcs; Los Alamos National Laboratory, KSL Site Support Services, Planning, Locating and Mapping Section; 06 January 2004; as published 28 May 2009.



Structures; Los Alamos National Laboratory, KSL Site Support Services, Planning, Locating and Mapping Section; 06 January 2004; as published 28 May 2009.

Technical Area Boundaries; Los Alamos National Laboratory, Site Planning & Project Initiation Group, Infrastructure Planning Division; 4 December 2009.

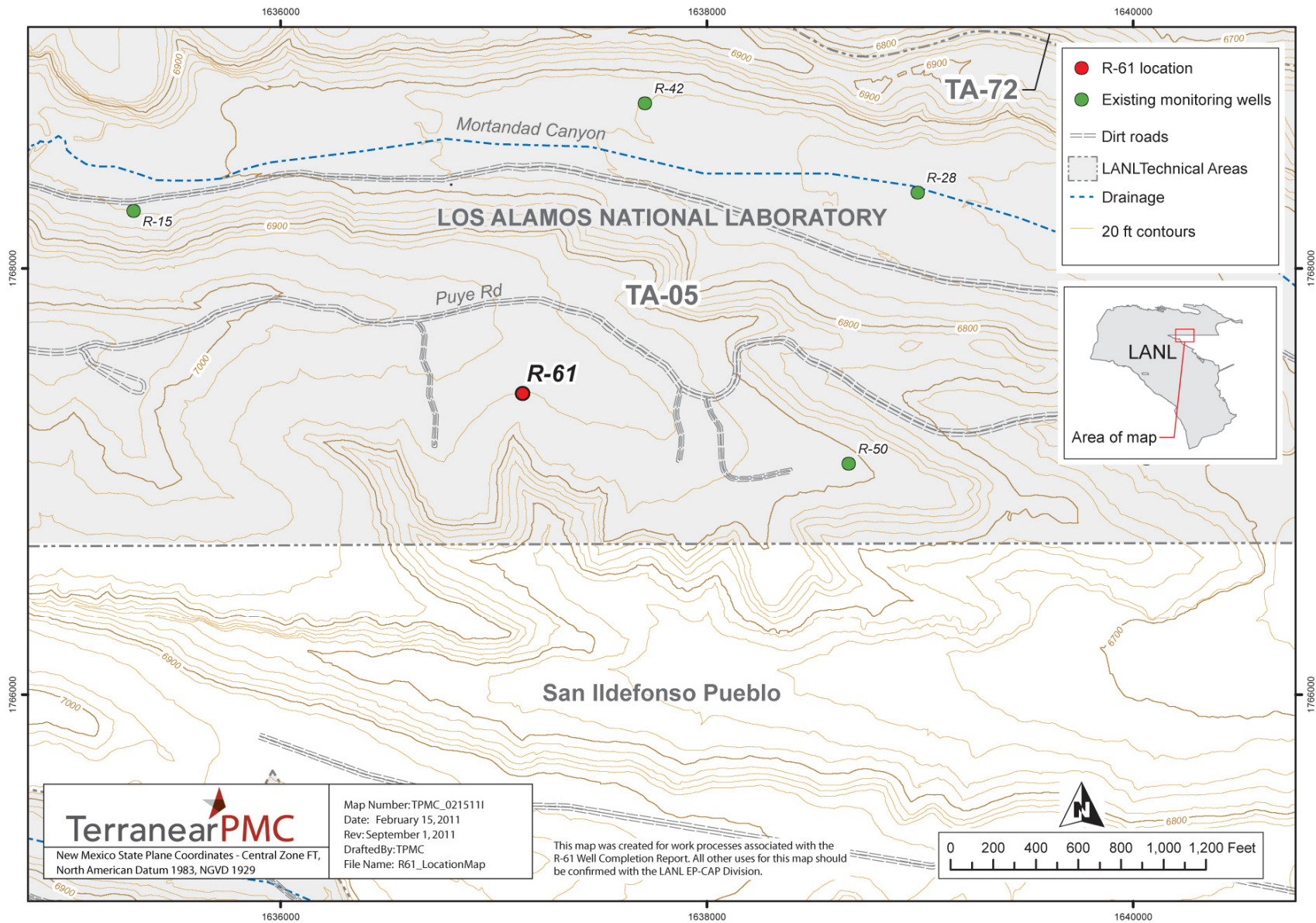


**Figure 1.0-1 Location of monitoring well R-61**

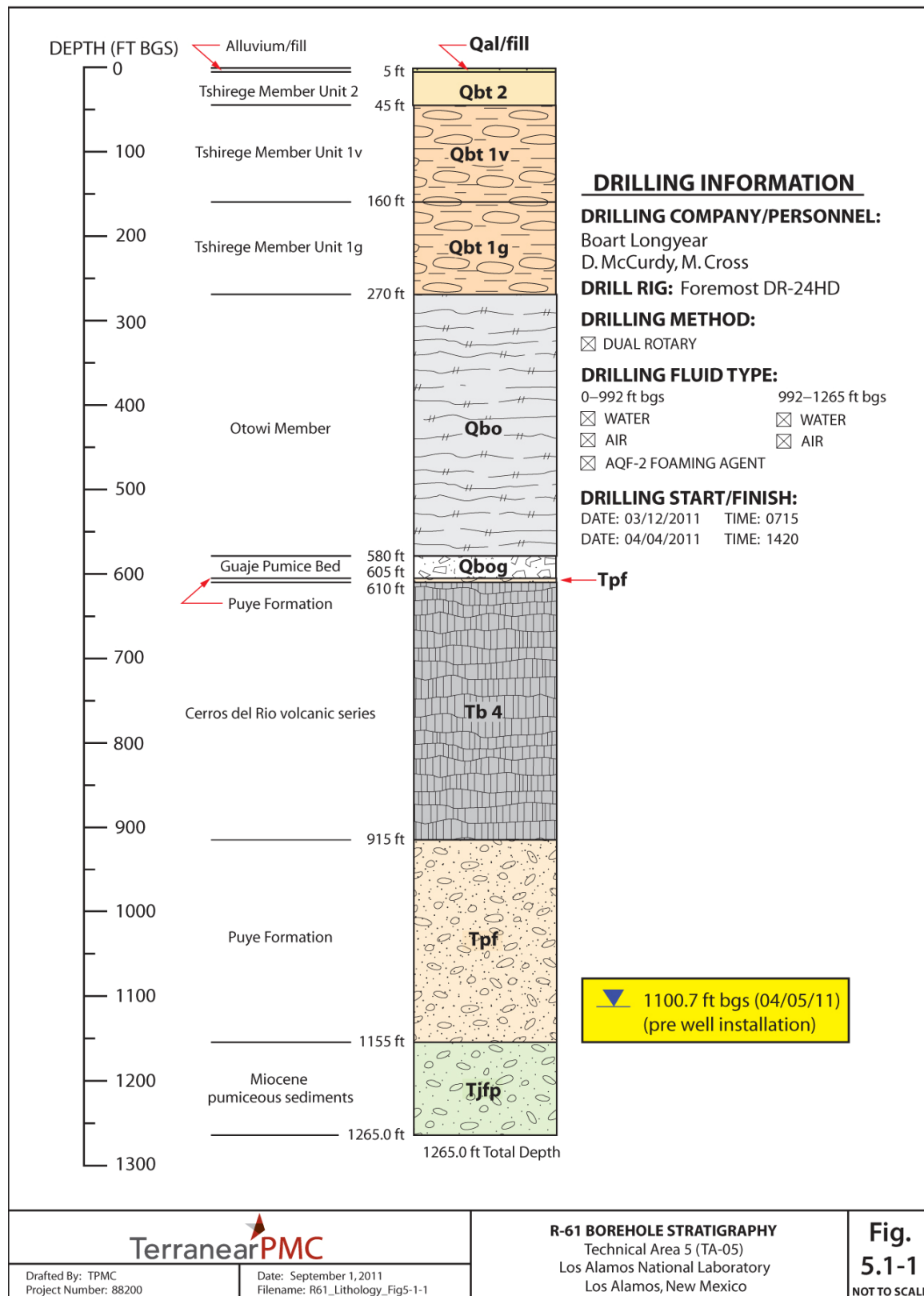


Figure 5.1-1 Monitoring well R-61 borehole stratigraphy





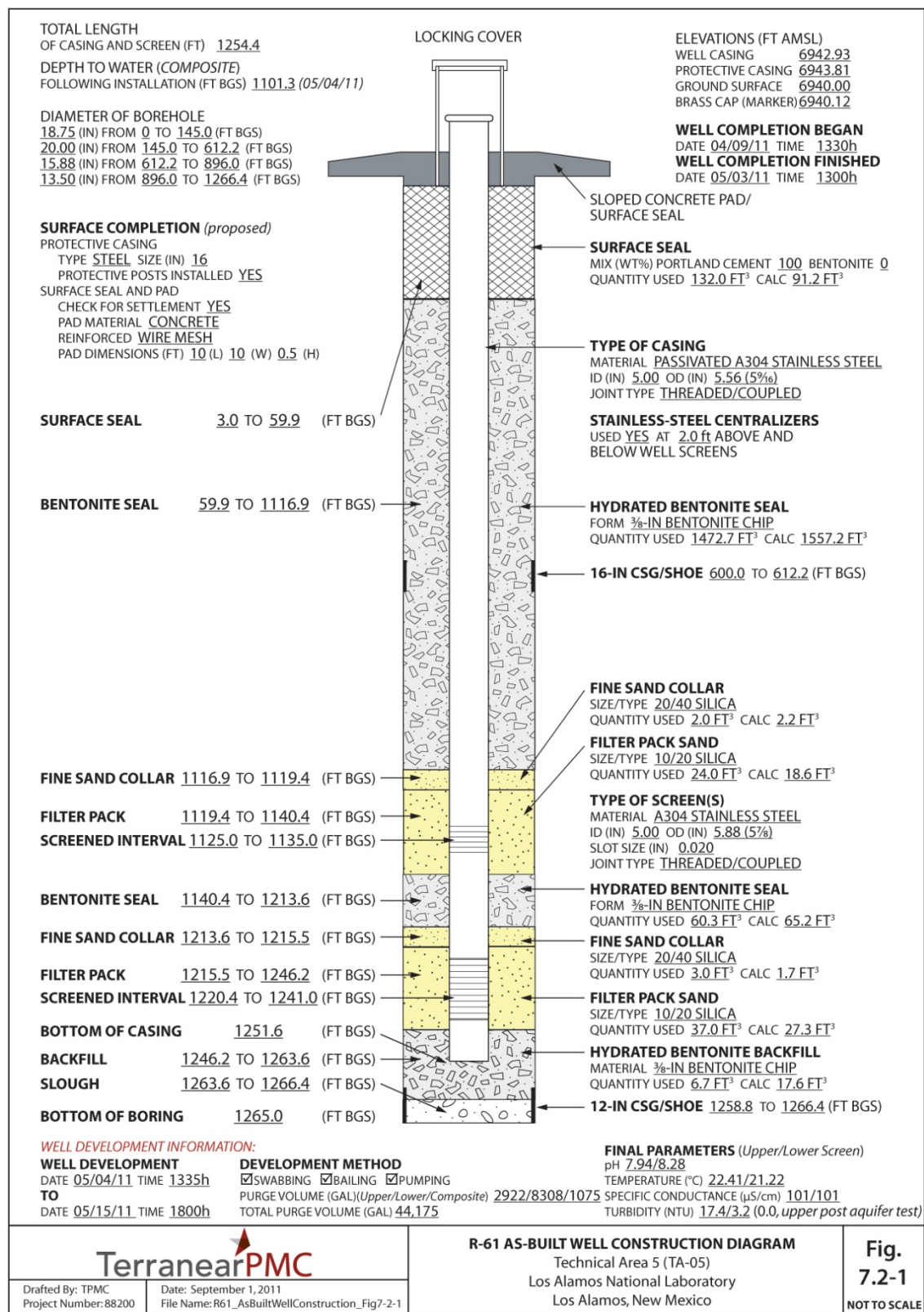


Figure 7.2-1 Monitoring well R-61 as-built well construction diagram

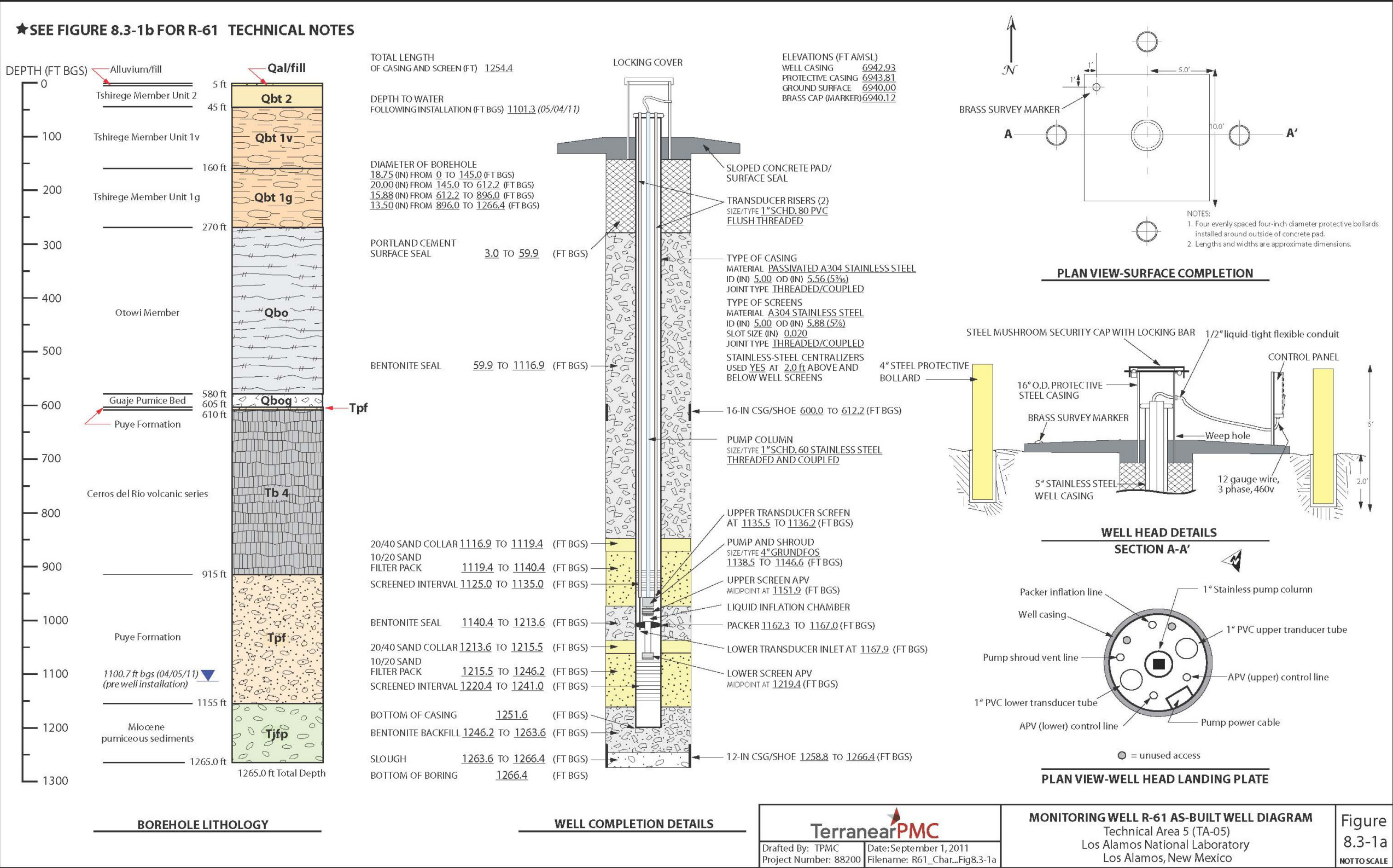


Figure 8.3-1a Monitoring well R-61 as-built diagram with borehole lithology and technical well completion details





**Table 3.1-1**  
**Fluid Quantities Used during R-61 Drilling and Well Construction**

Date	Depth Interval (ft bgs)	Water (gal.)	Cumulative Water (gal.)	AQF-2 Foam (gal.)	Cumulative AQF-2 Foam (gal.)
<b>Drilling</b>					
3/12/11	0-70	1500	1500	20	20
3/13/11	70-145	2000	3500	20	40
3/14/11	145-295	2500	6000	10	50
3/15/11	295-612	3000	9000	5	55
3/16/11	Ream	2000	11,000	5	60
3/17/11	Ream	2500	13,500	5	65
3/18/11	Ream	2000	15,500	5	70
3/22/11	612-645	700	16,200	3	73
3/23/11	645-865	4500	20,700	200	273
3/24/11	865-896	2000	22,700	50	323
3/30/11	896-955	1000	23,700	10	333
3/31/11	955-1049	2300	26,000	5 (above 992 ft bgs)	338
4/1/11	1049-1127	2200	28,200	0	338
4/2/11	1127-1208	2000	30,200	0	338
4/3/11	1208-1223	500	30,700	0	338
4/4/11	1223-1265	500	31,200	0	338
<b>Well Construction</b>					
4/12/11	1259-1251	350	350	n/a*	n/a
4/13/11	1251-1236	3200	3550	n/a	n/a
4/14/11	1236-1227	500	4050	n/a	n/a
4/15/11	1227-1213	1100	5150	n/a	n/a
4/17/11	1213-1203	2700	7850	n/a	n/a
4/18/11	1203-1186	2000	9850	n/a	n/a
4/19/11	1186-1146	5400	15,250	n/a	n/a
4/20/11	1146-1121	2600	17,850	n/a	n/a
4/21/11	1121-1106	1800	19,650	n/a	n/a
4/22/11	1106-1068	3200	22,850	n/a	n/a
4/23/11	1068-998	3100	25,950	n/a	n/a
4/24/11	998-867	5100	31,050	n/a	n/a
4/28/11	869-829	250	31,300	n/a	n/a
4/29/11	829-594	1800	33,100	n/a	n/a
4/30/11	594-486	1500	34,600	n/a	n/a



Table 3.1-1 (continued)

Date	Depth Interval (ft bgs)	Water (gal.)	Cumulative Water (gal.)	AQF-2 Foam (gal.)	Cumulative AQF-2 Foam (gal.)
<b>Well Construction</b>					
5/1/11	486-287	2500	37,100	n/a	n/a
5/2/11	287-62	3000	40,100	n/a	n/a
5/3/11	62-3	740	40,840	n/a	n/a
<b>Total Water Volume (gal.)</b>					
R-61	72,040				

Foam use terminated at 992 ft bgs during drilling; none used during well construction.

\*n/a = Not applicable.

**Table 4.2-1**  
**Summary of Groundwater Screening Samples Collected**  
**during Well Development and Aquifer Testing of Well R-61**

Location ID	Sample ID	Date and Time Collected	Collection Depth (ft bgs)	Sample Type	Analysis
<b>Aquifer Testing Upper Screen</b>					
R-61	GW61-11-5734	5/19/11; 1210	1125.9	Groundwater, pumped	TOC
R-61	GW61-11-5735	5/19/11; 1610	1125.9	Groundwater, pumped	TOC
R-61	GW61-11-5736	5/19/11; 2010	1125.9	Groundwater, pumped	TOC
R-61	GW61-11-5737	5/20/11; 0000	1125.9	Groundwater, pumped	TOC
R-61	GW61-11-5738	5/20/11; 0400	1125.9	Groundwater, pumped	TOC
R-61	GW61-11-5739	5/20/11; 0800	1125.9	Groundwater, pumped	TOC
<b>Well Development Lower Screen</b>					
R-61	GW61-11-5733	5/12/11; 1740	1215.9	Groundwater, pumped	TOC
<b>Aquifer Testing Lower Screen</b>					
R-61	GW61-11-5740	5/23/11; 1200	1184.2	Groundwater, pumped	TOC
R-61	GW61-11-5741	5/23/11; 1600	1184.2	Groundwater, pumped	TOC
R-61	GW61-11-5742	5/23/11; 2000	1184.2	Groundwater, pumped	TOC
R-61	GW61-11-5743	5/24/11; 0000	1184.2	Groundwater, pumped	TOC
R-61	GW61-11-5744	5/24/11; 0400	1184.2	Groundwater, pumped	TOC
R-61	CAMO-11-13848	5/24/11; 0630	1184.2	Groundwater, pumped	Dissolved gas content
R-61	GW61-11-5745	5/24/11; 0730	1184.2	Groundwater, pumped	TOC

**Table 7.2-1**  
**R-61 Monitoring Well Annular Fill Materials**

Material	Volume (ft <sup>3</sup> )
Upper surface seal: cement slurry	132.0
Upper bentonite seal: bentonite chips	1472.7
Fine sand collar: 20/40 silica sand	2.0
Filter pack: 10/20 silica sand	24.0
Middle bentonite seal: bentonite chips	60.3
Fine sand collar: 20/40 silica sand	3.0
Filter pack: 10/20 silica sand	37.0
Backfill: bentonite chips/pellets	6.7

**Table 8.5-1**  
**R-61 Survey Coordinates**

Identification	Northing	Easting	Elevation
R-61 brass cap embedded in pad	1767422.46	1637096.80	6940.12
R-61 ground surface near pad	1767422.04	1637094.60	6940.00
R-61 top of stainless-steel well casing	1767418.40	1637100.61	6942.93
R-61 top of 12-in. protective casing	1767419.19	1637101.06	6943.81

Note: All coordinates are expressed as New Mexico State Plane Coordinate System Central Zone (NAD 83); elevation is expressed in feet amsl using the National Geodetic Vertical Datum of 1929.

**Table 8.6-1**  
**Summary of Waste Samples Collected during Drilling, Construction, and Development of R-61**

Location ID	Sample ID	Date Collected	Description	Sample Type
R-61	WST61-11-5446	3/14/11	Drill cuttings—1st VOC <sup>a</sup> sample	Solids
R-61	WST61-11-5449 (FTB <sup>b</sup> )	3/14/11	Drill cuttings	Solids
R-61	WST61-11-5447	3/16/11	Drill cuttings—2nd VOC sample	Solids
R-61	WST61-11-5450 (FTB)	03/16/11	Drill cuttings	Solids
R-61	WST61-11-5448	4/5/11	Drill cuttings—3rd VOC sample	Solids
R-61	WST61-11-5451 (FTB)	4/5/11	Drill cuttings	Solids
R-61	WST61-11-6514 (F <sup>c</sup> )	5/24/11	Drill fluids	Liquid
R-61	WST61-11-6515 (F)	5/24/11	Drill fluids	Liquid
R-61	WST61-11-6516 (UF <sup>d</sup> )	5/24/11	Drill fluids	Liquid
R-61	WST61-11-6517 (FD <sup>e</sup> )	5/24/11	Drill fluids	Liquid
R-61	WST61-11-6518 (FTB)	5/24/11	Drill fluids	Liquid

Table 8.6-1 (continued)

Location ID	Sample ID	Date Collected	Description	Sample Type
R-61	WST61-11-6262 (F)	04/12/11	Decon <sup>f</sup> well casing not previously used at LANL	Liquid
R-61	WST61-11-6269 (UF)	4/12/11	Decon well casing not previously used at LANL	Liquid
R-61	WST61-11-6276 (FD)	4/12/11	Decon well casing not previously used at LANL	Liquid
R-61	WST61-11-6283 (FTB)	4/12/11	Decon well casing not previously used at LANL	Liquid
R-61	WST61-11-6263 (F)	4/13/11	Decon tremie pipe	Liquid
R-61	WST61-11-6270 (UF)	4/13/11	Decon tremie pipe	Liquid
R-61	WST61-11-6277 (FD)	4/13/11	Decon tremie pipe	Liquid
R-61	WST61-11-6284 (FTB)	4/13/11	Decon tremie pipe	Liquid
R-61	WST61-11-6519 (F)	5/19/11	Development water	Liquid
R-61	WST61-11-6520 (F)	5/19/11	Development water	Liquid
R-61	WST61-11-6521 (UF)	5/19/11	Development water	Liquid
R-61	WST61-11-6522 (FD)	5/19/11	Development water	Liquid
R-61	WST61-11-6523 (FTB)	5/19/11	Development water	Liquid

<sup>a</sup> VOC = Volatile organic compound.

<sup>b</sup> FTB = Field trip blank.

<sup>c</sup> F = Filtered.

<sup>d</sup> UF = Unfiltered.

<sup>e</sup> FD = Field duplicate.

<sup>f</sup> decon = Decontamination.

# **Appendix A**

---

## *Borehole R-61 Lithologic Log*

<b>Borehole Identification (ID):</b> R-61		<b>Technical Area (TA):</b> 05	<b>Page:</b> 1 of 12
<b>Drilling Company:</b> Boart Longyear Company		<b>Start Date/Time:</b> 3/12/2011; 0715	<b>End Date/Time:</b> 4/04/2011; 1420
<b>Drilling Method:</b> Dual Rotary		<b>Machine:</b> Foremost DR24 HD	<b>Sampling Method:</b> Grab
<b>Ground Elevation:</b> 6940.00 ft amsl			<b>Total Depth:</b> 1265.0 ft
<b>Drillers:</b> M. Cross, D. McCurdy		<b>Site Geologists:</b> T. Naibert, M. Jojola, A. Miller	
Depth (ft bgs)	Lithology	Lithologic Symbol	Notes
0–5	<b>ALLUVIUM/FILL:</b> Thin alluvium with construction fill—mixed constituents, including abundant quartzite and minor rounded volcanic pebbles (typical of construction base-course gravel); sand-sized quartz grains.	Qal/Fill	Note: Drill cuttings for microscopic and descriptive analysis were collected at 5-ft intervals from ground surface to borehole TD at 1265 ft bgs.
5–10	<b>UNIT 2 OF THE TSHIREGE MEMBER OF THE BANDELIER TUFF:</b> Tuff—very light gray (N8), poorly welded, moderately indurated, crystal-rich, pumice-bearing. 5'–10' WR: abundant fine volcanic ash. +10F: 50–90% fragments of poorly to moderately welded ash flow tuff [i.e., ignimbrite that is composed of 20–30% quartz and sanidine crystals, 10–15% compressed devitrified pumices set in an ash matrix that makes up 50–60% by volume]; 10–50% broken quartz and sanidine crystals; 1–2% small (up to 4 mm) obsidian fragments; trace volcanic lithic fragments. +35F: 70–95% quartz and sanidine crystals; 5–30% fragments of ash and pumice; trace obsidian; trace lithics.	Qbt 2	Unit 2 of the Tshirege Member of the Bandelier Tuff (Qbt 2), encountered from 5 to 45 ft bgs, is 40 ft thick.
10–45	Tuff—very light gray (N8), moderately welded, moderately indurated, crystal-rich, pumice-bearing. 10'–45' WR: abundant fine volcanic ash. +10F: 50–90% fragments of poorly to moderately welded ash flow tuff [i.e., ignimbrite that is composed of 20–30% quartz and sanidine crystals, 10–15% compressed devitrified pumices set in an ash matrix that makes up 50–60% by volume]; 10–50% broken quartz and sanidine crystals; 1–2% small (up to 4 mm) obsidian fragments; trace volcanic lithic fragments. +35F: 70–95% quartz and sanidine crystals; 5–30% fragments of ash and pumice; trace obsidian; trace lithics.	Qbt 2	The Qbt 2–Qbt 1v contact, estimated to be at 45 ft bgs, is based on natural gamma logging.
45–90	<b>UNIT 1v OF THE TSHIREGE MEMBER OF THE BANDELIER TUFF:</b> Tuff—light gray (N8) poorly welded, crystal-rich 45'–90' WR: abundant ash and large (up to 2 mm) quartz and sanidine crystals. +10F: 99–100% quartz and sanidine crystals; <1% tuff clasts; trace volcanic lithics. +35F: 99–100% quartz and sanidine crystals; <1% volcanic lithics.	Qbt 1v	Unit 1v of the Tshirege Member of the Bandelier Tuff (Qbt 1v), encountered from 45 to 145 ft bgs, is 100 ft thick.

<b>Borehole Identification (ID):</b> R-61		<b>Technical Area (TA):</b> 05	<b>Page:</b> 2 of 12
<b>Drilling Company:</b> Boart Longyear Company		<b>Start Date/Time:</b> 3/12/2011; 0715	<b>End Date/Time:</b> 4/04/2011; 1420
<b>Drilling Method:</b> Dual Rotary		<b>Machine:</b> Foremost DR24 HD	<b>Sampling Method:</b> Grab
<b>Ground Elevation:</b> 6940.00 ft amsl			<b>Total Depth:</b> 1265.0 ft
<b>Drillers:</b> M. Cross, D. McCurdy		<b>Site Geologists:</b> T. Naibert, M. Jojola, A. Miller	
<b>Depth (ft bgs)</b>	<b>Lithology</b>	<b>Lithologic Symbol</b>	<b>Notes</b>
90–125	Tuff—poorly welded, crystal-rich; lithic-bearing. 90'–125' +10F: 5–10% angular and broken volcanic lithic fragments (up to 15 mm, predominantly dacite with minor red rhyolite and welded tuff fragments); 90–95% quartz and sanidine crystals. +35F: 5–10% volcanic lithic fragments; 90–95% quartz and sanidine crystals.	Qbt 1v	
125–130	No sample collected due to lost circulation.	Qbt 1v	
130–145	Tuff—very light gray (N8) to pale yellowish gray (5Y 8/1), poorly welded, moderately indurated, pumiceous (pumices devitrified), crystal-bearing, lithic-bearing. 130'–135' +10F: 30–50% quartz and sanidine crystals; 20–30% pale tan fragments of pumiceous crystal-tuff; 20–40% volcanic lithic fragments (up to 15 mm) predominantly of gray hornblende-dacite. 135'–145' +10F: 60–85% pale tan fragments of weathered, strongly pumiceous (pumices distinctly devitrified) crystal-rich rhyolite ash flow tuff; 10–20% angular volcanic lithics (gray dacite); 5–30% quartz and sanidine crystals. 130'–145' +35F: 70–90% quartz and sanidine crystals; 5–20% fragments of strongly pumiceous ash flow tuff; 5–10% angular volcanic lithics (mostly dacite with minor weathered rhyolite).	Qbt 1v	
145–150	No sample collected due to lost circulation		
150–160	Tuff—very light gray (N8) to pale yellowish gray (5Y 8/1), poorly welded, moderately indurated, pumiceous (pumices devitrified), crystal-bearing, lithic-bearing. 150'–160' +10F: 40–50% quartz and sanidine crystals; 10–30% pale tan fragments of pumiceous crystal-tuff; 30–40% volcanic lithic fragments (up to 15 mm) predominantly of gray hornblende-dacite. +35F: 80–95% quartz and sanidine crystals; 5–10% fragments of strongly pumiceous ash flow tuff; 5–10% angular volcanic lithics (mostly dacite with minor weathered rhyolite).	Qbt 1v	The Qbt 1v–Qbt 1g contact, estimated to be at 160 ft bgs, is based on microscopic examination of drill cuttings and interpretation of natural gamma log data.

<b>Borehole Identification (ID):</b> R-61		<b>Technical Area (TA):</b> 05	<b>Page:</b> 3 of 12
<b>Drilling Company:</b> Boart Longyear Company		<b>Start Date/Time:</b> 3/12/2011; 0715	<b>End Date/Time:</b> 4/04/2011; 1420
<b>Drilling Method:</b> Dual Rotary		<b>Machine:</b> Foremost DR24 HD	<b>Sampling Method:</b> Grab
<b>Ground Elevation:</b> 6940.00 ft amsl			<b>Total Depth:</b> 1265.0 ft
<b>Drillers:</b> M. Cross, D. McCurdy		<b>Site Geologists:</b> T. Naibert, M. Jojola, A. Miller	
<b>Depth (ft bgs)</b>	<b>Lithology</b>	<b>Lithologic Symbol</b>	<b>Notes</b>
160–175	<p><b>UNIT 1g OF THE TSHIREGE MEMBER OF THE BANDELIER TUFF:</b></p> <p>Tuff—pale orange (10YR 8/2), poorly welded, moderately indurated, pumiceous (first appearance of glassy pumices noted), crystal-bearing, lithic-poor.</p> <p>160'–175' +10F: 60–80% pale orange fragments of indurated ash flow tuff containing abundant quartz and sanidine crystals and vitric pumices and black obsidian; 20–25% volcanic lithic fragments (up to 7 mm), predominantly dacite; 10–25% quartz and sanidine crystals. +35F: 30–60% tuff and pumice fragments; 30–50% quartz and sanidine crystals; 10–15% volcanic lithics.</p>	Qbt 1g	<p>Note: distinct color change to pinkish orange tuff fragments with glassy pumice observed below 155 ft bgs.</p> <p>Unit 1g of the Tshirege Member of the Bandelier Tuff (Qbt 1g), encountered from 160 to 270 ft bgs, is 110 ft thick.</p>
175–185	<p>Tuff—pale orange (10YR 8/2), poorly welded, weakly to moderately indurated, strongly pumiceous, crystal-bearing, lithic-poor.</p> <p>175'–185' +10F: 90–98% pale orange fragments of indurated ash flow tuff containing abundant quartz and sanidine crystals and vitric pumices and black obsidian (up to 20 mm); &lt;10% volcanic lithic fragments; &lt;5% quartz and sanidine crystals. +35F: 40–60% tuff and pumice fragments; 30–50% quartz and sanidine crystals; 10–15% volcanic lithics.</p>	Qbt 1g	
185–195	<p>Tuff—pale orange (10YR 8/2), poorly welded, weakly to moderately indurated, strongly pumiceous, crystal-bearing, lithic-poor.</p> <p>185'–195' +10F: very few to no clasts of this size collected in this interval. 80% pale orange pumiceous ash flow tuff fragments; 20% dacite fragments. +35F: 30–50% tuff and pumice fragments; 50–70% quartz and sanidine crystals; 10% volcanic lithics.</p>	Qbt 1g	

<b>Borehole Identification (ID):</b> R-61		<b>Technical Area (TA):</b> 05	<b>Page:</b> 4 of 12
<b>Drilling Company:</b> Boart Longyear Company		<b>Start Date/Time:</b> 3/12/2011; 0715	<b>End Date/Time:</b> 4/04/2011; 1420
<b>Drilling Method:</b> Dual Rotary		<b>Machine:</b> Foremost DR24 HD	<b>Sampling Method:</b> Grab
<b>Ground Elevation:</b> 6940.00 ft amsl			<b>Total Depth:</b> 1265.0 ft
<b>Drillers:</b> M. Cross, D. McCurdy		<b>Site Geologists:</b> T. Naibert, M. Jojola, A. Miller	
<b>Depth (ft bgs)</b>	<b>Lithology</b>	<b>Lithologic Symbol</b>	<b>Notes</b>
195–245	<p>Tuff—White (N9) to pale orange (10YR 8/2), poorly welded, weakly to moderately indurated, strongly pumiceous, crystal-bearing, lithic-poor.</p> <p>195'–205' +10F: 80–90% pale orange fragments of pumiceous ash flow tuff and vitric pumices containing black obsidian; 10–15% volcanic lithic fragments; &lt;5% quartz and sanidine crystals. +35F: 40–60% tuff and pumice fragments; 30–50% quartz and sanidine crystals; 10–15% volcanic lithics.</p> <p>205'–215' +10F: 60–70% pale orange fragments of pumiceous ash flow tuff and vitric pumices; 20–40% volcanic lithic fragments; &lt;5% quartz and sanidine crystals. +35F: 40–50% pumice fragments; 20–40% quartz and sanidine crystals; 20–30% volcanic lithics.</p> <p>215'–245' +10F: 80–90% white to pale orange vitric pumices containing black obsidian; 10–15% volcanic lithic fragments; &lt;5% quartz and sanidine crystals. +35F: 40–60% pumice fragments; 30–50% quartz and sanidine crystals; 10–15% volcanic lithics.</p>	Qbt 1g	
245–250	No sample collected due to lost circulation	Qbt 1g	
250–270	<p>Tuff—White (N9) to pale orange (10YR 8/2), poorly welded, weakly to moderately indurated, strongly pumiceous, crystal-bearing, lithic-poor.</p> <p>250'–270' +10F: 90–95% white to pale orange fragments of vitric pumices containing black obsidian; 5–10% volcanic lithic fragments; &lt;5% quartz and sanidine crystals. +35F: 40–60% pumice; 30–50% quartz and sanidine crystals; 10–15% volcanic lithics.</p>	Qbt 1g	The Qbt 1g–Qbo contact, estimated to be at 270 ft bgs, is based on natural gamma log data.
270–295	<p><b>OTOWI MEMBER OF THE BANDELIER TUFF:</b></p> <p>Tuff—white (N9) to pale yellowish gray (5Y 8/1) poorly welded, weakly indurated, pumice-rich, crystal bearing.</p> <p>270'–295' +10F: 90–95% white, glassy, lustrous pumice fragments/clasts with minor orange oxidation; 5–10% angular volcanic clasts (predominantly hornblende-dacite). +35F: 30–50% quartz and sanidine crystals; 35–65% pumice grains; 5–15% volcanic lithic grains.</p>	Qbo	The Otowi Member of the Bandelier Tuff (Qbo), intersected from 270 to 580 ft bgs, is 310 ft thick.



<b>Borehole Identification (ID):</b> R-61		<b>Technical Area (TA):</b> 05	<b>Page:</b> 5 of 12
<b>Drilling Company:</b> Boart Longyear Company		<b>Start Date/Time:</b> 3/12/2011; 0715	<b>End Date/Time:</b> 4/04/2011; 1420
<b>Drilling Method:</b> Dual Rotary		<b>Machine:</b> Foremost DR24 HD	<b>Sampling Method:</b> Grab
<b>Ground Elevation:</b> 6940.00 ft amsl			<b>Total Depth:</b> 1265.0 ft
<b>Drillers:</b> M. Cross, D. McCurdy		<b>Site Geologists:</b> T. Naibert, M. Jojola, A. Miller	
<b>Depth (ft bgs)</b>	<b>Lithology</b>	<b>Lithologic Symbol</b>	<b>Notes</b>
295–325	Tuff—white (N9) to pale yellowish gray (5Y 8/1) poorly welded, weakly indurated, pumice-rich, crystal bearing.  295'–325' +10F: 80–90% white, glassy, lustrous pumice fragments/clasts; 10–20% angular/broken and subrounded volcanic clasts (predominantly hornblende-dacite). +35F: 50–80% quartz and sanidine crystals; 10–35% pumice grains; 10–15% volcanic lithic grains.	Qbo	
325–360	Tuff—white (N9) to pale yellowish gray (5Y 8/1) poorly welded, weakly indurated, pumice-rich, crystal bearing.  325'–360' +10F: 60–90% white, glassy, lustrous pumice fragments/clasts (larger than above; up to 20 mm); 10–40% angular/broken and subrounded volcanic clasts (predominantly hornblende-dacite). +35F: 40–70% quartz and sanidine crystals; 20–40% pumice grains; 10–20% volcanic lithic grains.	Qbo	
360–375	Tuff—white (N9) to pale yellowish gray (5Y 8/1) poorly welded, weakly indurated, pumice-rich, crystal bearing.  360'–375' +10F: 60–80% white, glassy, lustrous pumice fragments/clasts (up to 10 mm); 20–40% angular/broken and subrounded volcanic clasts (predominantly hornblende-dacite). +35F: 40–80% quartz and sanidine crystals; 10–40% pumice grains; 10–20% volcanic lithic grains.	Qbo	
375–380	Tuff—white (N9) to pale yellowish gray (5Y 8/1) poorly welded, weakly indurated, pumice-rich, crystal bearing.  375'–380' +10F: 20–40% white, glassy, lustrous pumice fragments/clasts (up to 10 mm); 60–80% angular/broken and subrounded volcanic clasts (predominantly hornblende-dacite). +35F: 40–70% quartz and sanidine crystals; 20–40% pumice grains; 10–20% volcanic lithic grains.	Qbo	
380–395	No sample collected due to lost circulation.	Qbo	

<b>Borehole Identification (ID):</b> R-61		<b>Technical Area (TA):</b> 05	<b>Page:</b> 6 of 12
<b>Drilling Company:</b> Boart Longyear Company		<b>Start Date/Time:</b> 3/12/2011; 0715	<b>End Date/Time:</b> 4/04/2011; 1420
<b>Drilling Method:</b> Dual Rotary		<b>Machine:</b> Foremost DR24 HD	<b>Sampling Method:</b> Grab
<b>Ground Elevation:</b> 6940.00 ft amsl			<b>Total Depth:</b> 1265.0 ft
<b>Drillers:</b> M. Cross, D. McCurdy		<b>Site Geologists:</b> T. Naibert, M. Jojola, A. Miller	
<b>Depth (ft bgs)</b>	<b>Lithology</b>	<b>Lithologic Symbol</b>	<b>Notes</b>
395–405	Tuff—white (N9) to orange (10YR 8/2) poorly welded, pumice-rich, crystal bearing. 395'–405' +10F: 60–80% white, glassy pumice fragments/clasts (up to 20 mm); 20–40% subangular/subrounded volcanic clasts. +35F: 50–80% quartz and sanidine crystals; 20–40% pumice grains; 10–20% volcanic lithic grains.	Qbo	
405–490	Tuff—white (N9) to very pale orange (10YR 8/2), poorly welded, pumiceous, crystal-bearing. 405'–490' +10F: 80–90% glassy pumices; 10–20% volcanic lithic fragments (gray porphyritic dacites, dark gray andesite). +35F: 50–90% quartz and sanidine crystals; 10–40% pumice; 10–20% volcanic lithic fragments.	Qbo	Note: pumice size generally smaller (<5 mm) in +10F through this section, with larger pumices (<15 mm) between 435 to 440 ft bgs and 450 to 460 ft bgs.
490–500	Tuff—white (N9) poorly welded, pumiceous, crystal-bearing. 490'–500' +10F: 80–90% glassy quartz- and sanidine-phyric pumices (up to 15 mm) with minor black obsidian; 10–20% volcanic lithic fragments (gray porphyritic dacites, dark gray andesite). +35F: 60–90% quartz and sanidine crystals; 10–30% pumice; 10–20% volcanic lithic fragments.	Qbo	
500–525	Tuff—white (N9) to very pale orange (10YR 8/2), poorly welded, pumiceous, crystal-bearing. 500'–525' +10F: 80–90% glassy pumices; 10–20% volcanic lithic fragments (gray porphyritic dacites, dark gray andesite). +35F: 50–90% quartz and sanidine crystals; 10–40% pumice; 10–20% volcanic lithic fragments.	Qbo	
525–540	Tuff—white (N9) to very pale orange (10YR 8/2), poorly welded, pumiceous, crystal-bearing. 525'–540' +10F: 80–90% glassy pumices, lapilli are more angular than above; 10–20% volcanic lithic fragments (gray porphyritic dacites, dark gray andesite). +35F: 50–90% quartz and sanidine crystals; 10–40% pumice; 10–20% volcanic lithic fragments.	Qbo	
540–580	Tuff—white (N9) to very pale orange (10YR 8/2), poorly welded, pumiceous, crystal-bearing. 540'–580' +10F: 80–90% glassy pumices; 10–20% volcanic lithic fragments (gray porphyritic dacites, dark gray andesite). +35F: 50–90% quartz and sanidine crystals; 10–40% pumice; 10–20% volcanic lithic fragments.	Qbo	The Qbo–Qbog contact, estimated to be at 580 ft bgs, is based on microscopic examination of drill cuttings and interpretation of natural gamma log data.

<b>Borehole Identification (ID):</b> R-61		<b>Technical Area (TA):</b> 05	<b>Page:</b> 7 of 12
<b>Drilling Company:</b> Boart Longyear Company		<b>Start Date/Time:</b> 3/12/2011; 0715	<b>End Date/Time:</b> 4/04/2011; 1420
<b>Drilling Method:</b> Dual Rotary		<b>Machine:</b> Foremost DR24 HD	<b>Sampling Method:</b> Grab
<b>Ground Elevation:</b> 6940.00 ft amsl			<b>Total Depth:</b> 1265.0 ft
<b>Drillers:</b> M. Cross, D. McCurdy		<b>Site Geologists:</b> T. Naibert, M. Jojola, A. Miller	
<b>Depth (ft bgs)</b>	<b>Lithology</b>	<b>Lithologic Symbol</b>	<b>Notes</b>
580–605	<b>GUAJE PUMICE BED OF THE OTOWI MEMBER OF THE BANDELIER TUFF:</b> Tuff—white (N9) to very pale orange (10YR 8/2), poorly welded, pumiceous, crystal-bearing. 580'–605' +10F: 95–98% glassy pumices; 2–5% volcanic lithic fragments (gray porphyritic dacites, dark gray andesite). +35F: 70–90% quartz and sanidine crystals; 10–30% pumice; <5% volcanic lithic fragments.	Qbog	The Guaje Pumice Bed (Qbog), intersected from 580 to 605 ft bgs, is 25 ft thick.  The Qbog–Tpf contact, estimated to be at 605 ft bgs, is based on microscopic examination of drill cuttings and interpretation of natural gamma log data.
605–610	<b>PUYE FORMATION:</b> Volcaniclastic sediments—very pale orange (10YR 8/2) well rounded pumice gravels with fine to coarse sand, moderately sorted, moderately indurated. Samples consist of mixed volcanic and pumiceous detritus. 605'–610' +10F: 70–80% subrounded to rounded white vitric, pumice granules and pebbles (up to 10 mm); 20–30% subrounded volcanic clasts (vesicular basalt, dacite, black vitrophyre). +35F: samples of pumices and volcanic lithic grains in varying proportions; minor quartz and sanidine crystals.	Tpf	The upper section of Puye Fm. volcaniclastic sediments (Tpf), intersected from 605 to 610 ft bgs, is 5 ft thick.  The Tpf–Tb 4 contact, estimated to be at 610 ft bgs, is based on change in penetration rate during drilling operations.
610–630	<b>CERROS DEL RIO VOLCANIC SERIES:</b> Basalt lava—medium gray (N5) massive basalt clasts with minor rounded volcanic lithics similar to Puye Formation sediments. 610'–615' +10F: 70–80% angular to subrounded volcanic lithic fragments; 20–30% angular/broken chips of basalt. +35F: 90–95% volcanic lithic fragments; 5–10% basalt chips. 615'–630' WR/+10F/+35F: 80–90% angular/broken chips of basalt; 10–20% volcanic lithic fragments (mostly rhyolite and pumice).	Tb 4	Cerro del Rio volcanic series (Tb 4), including basalt lavas, cinder deposits, and volcanic sediments, were intersected from 610 to 915 ft bgs and are 05 ft thick.
630–670	Basaltic lava—medium gray (N5) massive basalt clasts with minor rounded volcanic lithic fragments. 630'–645' +10F: 90–95% subangular to subrounded clasts composed of massive, pyroxene-bearing basalt; 5–10% pumice and volcanic clasts. +35F: 95–98% massive basalt chips; 2–5% silicic volcanic fragments. 645'–670' WR/+10F/+35F: 98–100% subangular clasts of pyroxene-bearing massive basalt; <2% pumice and silicic volcanic clasts.	Tb 4	

<b>Borehole Identification (ID):</b> R-61		<b>Technical Area (TA):</b> 05	<b>Page:</b> 8 of 12
<b>Drilling Company:</b> Boart Longyear Company		<b>Start Date/Time:</b> 3/12/2011; 0715	<b>End Date/Time:</b> 4/04/2011; 1420
<b>Drilling Method:</b> Dual Rotary		<b>Machine:</b> Foremost DR24 HD	<b>Sampling Method:</b> Grab
<b>Ground Elevation:</b> 6940.00 ft amsl			<b>Total Depth:</b> 1265.0 ft
<b>Drillers:</b> M. Cross, D. McCurdy		<b>Site Geologists:</b> T. Naibert, M. Jojola, A. Miller	
<b>Depth (ft bgs)</b>	<b>Lithology</b>	<b>Lithologic Symbol</b>	<b>Notes</b>
670–680	Basalt lavas—medium dark gray (N4), fragments/chips of massive and weakly vesicular basalt. 670'–680' WR/+10F/+35F: 99–100% angular/broken chips of weakly porphyritic basalt with phenocrysts of clinopyroxene and olivine.	Tb 4	
680–685	Basaltic cinder deposits—grayish red (5R 4/2) to medium gray (N5), chips of vesicular basalt and gray olivine- and clinopyroxene-phyric basalt. 680'–685' +10F/+35F: 100% angular/broken chips of vesicular basalt.	Tb 4	
685–705	Basalt lavas—medium dark gray (N4), fragments/chips of massive and weakly vesicular basalt. 685'–705' WR/+10F/+35F: 99–100% angular/broken chips of weakly porphyritic basalt with phenocrysts of clinopyroxene and olivine with minor hematite alteration.	Tb 4	
705–725	Basalt lavas—medium (N5) to medium dark gray (N4) fragments of weakly vesicular basalt. 705'–725' WR/+10F/+35F: 100% angular/broken chips of weakly vesicular basalt with phenocrysts of olivine up to 3 mm.	Tb 4	
725–730	Basaltic sediments—medium gray (N5) rounded, moderately sorted basalt gravels and coarse sands. 725'–730' WR/+10F/+35F: 100% well rounded basalt sediments.	Tb 4	
730–760	Basalt lavas—medium (N5) to grayish red (5R 4/2) fragments of weakly vesicular basalt. 730'–760' WR/+10F/+35F: 100% angular chips of weakly vesicular basalt with some minor oxidation and phenocrysts of pyroxene and olivine.	Tb 4	
760–785	Basalt lavas—medium (N5) to grayish red (5R 4/2) fragments of weakly vesicular basalt. 760'–785' WR/+10F/+35F: 100% angular chips of weakly vesicular basalt with minor oxidation to grayish red and phenocrysts of pyroxene and olivine.	Tb 4	

<b>Borehole Identification (ID):</b> R-61		<b>Technical Area (TA):</b> 05	<b>Page:</b> 9 of 12
<b>Drilling Company:</b> Boart Longyear Company		<b>Start Date/Time:</b> 3/12/2011; 0715	<b>End Date/Time:</b> 4/04/2011; 1420
<b>Drilling Method:</b> Dual Rotary		<b>Machine:</b> Foremost DR24 HD	<b>Sampling Method:</b> Grab
<b>Ground Elevation:</b> 6940.00 ft amsl			<b>Total Depth:</b> 1265.0 ft
<b>Drillers:</b> M. Cross, D. McCurdy		<b>Site Geologists:</b> T. Naibert, M. Jojola, A. Miller	
<b>Depth (ft bgs)</b>	<b>Lithology</b>	<b>Lithologic Symbol</b>	<b>Notes</b>
785–795	Basaltic sediments—medium gray (N5) rounded, moderately sorted basalt granules and coarse sands. 785'–795' WR/+10F/+35F: 100% rounded to subrounded basalt sediments.	Tb 4	
795–825	Basalt lavas—medium gray (N5) angular chips of moderately oxidized, weakly vesicular basalt. 795'–825' WR/+10F: 90–100% weakly to moderately vesicular basalt with variable levels of oxidation; 0–10% pumice clasts. +35F: 100% basalt with minor oxidation.	Tb 4	
825–865	Basalt lavas—medium gray (N5) angular chips weakly vesicular basalt. 825'–865' WR/+10F: 100% weakly vesicular basalt. +35F: 100% medium gray basalt chips.	Tb 4	
865–895	No samples collected due to lost circulation	Tb 4	
895–915	Basalt lavas—medium gray (N5) angular chips of moderately oxidized, weakly vesicular basalt. 895'–915' WR/+10F: 90–100% weakly to moderately vesicular basalt with variable levels of oxidation; 0–10% volcanoclastic sediments. +35F: 95–100% basalt with minor oxidation; 0–5% volcanoclastic clasts.	Tb 4	
915–955	<b>PUYE FORMATION:</b> Volcanoclastic sediments—very light gray (N7) fine to medium gravels with silty fine to medium sand, moderately sorted. Samples consist of subangular to subrounded, predominantly dacitic pebbles. 915'–955' +10F/+35F: 98–100% broken chips (up to 15 mm) of subangular pebbles/granules of dacite; 0–2% quartz crystals.	Tpf	The lower section of Puye Fm. volcanoclastic sediments (Tpf), intersected from 915 to 1155 ft bgs, is 240 ft thick.
955–1030	Volcanoclastic sediments—very light gray (N7) fine to medium gravels with silty fine to medium sand, moderately sorted. Samples consist of subangular to subrounded, predominantly dacitic pebbles with slight alteration. 955'–1030' +10F/+35F: 98–100% broken chips (up to 25 mm) of subangular pebbles/granules of dacite; 0–2% quartz crystals.	Tpf	

<b>Borehole Identification (ID):</b> R-61		<b>Technical Area (TA):</b> 05	<b>Page:</b> 10 of 12
<b>Drilling Company:</b> Boart Longyear Company		<b>Start Date/Time:</b> 3/12/2011; 0715	<b>End Date/Time:</b> 4/04/2011; 1420
<b>Drilling Method:</b> Dual Rotary		<b>Machine:</b> Foremost DR24 HD	<b>Sampling Method:</b> Grab
<b>Ground Elevation:</b> 6940.00 ft amsl			<b>Total Depth:</b> 1265.0 ft
<b>Drillers:</b> M. Cross, D. McCurdy		<b>Site Geologists:</b> T. Naibert, M. Jojola, A. Miller	
<b>Depth (ft bgs)</b>	<b>Lithology</b>	<b>Lithologic Symbol</b>	<b>Notes</b>
1030– 1040	Volcaniclastic sediments—very light gray (N7) fine to medium gravels with silty fine to medium sand, moderately sorted. Samples consist of subangular to subrounded, predominantly dacitic pebbles with slight alteration. 1030'–1040' +10F/+35F: 98–100% broken chips (up to 10 mm) of subangular pebbles/granules of dacite; 0–2% quartz crystals.	Tpf	
1040– 1110	Volcaniclastic sediments—very light gray (N7) fine to medium gravels with silty fine to medium sand, moderately sorted. Samples consist of subangular to subrounded, predominantly dacitic pebbles. 1040'–1110' +10F: 100% broken chips (up to 25 mm) of subangular pebbles/granules of dacite, +35F: 95–98% subangular volcanic clasts; 2–5% quartz crystals.	Tpf	
1110– 1145	Volcaniclastic sediments—varicolored, medium (N5) to very light gray (N7) coarse gravels with detritus composed of nearly monolithologic coarsely porphyritic hornblende-phyric dacites. 1110'–1145' +10F: 100% broken chips (up to 10 mm) of subangular pebbles/granules of dacite, +35F: 95–98% subangular volcanic clasts; 2–5% quartz crystals.	Tpf	
1145– 1155	Volcaniclastic sediments—varicolored, medium (N5) to very light gray (N7) coarse gravels with larger clasts than above. 1145'–1155' +10F: 100% broken chips (up to 25 mm) of subangular pebbles/granules of dacite, +35F: 95–98% subangular volcanic clasts; 2–5% quartz crystals.	Tpf	The contact between Tpf and underlying Miocene pumiceous sediments, estimated to be at 1155 ft bgs, is based on natural gamma logs and microscopic examination of drill cuttings.
1155– 1165	<b>MIOCENE PUMICEOUS SEDIMENTS:</b> Volcaniclastic sediments—varicolored, medium (N5) to very light gray (N7) coarse gravels with detritus composed of porphyritic hornblende-phyric dacites and pumice. 1155'–1165' +10F: 80–90% broken chips (up to 15 mm) of subangular pebbles/granules of dacite; 10–20% glassy pumice clasts, +35F: 95–98% subangular volcanic clasts; 2–5% quartz crystals.	Tjfp	Pumiceous volcaniclastic sediments of Miocene age were intersected from 1155 ft bgs to the bottom of the R-61 borehole at 1265 ft bgs. Miocene pumiceous sediments are locally a minimum of 110 ft thick.

<b>Borehole Identification (ID):</b> R-61		<b>Technical Area (TA):</b> 05	<b>Page:</b> 11 of 12
<b>Drilling Company:</b> Boart Longyear Company		<b>Start Date/Time:</b> 3/12/2011; 0715	<b>End Date/Time:</b> 4/04/2011; 1420
<b>Drilling Method:</b> Dual Rotary		<b>Machine:</b> Foremost DR24 HD	<b>Sampling Method:</b> Grab
<b>Ground Elevation:</b> 6940.00 ft amsl			<b>Total Depth:</b> 1265.0 ft
<b>Drillers:</b> M. Cross, D. McCurdy		<b>Site Geologists:</b> T. Naibert, M. Jojola, A. Miller	
<b>Depth (ft bgs)</b>	<b>Lithology</b>	<b>Lithologic Symbol</b>	<b>Notes</b>
1165– 1175	Volcaniclastic sediments—varicolored, medium (N5) to very light gray (N7) coarse gravels with detritus composed of porphyritic hornblende-phyric dacites and glassy pumice. 1165'–1175' +10F: 30–60% broken chips of subangular pebbles/granules of dacite; 40–70% glassy pumice clasts, +35F: 50–60% subangular volcanic clasts; 25–45% pumice fragments; 5–15% quartz crystals.	Tjfp	
1175– 1180	Volcaniclastic sediments—varicolored, medium (N5) to very light gray (N7) coarse gravels with detritus composed of porphyritic hornblende-phyric dacites and glassy pumice. 1175'–1180' WR/+10F: 40–50% subangular volcanic (mostly dacite) pebbles; 50–60% glassy pumice clasts. No +35F samples collected.	Tjfp	
1180– 1210	Volcaniclastic sediments—varicolored, medium (N5) to very light gray (N7) coarse gravels with detritus composed of porphyritic hornblende-phyric dacites and glassy pumice. 1180'–1210' +10F: 30–60% broken chips of subangular pebbles/granules of dacite; 40–70% glassy pumice clasts, +35F: 50–60% subangular volcanic clasts; 25–45% pumice fragments; 5–15% quartz crystals.	Tjfp	
1210– 1230	Pumiceous volcaniclastic sediments—varicolored, white (N9) to medium light gray (N7) fine to medium gravels with fine to coarse sand, moderately to poorly sorted, detrital dacite clasts and glassy pumices. 1210'–1230' +10F: 30% angular/broken chips of light gray biotite-phyric dacite; trace white dacite with very fine hornblende phenocrysts; 70% white phenocryst-poor pumices. +35F: 10–50% subangular volcanic clasts; 50–80% pumice fragments; 10% quartz crystals.	Tjfp	

<b>Borehole Identification (ID):</b> R-61		<b>Technical Area (TA):</b> 05	<b>Page:</b> 12 of 12
<b>Drilling Company:</b> Boart Longyear Company		<b>Start Date/Time:</b> 3/12/2011; 0715	<b>End Date/Time:</b> 4/04/2011; 1420
<b>Drilling Method:</b> Dual Rotary		<b>Machine:</b> Foremost DR24 HD	<b>Sampling Method:</b> Grab
<b>Ground Elevation:</b> 6940.00 ft amsl			<b>Total Depth:</b> 1265.0 ft
<b>Drillers:</b> M. Cross, D. McCurdy		<b>Site Geologists:</b> T. Naibert, M. Jojola, A. Miller	
<b>Depth (ft bgs)</b>	<b>Lithology</b>	<b>Lithologic Symbol</b>	<b>Notes</b>
1230– 1240	Pumiceous volcanoclastic sediments—varicolored, white (N9) to medium light gray (N7) fine to medium gravels with fine to coarse sand, moderately to poorly sorted, detrital volcanic clasts and glassy pumices. 1230'–1240' +10F: 30% large (up to 30 mm), rounded clasts of various volcanic lithologies (dacites, andesite scoria); 70% white phenocryst-poor pumices. +35F: 10–50% subangular volcanic clasts; 50–80% pumice fragments; 10% quartz crystals.	Tjfp	
1240– 1265	Pumice-rich volcanoclastic sediments—varicolored, white (N9) to medium light gray (N7) fine gravels with fine to medium sand, moderately sorted. Samples composed of more than 50% detrital pumices and less than 50% grains and granules of various volcanic compositions. 1240'–1265' +10F: 60–80% well rounded granules/pebbles (up to 20 mm) of white to tan, phenocryst-poor, vitric pumices; 20–40% subangular to subrounded pebbles (up to 10 mm) composed of various volcanic lithologies including hornblende-dacite, white biotite-dacites, andesite and banded vitrophyre.	Tjfp	Note: The total depth of R-61 was 1265 ft bgs.



## Borehole Lithologic Log (continued)

### Abbreviations

5YR 8/4 (example) = Munsell rock color notation where hue (e.g., 5YR), value (e.g., 8), and chroma (e.g., 4) are expressed. Hue indicates soil color's relation to red, yellow, green, blue, and purple. Value indicates soil color's lightness. Chroma indicates soil color's strength.

% = estimated percent by volume of a given sample constituent

amsl = above mean sea level

bgs = below ground surface

Qbo = Otowi Member of the Bandelier Tuff

Qbog = Guaje Pumice Bed of the Otowi Member of the Bandelier Tuff

Qbt = Tshirege Member of the Bandelier Tuff

Tb 4 = Cerros del Rio volcanic series

Tjfp = Jemez fanglomerate pumiceous (called Miocene pumiceous sediments in this report)

Tpf = Puye Formation

+10F = plus No. 10 sieve sample fraction

+35F = plus No. 35 sieve sample fraction

WR = whole rock (unsieved sample)

1 mm = 0.039 in.

1 in. = 25.4 mm



## **Appendix B**

---

### *Screening Groundwater Analytical Results*

## **B-1.0 SCREENING GROUNDWATER ANALYSES AT R-61**

R-61 is a regional aquifer monitoring well with two screened intervals. The upper screen is set between 1125 and 1135 ft below ground surface (bgs) in Puye Formation sediments, and the lower screen is set between 1220.4 and 1241 ft bgs in Miocene pumiceous sediments. This appendix presents screening analytical results for samples collected during well development and aquifer testing at R-61.

### **Laboratory Analyses**

Regional groundwater samples were collected at the end of development of the lower screened interval and during aquifer testing of each screened interval and analyzed for total organic carbon (TOC). Los Alamos National Laboratory's Earth and Environmental Sciences Group 14 (EES-14) conducted the TOC and dissolved gas content analyses. Table B-1.0-1 lists the samples submitted for analyses from R-61.

Additionally, because of the observed effervescent groundwater discharging from the lower screen during aquifer testing, a groundwater sample was collected from the lower screened interval and analyzed for dissolved gas content near the end of aquifer testing. The dissolved gas analysis was also conducted by EES-14 in an effort to determine the content and origin of the effervescing bubbles.

### **Field Analyses**

Groundwater samples were collected from a flow-through cell during well development and aquifer testing in the lower screen and during aquifer testing in the upper screen and measured for pH, conductivity, temperature, dissolved oxygen (DO), oxidation-reduction potential (ORP) and turbidity.

## **B-2.0 SCREENING ANALYTICAL RESULTS**

This section presents the TOC results, dissolved gas content analyses, and field parameters measured during well development and aquifer testing.

### **B-2.1 Total Organic Carbon**

During well development and aquifer testing of the lower screen, TOC values ranged from 0.2 to 0.4 mgC/L in seven samples. During aquifer testing of the upper screen, TOC concentrations varied from 2.8 to 0.4 mgC/L in six groundwater samples (Table B-2.1-1). The final concentrations for each screen are below the target concentration of 2.0 mgC/L for TOC.

### **B-2.2 Dissolved Gas Analysis**

Dissolved nitrogen, oxygen, and carbon dioxide were the three primary gases detected in the groundwater sample from the lower screened interval. Dissolved carbon dioxide (CO<sub>2</sub>) was of most interest because elevated concentrations might represent deep-seated hydrothermal sources for the groundwater.

CO<sub>2</sub> concentrations of 2.07 and 2.57 g/L were measured in the lower screen sample; these concentrations, although slightly elevated, do not imply deep-seated CO<sub>2</sub> sources. The alkalinity of the lower screen sample was also measured, and it was low, typical of other regional aquifer groundwater

measurements. If the sample had experienced extended periods of time in groundwater with elevated CO<sub>2</sub>, a higher total alkalinity would be expected, which was not the case. It also had a neutral pH (6.5).

The interpretation regarding the lower screen sample is that the elevated CO<sub>2</sub> was the result of compressed air drilling techniques, and that the sample was saturated with respect to CO<sub>2</sub> at the temperature and pressure of the groundwater at depth. Upon being sampled at the ground surface, the water became oversaturated with respect to CO<sub>2</sub>, causing it to effervesce. It should also be noted that the effervescence of the lower screen groundwater had decreased significantly by the time the sampling system was installed in late July 2011, some 2 mo after aquifer testing.

### **B-2.3 Field Parameters**

A handheld YSI 6920 multi-parameter instrument was used to measure field parameters during well development and aquifer testing. Performance checks were conducted at the beginning of each shift, and the same meter was used throughout well development and aquifer testing at R-61. Field parameters measured during well development and aquifer testing are presented in Table B-2.3-1.

During well development and aquifer testing of the lower screen, pH varied from 7.53 to 8.36, and temperature ranged from 16.45°C to 23.04°C. DO concentrations varied from 6.29 to 8.37 mg/L. Specific conductance ranged from 101 to 198 µS/cm, and turbidity values varied from 0 to 122.9 nephelometric turbidity units (NTU). Corrected oxidation-reduction potential (Eh) values, determined from field ORP measurements, varied from 260.0 to 349.6 mV. Figure B-2.3-1 shows the lower screen field parameters measured over the course of well development and aquifer testing.

During well development and aquifer testing of the upper screen, pH varied from 6.95 to 8.11, and temperature ranged from 17.03°C to 24.78°C. DO concentrations varied from 1.27 to 6.51 mg/L. Specific conductance ranged from 101 to 188 µS/cm, and turbidity values varied from 0 to 134.3 NTU. Corrected Eh values, determined from field ORP measurements, varied from 304.5 to 416.8 mV. Three temperature-dependent correction factors were used to calculate Eh values from field ORP measurements obtained from the lower and upper screens: 208.9, 203.9, and 198.5 mV at 15°C, 20°C, and 25°C, respectively. Figure B-2.3-2 shows the upper screen field parameters measured over the course of well development and aquifer testing.

The final parameters measured at the end of aquifer testing at the lower screen were pH of 8.19, temperature of 16.55°C, DO of 7.66 mg/L, specific conductance of 134 µS/cm, and turbidity of 0 NTU. The final parameters measured at the end of aquifer testing at the upper screen were pH of 7.67, temperature of 18.75°C, DO of 5.30 mg/L, specific conductance of 167 µS/cm, and turbidity of 0 NTU.

### **B-3.0 SUMMARY OF SCREENING ANALYTICAL RESULTS**

At the end of aquifer testing of both screened intervals, TOC concentrations were below the target level of 2.0 mgC/L, and turbidity was below 5 NTU. Dissolved gas concentrations indicate that the source of the effervescence observed in the lower screened interval's discharge is likely attributed to compressed air used during the borehole drilling process.

R-61 will be sampled quarterly for 1 yr, and then data will be incorporated into the appropriate periodic monitoring report. The revised sampling suite and schedule will be reported in the annual updates to the Interim Facility-Wide Groundwater Monitoring Plan.

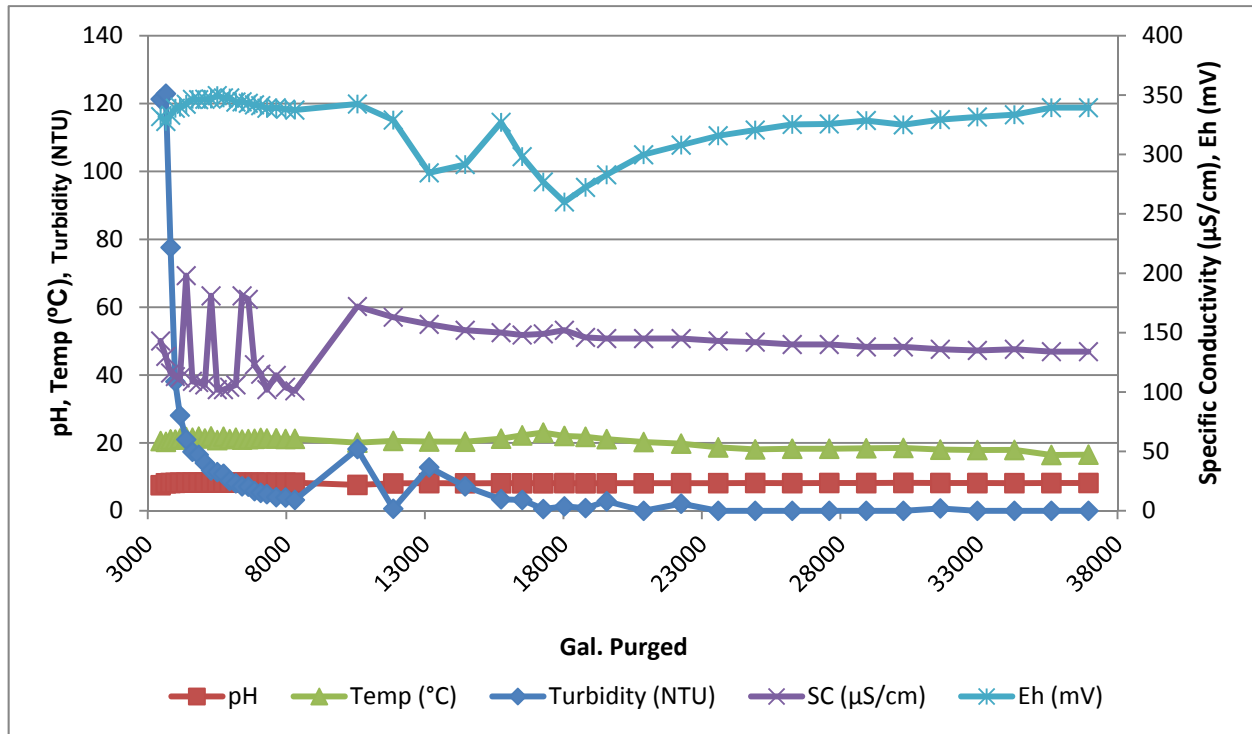


Figure B-2.3-1 Field parameters vs. volume purged during R-61 lower screen well development and aquifer testing

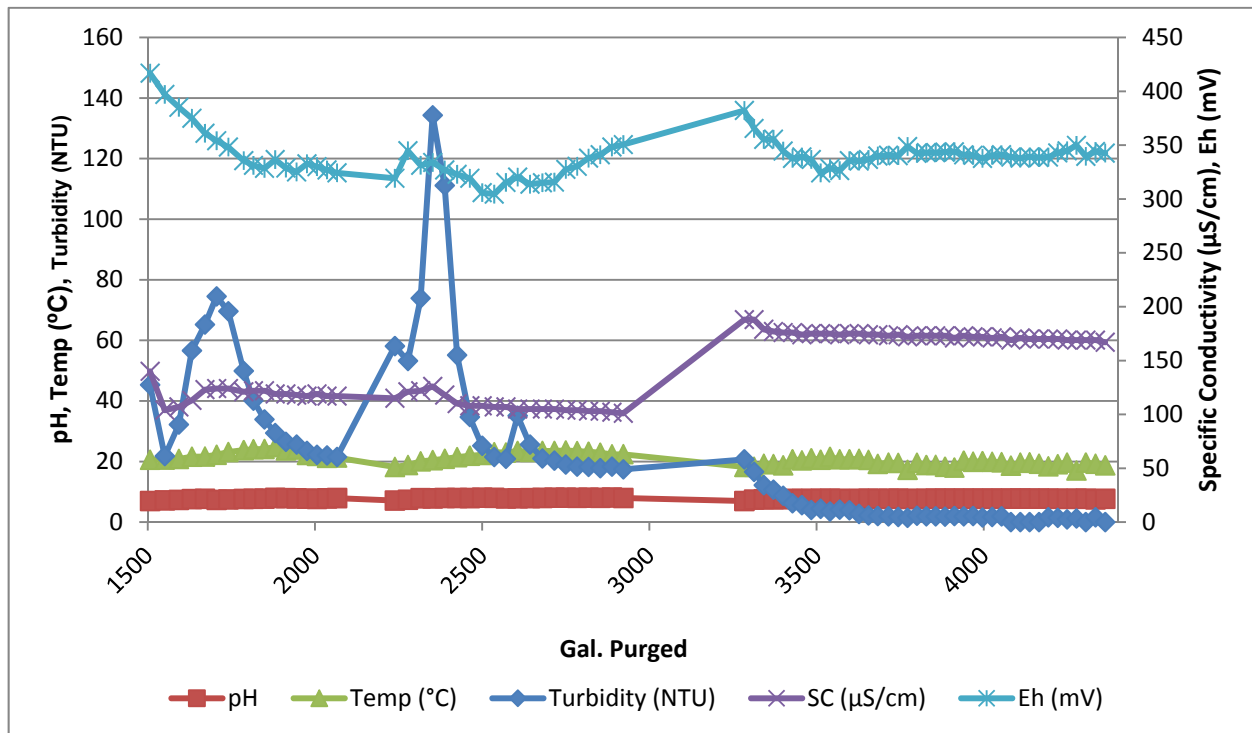


Figure B-2.3-2 Field parameters vs. volume purged during R-61 upper screen well development and aquifer testing



**Table B-1.0-1**  
**Summary of Groundwater Screening Samples Collected**  
**during Well Development and Aquifer Testing at Well R-61**

Location ID	Sample ID	Date and Time Collected	Collection Depth (ft bgs)	Sample Type	Analysis
<b>Well Development Lower Screen</b>					
R-61	GW61-11-5733	5/12/11; 1740 h	1215.9	Groundwater, pumped	TOC
<b>Aquifer Testing Upper Screen</b>					
R-61	GW61-11-5734	5/19/11; 1210 h	1125.9	Groundwater, pumped	TOC
R-61	GW61-11-5735	5/19/11; 1610 h	1125.9	Groundwater, pumped	TOC
R-61	GW61-11-5736	5/19/11; 2010 h	1125.9	Groundwater, pumped	TOC
R-61	GW61-11-5737	5/20/11; 0000 h	1125.9	Groundwater, pumped	TOC
R-61	GW61-11-5738	5/20/11; 0400 h	1125.9	Groundwater, pumped	TOC
R-61	GW61-11-5739	5/20/11; 0800 h	1125.9	Groundwater, pumped	TOC
<b>Aquifer Testing Lower Screen</b>					
R-61	GW61-11-5740	5/23/11; 1200 h	1184.2	Groundwater, pumped	TOC
R-61	GW61-11-5741	5/23/11; 1600 h	1184.2	Groundwater, pumped	TOC
R-61	GW61-11-5742	5/23/11; 2000 h	1184.2	Groundwater, pumped	TOC
R-61	GW61-11-5743	5/24/11; 0000 h	1184.2	Groundwater, pumped	TOC
R-61	GW61-11-5744	5/24/11; 0400 h	1184.2	Groundwater, pumped	TOC
R-61	CAMO-11-13848	5/24/11; 0630 h	1184.2	Groundwater, pumped	Dissolved gas content
R-61	GW61-11-5745	5/24/11; 0730 h	1184.2	Groundwater, pumped	TOC

**Table B-2.1-1**  
**TOC Results**

Sample ID	EPA* Method	TOC Concentration (mgC/L)
<b>Upper Screen</b>		
GW61-11-5734	415.1	2.8
GW61-11-5735	415.1	1.0
GW61-11-5736	415.1	0.6
GW61-11-5737	415.1	0.6
GW61-11-5738	415.1	0.4
GW61-11-5739	415.1	0.4
<b>Lower Screen</b>		
GW61-11-5733	415.1	0.2
GW61-11-5740	415.1	0.3
GW61-11-5741	415.1	0.4
GW61-11-5742	415.1	0.3
GW61-11-5743	415.1	0.4
GW61-11-5744	415.1	0.3
GW61-11-5745	415.1	0.3

\*EPA = U.S. Environmental Protection Agency.



**Table B-2.3-1**  
**Purge Volumes and Field Parameters**  
**during Well Development and Aquifer Testing at R-61**

Date	pH	Temp (°C)	DO (mg/L)	ORP (mV)	Eh (mV)	Specific Conductivity (μS/cm)	Turbidity (NTU)	Purge Volume between Samples (gal.)	Cumulative Purge Volume (gal.)
Well Development Composite Water from Both Screens									
5/4/11	n/r*; bailing							325	325
5/5/11	n/r; bailing							750	1075
Well Development Lower Screen									
5/11/11	n/r, pumping while swabbing screen							1430	1430
5/12/11	n/r, pumping sump							1986	3416
	7.53	20.56	7.55	128.0	331.9	143	121.3	48	3464
	8.10	20.32	7.80	123.9	327.8	130	122.9	189	3653
	8.21	21.06	8.07	129.1	333.0	116	77.6	171	3824
	8.25	20.98	8.11	135.0	338.9	113	38.1	170	3994
	8.28	21.29	8.08	136.0	339.9	112	28.1	170	4164
	8.30	21.74	8.06	138.4	342.3	198	21.0	224	4388
	8.31	21.52	8.16	142.5	346.4	109	17.4	224	4612
	8.30	21.86	8.00	142.3	346.2	108	16.5	224	4836
	8.31	21.32	8.06	142.6	346.5	106	14.1	224	5060
	8.36	21.92	7.78	142.8	346.7	181	11.9	224	5284
	8.32	20.82	8.23	145.7	349.6	102	11.4	224	5508
	8.33	21.84	8.06	143.8	347.7	102	10.9	224	5732
	8.30	21.13	8.37	143.7	347.6	104	8.8	224	5956
	8.29	21.55	8.23	140.2	344.1	106	8.1	224	6180
	8.28	20.97	8.32	140.5	344.4	181	7.2	224	6404
	8.28	21.11	8.18	139.2	343.1	178	7.1	224	6628
	8.28	21.21	8.30	137.9	341.8	123	5.8	224	6852
	8.28	21.48	8.11	137.2	341.1	115	5.3	224	7076
	8.29	21.32	8.28	135.0	338.9	102	4.9	224	7300
5/12/11	8.27	21.36	8.19	135.4	339.3	114	4.0	336	7636
	8.27	21.16	8.28	134.2	338.1	104	3.9	336	7972
	8.28	21.22	8.14	133.5	337.4	101	3.2	336	8308
Well Development Upper Screen									
5/13/11	n/r, pumping while swabbing screen							1320	1320
5/14/11	6.95	20.58	6.51	212.9	416.8	140	45.3	187	1507
	7.18	20.65	6.48	193.2	397.1	104	21.8	44	1551
	7.32	20.86	6.18	181.2	385.1	107	32.2	42	1593
	7.58	21.57	5.24	171.0	374.9	113	56.6	39	1632
	7.70	21.62	4.70	157.1	361.0	123	65.2	39	1671

Table B-2.3-1 (continued)

Date	pH	Temp (°C)	DO (mg/L)	ORP (mV)	Eh (mV)	Specific Conductivity (μS/cm)	Turbidity (NTU)	Purge Volume between Samples (gal.)	Cumulative Purge Volume (gal.)
<b>Well Development Upper Screen</b>									
05/14/11	7.34	22.22	4.90	150.2	354.1	124	74.5	35	1706
	7.47	23.12	4.01	149.7	348.2	124	69.6	35	1741
	7.63	23.75	4.32	137.1	335.6	121	49.9	46	1787
	7.69	24.05	3.86	132.7	331.2	122	40.1	29	1816
	7.74	24.12	3.76	129.9	328.4	122	33.9	33	1849
	7.98	24.78	3.99	138.1	336.6	119	29.4	32	1881
	7.91	23.67	4.24	130.2	328.7	119	26.5	32	1913
	7.82	23.94	3.85	126.6	325.1	118	25.6	32	1945
	7.74	22.17	3.98	128.8	332.7	117	23.5	31	1976
	7.66	21.87	3.60	126.1	330.0	119	22.2	30	2006
	7.82	21.24	3.64	123.1	327.0	117	22.0	30	2036
	7.93	21.30	3.36	120.4	324.3	117	21.5	30	2066
05/15/11	7.11	18.19	3.23	115.3	319.2	115	58.1	173	2239
	7.37	18.82	3.64	140.9	344.8	121	53.2	39	2278
	7.88	20.04	3.11	127.4	331.3	122	73.9	38	2316
	7.82	20.45	3.61	130.0	333.9	126	134.3	36	2352
	7.97	20.89	3.55	123.1	327.0	118	111.1	36	2388
	7.94	21.42	3.90	119.0	322.9	110	55.1	37	2425
	7.93	21.90	3.91	115.3	319.2	108	34.7	38	2463
	8.05	22.17	3.33	102.0	305.9	108	25.2	37	2500
	7.99	23.08	3.54	106.0	304.5	107	21.5	36	2536
	7.81	22.96	3.60	116.9	315.4	107	20.9	35	2571
	7.86	23.49	3.89	121.8	320.3	105	35.1	35	2606
	7.91	23.16	4.52	115.2	313.7	105	25.6	37	2643
	7.98	23.50	4.48	116.6	315.1	105	21.0	37	2680
	8.04	23.50	5.02	117.1	315.6	105	20.3	36	2716
	8.04	23.65	5.09	129.0	327.5	104	19.0	34	2750
	8.03	23.45	5.14	131.8	330.3	104	18.3	34	2784
	8.05	23.22	5.29	139.4	337.9	103	18.2	34	2818
	7.99	22.89	4.71	142.6	341.1	103	17.8	35	2853
	8.11	22.35	4.78	144.4	348.3	102	18.3	35	2888
	7.94	22.41	4.23	146.6	350.5	101	17.4	34	2922

Table B-2.3-1 (continued)

Date	pH	Temp (°C)	DO (mg/L)	ORP (mV)	Eh (mV)	Specific Conductivity (µS/cm)	Turbidity (NTU)	Purge Volume between Samples (gal.)	Cumulative Purge Volume (gal.)
<b>Aquifer Pump Test Upper Screen</b>									
05/17/11	n/r, pumping, mini-tests							89	89
05/19/11 to 05/20/11	6.96	18.22	1.33	178.3	382.2	188	20.7	273	362
	7.42	18.26	1.27	161.6	365.5	188	16.6	29	391
	7.53	19.25	1.71	151.4	355.3	179	12.2	29	420
	7.56	19.13	1.88	151.6	355.5	177	10.7	29	449
	7.59	18.73	2.48	140.6	344.5	176	8.7	29	478
	7.63	20.74	2.68	133.8	337.7	176	6.2	28	506
	7.64	20.36	2.97	135.1	339.0	174	5.6	28	534
	7.65	21.05	2.97	132.8	336.7	175	4.0	28	562
	7.67	20.59	3.33	120.3	324.2	175	4.4	28	590
	7.70	21.53	3.66	124.5	328.4	175	3.5	28	618
	7.69	20.73	3.80	122.5	326.4	174	4.1	29	647
	7.54	20.75	3.79	131.7	335.6	175	3.9	29	676
	7.70	20.88	4.00	131.3	335.2	175	2.7	29	705
	7.69	20.51	4.01	132.8	336.7	174	2.2	28	733
	7.68	19.20	4.33	136.0	339.9	174	2.0	28	761
	7.70	19.62	4.54	136.8	340.7	173	1.9	32	793
	7.73	19.53	4.33	136.3	340.2	174	1.7	29	822
	7.66	17.27	4.87	144.8	348.7	172	1.4	28	850
	7.64	19.58	4.64	138.5	342.4	173	2.1	28	878
	7.69	18.84	4.66	139.1	343.0	173	1.9	28	906
	7.73	18.87	4.83	139.1	343.0	173	1.9	28	934
	7.74	18.25	4.93	139.6	343.5	173	1.8	28	962
	7.75	18.01	5.03	139.9	343.8	171	2.0	28	990
	7.74	20.28	4.91	137.1	341.0	173	1.9	28	1018
	7.72	19.92	5.0	136.7	340.6	172	2.0	28	1046
	7.75	20.10	4.98	133.8	337.7	172	1.5	28	1074
	7.72	19.88	5.09	136.6	340.5	171	1.7	29	1103
	7.73	19.76	5.02	137.2	341.1	172	1.9	28	1131
	7.75	18.64	5.36	135.0	338.9	169	0	28	1159
	7.77	19.60	5.40	134.0	337.9	171	0	28	1187
	7.74	19.72	5.42	135.2	339.1	170	0	28	1215

Table B-2.3-1 (continued)

Date	pH	Temp (°C)	DO (mg/L)	ORP (mV)	Eh (mV)	Specific Conductivity (μS/cm)	Turbidity (NTU)	Purge Volume between Samples (gal.)	Cumulative Purge Volume (gal.)	
Aquifer Pump Test Upper Screen										
05/19/11 to 05/20/11	7.75	19.27	5.64	134.6	338.5	170	0	28	1243	
	7.75	18.40	5.42	135.0	338.9	170	1.6	28	1271	
	7.71	19.10	5.53	138.9	342.8	170	1.4	28	1299	
	7.70	19.64	5.74	140.8	344.7	169	0.9	28	1327	
	7.71	17.03	5.76	140.9	349.8	169	1.2	28	1355	
	7.74	19.65	5.52	135.7	339.6	169	0	28	1383	
	7.47	19.25	5.85	140.2	344.1	169	1.6	29	1412	
	7.67	18.75	5.30	138.7	342.6	167	0	29	1441	
05/21/11	n/r, pumping							490	1931	
Aquifer Pump Test Lower Screen										
05/22/11	n/r, pumping, mini-tests							963	963	
05/23/11 to 05/24/11	7.61	20.07	6.64	138.6	342.5	172	18.2	1294	2257	
	8.07	20.60	8.50	125.1	329.0	163	0.6	1294	3551	
	8.16	20.40	7.14	80.7	284.6	157	12.8	1297	4848	
	8.11	20.36	7.18	87.6	291.5	152	7.2	1298	6146	
	8.12	21.27	6.29	123.2	327.1	150	3.4	1298	7444	
	8.12	22.22	6.60	94.3	298.2	148	3.2	760	8204	
	8.12	23.04	6.72	78.4	276.9	149	0.5	761	8965	
	8.13	22.06	6.91	56.1	260.0	152	1.3	762	9727	
	8.11	21.80	6.94	68.4	272.3	146	0.8	763	10,490	
	8.12	21.11	6.98	79.0	282.9	145	2.8	763	11,253	
	8.12	20.25	7.63	95.9	299.8	145	0	1334	12,587	
	8.13	19.80	7.27	104.0	307.9	145	2.1	1355	13,942	
	8.16	18.69	7.60	111.9	315.8	143	0	1336	15,278	
	8.19	18.10	7.69	116.7	320.6	142	0	1336	16,614	
	8.15	18.30	7.41	121.4	325.3	140	0	1336	17,950	
	8.19	18.29	7.50	121.8	325.7	140	0	1337	19,287	
	8.17	18.42	7.61	124.7	328.6	138	0	1336	20,623	
	8.22	18.51	7.40	121.1	325.0	138	0	1336	21,959	
	8.19	18.03	7.66	125.5	329.4	136	0.7	1336	23,295	
	8.17	17.89	7.59	127.7	331.6	135	0	1336	24,631	
	8.13	17.93	7.67	129.6	333.5	136	0	1336	25,967	
	8.17	16.45	7.53	130.5	339.4	134	0	1336	27,303	
	8.19	16.55	7.66	130.5	339.4	134	0	1337	28,640	
	nr, aquifer pump test								1299	29,939

Note: Eh values were derived from ORP concentrations using the following temperature-based correction factors: 208.9 mV at 15°C, 203.9 mV at 20°C, and 198.5 mV at 25°C.

\*n/r = Not recorded.



## **Appendix C**

---

### *Aquifer Testing Report*

## **C-1.0 INTRODUCTION**

This appendix describes the hydraulic analysis of pumping tests conducted during May 2011 at R-61, a dual-screen regional aquifer well located on the mesa above Mortandad Canyon. The tests on R-61 were conducted to quantify the hydraulic properties of the two zones in which the well is screened, evaluate the hydraulic interconnection of the zones, and check for interference effects at neighboring wells.

Testing conducted on each screened interval consisted of brief trial pumping, background water level data collection, and a 24-h pumping test. Water levels were monitored in both zones during each of the pumping tests in each screen as well as at nearby regional wells R-15 (2020 ft away), R-42 (1508 ft away), R-43 screens 1 and 2 (2289 ft away), and R-50 screens 1 and 2 (1560 ft away).

As in most of the R-well pumping tests conducted on the Pajarito Plateau, an inflatable packer system was used in R-61 both to hydraulically isolate the screened zones and to try to eliminate casing storage effects on the test data. The implementation of the inflatable packer system was only partially successful in limiting storage effects on the tests. Screen 1 was apparently partially dewatered during well development—difficult to avoid because of the low yield of the screen 1 interval. This would have allowed air to enter the filter pack adjacent to the blank casing just above the well screen. The trapped air could then have expanded and contracted in response to pumping and recovery, causing a storage-like effect at screen 1. Also, both screened zones produced aerated water, indicative of substantial amounts of air trapped in the formation pore spaces around the screens. Again, expansion and contraction of this air, and possibly release of additional air from solution in response to pressure reduction via pumping, likely contributed to storage effects in the test data from both screens. It is estimated that the observed duration of apparent storage effects in each screened zone was an order of magnitude shorter than what would have occurred without an inflatable packer system.

### **Conceptual Hydrogeology**

The static water level measured in the open well on May 16 was 1100.95 ft below ground surface (bgs). Drilling logs showed continuous granular media from above the static water level to the maximum depth penetrated by the borehole at 1265 ft bgs. The Puye Formation extends from well above the water table to 1155 ft bgs, with Miocene pumiceous sediments from that depth to the bottom of the borehole.

Screen 1 is 10 ft long, extending from 1125 to 1135 ft bgs within the Puye Formation. Screen 2 is 20.6 ft long and is positioned over 85 ft beneath screen 1, extending from 1220.4 to 1241 ft bgs within the pumiceous sediments.

When the screened zones were isolated using an inflatable packer, there was no consistent, discernable change in the water level in either zone. There were, however, tiny, irregular changes in measured pressure that were not consistent or repeatable from deflation to inflation or from one inflation/deflation cycle to another. These perturbations are attributed to slight vertical movements of the pumping string and transducers associated with compression and relaxation of the drop pipe that occurred when the packers were inflated or deflated. The static water level appeared to be 1100.95 ft bgs for both screened zones.

### **R-61 Screen 1 Testing**

Screen 1 was tested from May 16 to 21, 2011. After running the pump and filling the drop pipe on May 16, testing began with brief trial pumping on May 17, followed by background data collection and a 24-h

constant-rate pumping test that was started on May 19. Following shutdown of the 24-h test on May 20, recovery data were recorded for 24 h until May 21.

Trial testing of screen 1 began at 10:00 a.m. on May 17 at a discharge rate of 1.02 gallons per minute (gpm) and continued for 30 min until 10:30 a.m. Recovery data were recorded for 30 min until 11:00 a.m. when trial 2 pumping began at a discharge rate of 0.98 gpm. Following shutdown at 12:00 a.m., trial 2 recovery and background data were collected for 2640 min until 8:00 a.m. on May 19.

At 8:00 a.m. on May 19, the 24-h pumping test was initiated at a discharge rate of 0.95 gpm. Pumping continued for 1440 min until 8:00 a.m. on May 20. Following shutdown, recovery data were recorded for 1440 min until 8:00 a.m. on May 21.

## **R-61 Screen 2 Testing**

Screen 2 was tested from May 21 to 26. After filling the drop pipe and confirming the yield capability of screen 2 on May 21, testing began with brief trial pumping on May 22, a 24-h pumping test that began on May 23, and recovery/background data collection until May 26.

Two trial tests were conducted on May 22. Trial 1 was conducted at a discharge rate of 21.8 gpm, starting at 10:00 a.m. and continuing for 30 min, followed by 30 min of recovery until 11:00 a.m. Trial 2 was conducted for 60 min from 11:00 a.m. to 12:00 p.m. at a rate of 21.7 gpm. Following shutdown, recovery data were recorded for 1200 min until 8:00 a.m. on May 23.

At 8:00 a.m. on May 23, the 24-h pumping test began. At Los Alamos National Laboratory's request, as an experiment, a variable-rate test was conducted. To minimize the complexity of the data set, the pumping rate variation was limited to three steps. Initially, the pump was operated at its maximum rate of 21.6 gpm for 5 h. Then the rate was cut back to 12.7 gpm for 5 h. Finally, the valve was opened again, producing 22.3 gpm for the remainder of the test period—an additional 14 h. Pumping was conducted for 1440 min until 8:00 a.m. on May 24. Following shutdown, recovery/background measurements were recorded for 2880 min until 8:00 a.m. on May 26 when the pump was tripped out of the well.

## **Aerated Water**

Consistent with observations in many of the recent R-well pumping tests, air was observed in the groundwater pumped from both screens during the R-61 pumping tests. Based upon the results of the dissolved gas analysis conducted on water from the lower screen, it appears that high-pressure compressed air used in the drilling process invaded the aquifer zones during drilling, collecting in the formation pore spaces and/or dissolving into the groundwater. When water is pumped from the aquifer, trapped air in the formation pores can move with the pumped water as well as expand and contract in response to pressure changes. Also, pressure reduction associated with pumping can allow dissolved gas or air to come out of solution. The air present in the formations in recently tested wells has had several effects, including (1) interfering with pump operating efficiency, (2) causing transient changes in aquifer permeability, (3) inducing pressure transients as the gas or air expands and contracts, and (4) causing storage-like effects associated with changes in air volume in the formation voids, filter pack, and/or well casing.

As stated above, the trapped air in the formation pores contributed to storage-like effects in the early pumping and recovery data. Also, varying air content affected the well efficiency in each zone. During the 24-h test on screen 1, gradual accumulation of air in the formation pores degraded the permeability of the sediments near the well and annulus, eventually nearly doubling the drawdown in the well. The opposite effect was observed at screen 2. The air content in the pumped water declined steadily throughout the



24-h pumping test. Over that last half of the test, the pumping water level rose gradually as the air content in the formation pores evidently declined somewhat over time, increasing the permeability of the sediments correspondingly.

### **Drop Pipe Leakage**

The data sets from the aquifer tests show that water leaked from the drop pipe during testing. There are two possible sources of this. First, it is possible that some leakage occurred through the threaded coupling joints in the stainless-steel drop pipe. Such leakage has been observed occasionally in previous tests. Repeated use of the drop pipe in numerous tests likely wears the threads, increasing the susceptibility to leakage.

A second possible source of leakage is in the crossover assemblies on the inflatable packer where the pump wires pass from outside the drop pipe to inside. The pump-wire pass-through setup on the packer was rebuilt just before the R-61 pumping tests and was not pressure tested to verify water tightness. The O-ring seals where the pump wires pass into the drop pipe are often subjected to water pressures in excess of 700 psi and, therefore, are potential leakage sources.

## **C-2.0 BACKGROUND DATA**

The background water level data collected before the pumping tests help distinguish the naturally occurring water level fluctuations from those caused by the pumping test.

Background water level fluctuations have several causes, among them barometric pressure changes, operation of other wells in the aquifer, Earth tides, and long-term trends related to weather patterns. The background data hydrographs from the monitored wells were compared with barometric pressure data from the area to determine if a correlation existed.

Previous pumping tests on the Pajarito Plateau have demonstrated a barometric efficiency for most wells of between 90% and 100%. Barometric efficiency is defined as the ratio of water level change divided by barometric pressure change, expressed as a percentage. In the initial pumping tests conducted on the early R-wells, downhole pressure was monitored using a vented pressure transducer. This equipment measures the difference between the total pressure applied to the transducer and the barometric pressure, with this difference being the true height of water above the transducer.

Subsequent pumping tests, including those at R-61, have utilized nonvented transducers. These devices simply record the total pressure on the transducer, that is, the sum of the water height plus the barometric pressure. This results in an attenuated "apparent" hydrograph in a barometrically efficient well. For example, when monitoring a 90% barometrically efficient well with a vented transducer, an increase in barometric pressure of 1 unit causes a decrease in recorded downhole pressure of 0.9 unit because the water level is forced downward 0.9 unit by the barometric pressure change. However, with a nonvented transducer, the total measured pressure increases by 0.1 unit (the combination of the barometric pressure increase and the water level decrease). Thus, the resulting apparent hydrograph changes by a factor of 100 minus the barometric efficiency and in the same direction as the barometric pressure change, rather than in the opposite direction.

Barometric pressure data were obtained from Technical Area 54 (TA-54) tower site from the Waste and Environmental Services Division–Environmental Data and Analysis (WES-EDA) Group. The TA-54 measurement location is at an elevation of 6548 ft above mean sea level (amsl), whereas the wellhead elevation is at approximately 6940 ft amsl. The static water level in R-61 at the time of the aquifer tests was 1100.95 ft bgs, making the estimated water table elevation 6839.05 ft amsl. Therefore, the measured

barometric pressure data from TA-54 had to be adjusted to reflect the pressure at the elevation of the water table within R-61.

The following formula was used to adjust the measured barometric pressure data:

$$P_{WT} = P_{TA54} \exp \left[ -\frac{g}{3.281R} \left( \frac{E_{R-61} - E_{TA54}}{T_{TA54}} + \frac{E_{WT} - E_{R-61}}{T_{WELL}} \right) \right] \quad \text{Equation C-1}$$

where  $P_{WT}$  = barometric pressure at the water table inside R-61

$P_{TA54}$  = barometric pressure measured at TA-54

$g$  = acceleration of gravity, in m/sec<sup>2</sup> (9.80665 m/sec<sup>2</sup>)

$R$  = gas constant, in J/kg/degrees kelvin (287.04 J/kg/degrees kelvin)

$E_{R-61}$  = land surface elevation at R-61 site, in feet (estimated at 6940 ft)

$E_{TA54}$  = elevation of barometric pressure measuring point at TA-54, in feet (6548 ft)

$E_{WT}$  = elevation of the water level in R-61, in feet (estimated at 6839.05 ft)

$T_{TA54}$  = air temperature near TA-54, in degrees kelvin (assigned a value of 52.7°F or 284.7 K)

$T_{WELL}$  = air temperature inside R-61, in degrees kelvin (assigned a value of 66.8°F or 292.5 K)

This formula is an adaptation of an equation WES-EDA provided. It can be derived from the ideal gas law and standard physics principles. An inherent assumption in the derivation of the equation is that the air temperature between TA-54 and the well is temporally and spatially constant, and that the temperature of the air column in the well is similarly constant.

The corrected barometric pressure data reflecting pressure conditions at the water table were compared with the water level hydrograph to discern the correlation between the two and determine whether water level corrections would be needed before data analysis.

### C-3.0 IMPORTANCE OF EARLY DATA

When pumping or recovery first begins, the vertical extent of the cone of depression is limited to approximately the well screen length, the filter pack length, or the aquifer thickness in relatively thin permeable strata. For many pumping tests on the plateau, the early pumping period is the only time that the effective height of the cone of depression is known with certainty because, soon after startup, the cone of depression expands vertically through permeable materials above and/or below the screened interval. Thus, the early data often offer the best opportunity to obtain hydraulic conductivity information because conductivity would equal the earliest-time transmissivity divided by the well screen length.

Unfortunately, in many pumping tests, casing-storage effects dominate the early-time data, potentially hindering the effort to determine the transmissivity of the screened interval. The duration of casing-storage effects can be estimated using the following equation (Schafer 1978, 098240).

$$t_c = \frac{0.6(D^2 - d^2)}{\frac{Q}{s}} \quad \text{Equation C-2}$$

where  $t_c$  = duration of casing-storage effect, in minutes

$D$  = inside diameter of well casing, in inches

$d$  = outside diameter of column pipe, in inches

$Q$  = discharge rate, in gallons per minute

$s$  = drawdown observed in pumped well at time  $t_c$ , in feet

The calculated casing-storage time is quite conservative. Often, the data show that significant effects of casing storage have dissipated after about half the computed time.

For wells screened across the water table, there can be an additional storage contribution from the filter pack around the screen. The following equation provides an estimate of the storage duration accounting for both casing and filter pack storage.

$$t_c = \frac{0.6[(D^2 - d^2) + S_y(D_B^2 - D_C^2)]}{\frac{Q}{s}} \quad \text{Equation C-3}$$

where  $S_y$  = short term specific yield of filter media (typically 0.2)

$D_B$  = diameter of borehole, in inches

$D_C$  = outside diameter of well casing, in inches

This equation was derived from Equation C-2 on a proportional basis by increasing the computed time in direct proportion to the additional volume of water expected to drain from the filter pack. (To prove this, note that the left-hand term within the brackets is directly proportional to the annular area [and volume] between the casing and drop pipe while the right-hand term is proportional to the area [and volume] between the borehole and the casing, which is corrected for the drainable porosity of the filter pack. Thus, the summed term within the brackets accounts for all of the volume [casing water and drained filter pack water] appropriately.)

In some instances, it is possible to eliminate casing-storage effects by setting an inflatable packer above the tested screened interval before conducting the test. As described earlier, this approach was only partially successful in the R-61 pumping test effort.

#### C-4.0 TIME-DRAWDOWN METHODS

Time-drawdown data can be analyzed using a variety of methods, one of which is the Theis method (1934-1935, 098241). The Theis equation describes drawdown around a well as follows:

$$s = \frac{114.6Q}{T} W(u) \quad \text{Equation C-4}$$

where

$$W(u) = \int_u^{\infty} \frac{e^{-x}}{x} dx \quad \text{Equation C-5}$$

and

$$u = \frac{1.87r^2S}{Tt}$$

**Equation C-6**

where  $s$  = drawdown, in feet

$Q$  = discharge rate, in gallons per minute

$T$  = transmissivity, in gallons per day per foot

$S$  = storage coefficient (dimensionless)

$t$  = pumping time, in days

$r$  = distance from center of pumpage, in feet

To use the Theis method of analysis, the time-drawdown data are plotted on log-log graph paper. Then, Theis curve matching is performed using the Theis type curve—a plot of the Theis well function  $W(u)$  versus  $1/u$ . Curve matching is accomplished by overlaying the type curve on the data plot and, while keeping the coordinate axes of the two plots parallel, shifting the data plot to align with the type curve, effecting a matched position. An arbitrary point, referred to as the match point, is selected from the overlapping parts of the plots. Match-point coordinates are recorded from the two graphs, yielding four values:  $W(u)$ ,  $1/u$ ,  $s$ , and  $t$ . Using these match-point values, transmissivity and storage coefficient are computed as follows:

$$T = \frac{114.6Q}{s} W(u)$$

**Equation C-7**

$$S = \frac{Tut}{2693r^2}$$

**Equation C-8**

where  $T$  = transmissivity, in gallons per day per foot

$S$  = storage coefficient (dimensionless)

$Q$  = discharge rate, in gallons per minute

$W(u)$  = match-point value

$s$  = match-point value, in feet

$u$  = match-point value

$t$  = match-point value, in minutes

$r$  = distance from center of pumpage, in feet

An alternative solution method applicable to time-drawdown data is the Cooper-Jacob method (1946, 098236), a simplification of the Theis equation that is mathematically equivalent to the Theis equation for most pumped well data. The Cooper-Jacob equation describes drawdown around a pumping well as follows:

$$s = \frac{264Q}{T} \log \frac{0.3Tt}{r^2S}$$

**Equation C-9**

The Cooper-Jacob equation is a simplified approximation of the Theis equation and is valid whenever the  $u$  value is less than about 0.05. For small radius values (e.g., corresponding to borehole radii),  $u$  is less than 0.05 at very early pumping times and therefore is less than 0.05 for most or all measured drawdown values. Thus, for the pumped well, the Cooper-Jacob equation usually can be considered a valid approximation of the Theis equation. An exception occurs when the transmissivity of the aquifer is very low. In that case, some of the early pumped well drawdown data may not be well approximated by the Cooper-Jacob equation.

According to the Cooper-Jacob method, the time-drawdown data are plotted on a semilog graph, with time plotted on the logarithmic scale. Then a straight line of best fit is constructed through the data points and transmissivity is calculated using the following:

$$T = \frac{264Q}{\Delta s} \quad \text{Equation C-10}$$

where  $T$  = transmissivity, in gallons per day per foot

$Q$  = discharge rate, in gallons per minute

$\Delta s$  = change in head over one log cycle of the graph, in feet

Because many of the test wells completed on the plateau are severely partially penetrating, an alternate solution considered for assessing aquifer conditions is the Hantush equation for partially penetrating wells (Hantush 1961, 098237; Hantush 1961, 106003). The Hantush equation is as follows:

**Equation C-11**

$$s = \frac{Q}{4\pi T} \left[ W(u) + \frac{2b^2}{\pi^2(l-d)(l'-d')} \sum_{n=1}^{\infty} \frac{1}{n^2} \left( \sin \frac{n\pi l}{b} - \sin \frac{n\pi d}{b} \right) \left( \sin \frac{n\pi l'}{b} - \sin \frac{n\pi d'}{b} \right) W \left( u, \sqrt{\frac{K_z}{K_r}} \frac{n\pi r}{b} \right) \right]$$

where, in consistent units,  $s$ ,  $Q$ ,  $T$ ,  $t$ ,  $r$ ,  $S$ , and  $u$  are as previously defined and

$b$  = aquifer thickness

$d$  = distance from top of aquifer to top of well screen in pumped well

$l$  = distance from top of aquifer to bottom of well screen in pumped well

$d'$  = distance from top of aquifer to top of well screen in observation well

$l'$  = distance from top of aquifer to bottom of well screen in observation well

$K_z$  = vertical hydraulic conductivity

$K_r$  = horizontal hydraulic conductivity

In this equation,  $W(u)$  is the Theis well function, and  $W(u, \beta)$  is the Hantush well function for leaky aquifers where

$$\beta = \sqrt{\frac{K_z}{K_r}} \frac{n\pi r}{b} \quad \text{Equation C-12}$$

Note that for single-well tests,  $d = d'$  and  $l = l'$ .

### C-5.0 RECOVERY METHODS

Recovery data were analyzed using the Theis recovery method. This is a semilog analysis method similar to the Cooper-Jacob procedure.

In this method, residual drawdown is plotted on a semilog graph versus the ratio  $t/t'$ , where  $t$  is the time since pumping began, and  $t'$  is the time since pumping stopped. A straight line of best fit is constructed through the data points, and  $T$  is calculated from the slope of the line as follows:

$$T = \frac{264Q}{\Delta s} \quad \text{Equation C-13}$$

The recovery data are particularly useful when compared with time-drawdown data. Because the pump is not running, spurious data responses associated with dynamic discharge rate fluctuations are eliminated. The result is that the data set is generally "smoother" and easier to analyze.

Recovery data also can be analyzed using the Hantush equation for partial penetration. This approach is generally applied to the early data in a plot of recovery versus recovery time.

### C-6.0 SPECIFIC CAPACITY METHOD

The specific capacity of the pumped well can be used to obtain a lower-bound value of hydraulic conductivity. The hydraulic conductivity is computed using formulas that are based on the assumption that the pumped well is 100% efficient. The resulting hydraulic conductivity is the value required to sustain the observed specific capacity. If the actual well is less than 100% efficient, it follows that the actual hydraulic conductivity would have to be greater than calculated to compensate for well inefficiency. Thus, because the efficiency is unknown, the computed hydraulic conductivity value represents a lower bound. The actual conductivity is known to be greater than or equal to the computed value.

For fully penetrating wells, the Cooper-Jacob equation can be iterated to solve for the lower-bound hydraulic conductivity. However, the Cooper-Jacob equation (assuming full penetration) ignores the contribution to well yield from permeable sediments above and below the screened interval. To account for this contribution, it is necessary to use a computation algorithm that includes the effects of partial penetration. One such approach was introduced by Brons and Marting (1961, 098235) and augmented by Bradbury and Rothschild (1985, 098234).

Brons and Marting introduced a dimensionless drawdown correction factor,  $s_p$ , approximated by Bradbury and Rothschild as follows:

$$s_p = \frac{1 - \frac{L}{b}}{\frac{L}{b}} \left[ \ln \frac{b}{r_w} - 2.948 + 7.363 \frac{L}{b} - 11.447 \left( \frac{L}{b} \right)^2 + 4.675 \left( \frac{L}{b} \right)^3 \right] \quad \text{Equation C-14}$$

In this equation,  $L$  is the well screen length, in ft. Incorporating the dimensionless drawdown parameter, the conductivity is obtained by iterating the following formula:

$$K = \frac{264Q}{sb} \left( \log \frac{0.3Tt}{r_w^2 S} + \frac{2s_p}{\ln 10} \right) \quad \text{Equation C-15}$$

The Brons and Marting procedure can be applied to both partially penetrating and fully penetrating wells.

To apply this procedure, a storage coefficient value must be assigned. Storage coefficient values generally range from  $10^{-5}$  to  $10^{-3}$  for confined aquifers and 0.01 to 0.25 for unconfined aquifers (Driscoll 1986, 104226). Unconfined conditions were assumed for screen 1, and a storage coefficient of 0.05 was arbitrarily assigned. Pumping screen 2 drew down water levels in screen 1 slightly, suggesting that some lowering of the phreatic surface also might have occurred during the screen 2 test. Therefore, a leaky-confined storage coefficient value of 0.003 (between the unconfined and confined ranges) was used for the calculations for screen 2. The calculation result is not particularly sensitive to the choice of storage coefficient value, so a rough estimate is generally adequate to support the calculations.

The analysis also requires assigning a value for the saturated aquifer thickness,  $b$ . For both screens, an arbitrary thickness of 200 ft was used in the calculations. For partially penetrating conditions, the calculations are not particularly sensitive to the choice of aquifer thickness because sediments far above or below the screen typically contribute little flow.

### C-7.0 BACKGROUND DATA ANALYSIS

Background aquifer pressure data collected during the R-61 tests were plotted along with barometric pressure to determine the barometric effect on water levels.

Figure C-7.0-1 shows aquifer pressure data from R-61 screen 1 during the test period along with barometric pressure data from TA-54 that have been corrected to equivalent barometric pressure in feet of water at the water table. The R-61 data are referred to in the figure as the “apparent hydrograph” because the measurements reflect the sum of water pressure and barometric pressure, as recorded using a nonvented pressure transducer. The times of the pumping periods for the R-61 pumping tests are included in the figure for reference. The minimal fluctuations in the hydrograph compared with those in the barometric pressure curve imply a high barometric efficiency for screen 1.

Portions of the apparent hydrograph measured during the screen 1 background data collection period on May 18 and 19 had a strikingly similar shape to the barometric pressure curve, although subdued significantly. The apparent hydrograph data were replotted on the expanded scale shown in Figure C-7.0-2 to align the data more closely with the barometric pressure curve. Although the shapes of the curves are similar, changes in the hydrograph *preceded* those in the barometric pressure record by a few hours, ostensibly impossible, although observed anecdotally in other wells on the plateau. It is possible that this could be explained by barometric pressure effects being transmitted through certain portions of the subsurface geology faster than through the atmosphere. Alternatively, it is possible that the sinusoidal fluctuations in the apparent hydrograph were Earth-tide effects rather than barometric pressure effects. The magnitude of the perturbations in the hydrograph (a couple hundredths of a foot) is consistent with Earth-tide effects observed at Los Alamos. Because both Earth tides and barometric pressure fluctuations are diurnal, the similar appearance of the two curves in Figure C-7.0-2 may have been coincidental.

The data in Figure C-7.0-1 show that pumping screen 2 caused water level changes at screen 1. Data from the screen 2 pumping period on May 23 and 24 are plotted on the expanded-scale graph in Figure C-7.0-3 to illustrate this more clearly.

As shown in the figure, initial pumping of screen 2 caused drawdown in screen 1, reaching about 0.16 ft after 5 h. During this period, the control valve in the discharge line was wide open, thus minimizing the hydraulic backpressure on the drop pipe. In this configuration, the maximum pressure in the lower reaches of the drop pipe was around 470 psi. It is not known if water was leaking from the drop pipe into

the screen 1 zone at this point. If leakage into screen 1 was occurring, the corresponding rise in water level associated with the injection into screen 1 was masked by drawdown induced by pumping screen 2. The net decline in the screen 1 water level observed during this period is evidence of this effect.

After 5 h of pumping, the discharge valve was partially closed to reduce the flow rate in accordance with the desired variable-rate test. This change imposed an additional backpressure on the drop pipe of 250 psi, raising the total internal pressure within the packer tubing (pump-wire pass-through assembly) and lower reaches of the drop pipe to more than 720 psi. This increase in pressure clearly caused water to leak from the drop pipe string into screen 1, raising its water level by about 0.5 ft.

After 5 h of operation in this configuration, the valve was opened again to increase the discharge rate to the maximum obtainable from the submersible pump. This should have restored the internal pressure within the lower portion of the drop pipe string to near 470 psi. However, the water levels in screen 1 remained elevated above the original static water level, indicating that the leakage into screen 1 was greater than it had been initially at the same hydraulic pressure. Thus, temporarily raising the backpressure to 720 psi either caused a leak (through coupling joints or the packer's crossover assembly) where there had been none or exacerbated a small existing leak. Over the balance of the pumping period, the screen 1 water levels continued to rise gradually, possibly indicating a steady worsening of the leak.

Once pumping stopped, the presence of the check valves in the drop pipe string would have suspended most of the overlying weight of water in the drop pipe, greatly reducing the internal pressure at the bottom of the drop pipe and, presumably, reducing or essentially eliminating the leakage. Absent leakage, the screen 1 water level showed residual effects of screen 2 pumping when it dropped below the original static level and gradually recovered over time.

Figure C-7.0-4 shows aquifer pressure data from R-61 screen 2 obtained during the test effort. The lack of correspondence between the barometric pressure curve and the apparent hydrograph implies a high barometric efficiency for screen 2. The low-amplitude, diurnal perturbations in the water level data are Earth-tide effects. The data do not show a discernable response in screen 2 to pumping screen 1. This is not surprising given the large separation distance between the screens and the low discharge rate from screen 1 (around 1 gpm).

Hydrograph data from additional nearby R-wells were downloaded to check for a possible pumping response to the R-61 tests. Screened zones examined included regional wells R-15 (2020 ft away), R-42 (1508 ft away), R-43 screens 1 and 2 (2289 ft away), and R-50 screens 1 and 2 (1560 ft away). None of the monitored zones showed any response to pumping either screen in R-61. The hydrographs for these wells are not included in this report.

## **C-8.0 WELL R-61 SCREEN 1 DATA ANALYSIS**

This section presents the data obtained from the R-61 screen 1 pumping tests and the results of the analytical interpretations. Data are presented for drawdown and recovery from trial 1, trial 2, and the 24-h constant-rate test.

### **C-8.1 Well R-61 Screen 1 Trial Test**

Figure C-8.1-1 shows a semilog plot of the drawdown data collected from the trial 1 test on screen 1. The earliest data show exaggerated drawdown likely caused by a brief period of a greater than expected discharge rate. This is probably an indication of antecedent drainage of a minor volume of drop pipe. This



would have allowed the pump to operate against reduced head momentarily on startup, thus producing a greater flow rate for a few seconds until the void caused by drainage had refilled.

Subsequent data show a storage effect of several minutes duration. As discussed above, this may have been caused by air trapped in the filter pack above the screen (that had entered during well development), air bubbles in the formation pores (either naturally occurring or placed there during drilling via the air compressor), or a combination of both.

The transmissivity estimated from the line of fit shown in Figure C-8.1-1 is 150 gallons per day (gpd)/ft. If the height of the cone of depression had been equal to the screen length of 10 ft at that time, the corresponding hydraulic conductivity would be 15 gpd/ft<sup>2</sup>, or 2.0 ft/d. Because several minutes passed after pumping began, it is likely that the cone of depression had already expanded vertically and that the computed transmissivity value reflects a greater thickness of sediment. This would make the actual hydraulic conductivity correspondingly less.

Figure C-8.1-2 shows the recovery data collected following shutdown of the trial 1 pumping test. The transmissivity computed from the line of fit shown on the plot is 200 gpd/ft.

The late recovery data are replotted on the graph shown in Figure C-8.1-3, revealing a steady, continuous slope change not seen in the drawdown data. Note that extrapolation of the line of fit predicted full recovery prematurely, i.e., well before a  $t/t'$  value of 1.0, possibly an indication of hysteretic effects. In unconfined aquifers, the early rate of recovery can be more rapid than that of drawdown because of a smaller effective storage coefficient during recovery. During pumping the capillary fringe above the water table increases in thickness, while during recovery it gets thinner (Bevan et al. 2005, 105186). If the rate of thinning during recovery exceeds the rate of growth during pumping, the effective storage coefficient during recovery will be less than that during pumping, resulting in a more rapid initial recovery rate than drawdown rate, followed by a corresponding slowing of the recovery rate at late time. Additionally, as the water table rebounds during recovery, it can trap air in the previously dewatered pore spaces, further decreasing the effective recovery storage coefficient. It is also possible that extraneous air already in the formation, or air that was dissolved in the groundwater and came out of solution during pumping, contributed to a reduced storage coefficient initially and then a greater storage coefficient as rising water levels compressed the air bubbles. Because of these probable effects, the computed transmissivity value is considered only approximate, not necessarily representative.

## C-8.2 Well R-61 Screen 1 Trial 2 Test

Figure C-8.2-1 shows a semilog plot of the drawdown data collected from the trial 2 test on screen 1 at a discharge rate of 0.98 gpm. As observed in trial 1, early data show symptoms of antecedent drainage of a trivial volume of drop pipe as well as a storage effect associated with air in the formation or filter pack.

The transmissivity estimated from the line of fit shown on the graph is 140 gpd/ft. The corresponding computed hydraulic conductivity for a 10-ft-thick zone is 14 gpd/ft<sup>2</sup>, or 1.9 ft/day. The actual height of the cone of depression was likely greater than 10 ft, making the true hydraulic conductivity less than this.

Figure C-8.2-2 shows the recovery data that were collected following shutdown of the trial 2 pumping test. The bulk of the curve shows storage effects, while the later data, shown on the expanded-scale plot on Figure C-8.2-3 shows the hysteretic effects of gradually changing storage coefficient rendering the curve not analyzable.

### C-8.3 Well R-61 Screen 1 24-H Constant-Rate Test

Figure C-8.3-1 shows a semilog plot of the drawdown data collected from the 24-h test on screen 1 at a discharge rate of 0.95 gpm. As observed in trials 1 and 2, early data show symptoms of antecedent drainage of a trivial volume of drop pipe as well as a storage effect associated with air in the formation or filter pack. Throughout the 24-h screen 1 test, the presence of air was persistent, with no obvious reduction in content over time.

The transmissivity estimated from the line of fit shown on the graph is 170 gpd/ft. The corresponding computed hydraulic conductivity for a 10-ft-thick zone is  $17 \text{ gpd/ft}^2$ , or 2.3 ft/day. The actual height of the cone of depression was likely greater than 10 ft, making the true hydraulic conductivity lower.

After an hour of pumping, the slope of the drawdown curve steepens significantly with a steadily increasing slope throughout the remainder of the test. Air was produced continuously throughout the test, and, although it was not possible to quantify the amount, there was no obvious reduction in the air content. It is likely that accumulation of air in the formation pores around the well degraded the permeability of the sediments continuously. A possible boundary effect was ruled out as the cause because the data pattern observed during drawdown is not replicated in the recovery data set, as discussed below.

Figure C-8.3-2 shows the recovery data collected following shutdown of the 24-h pumping test. The bulk of the curve shows storage effects. Later data show a remarkable effect not previously seen in any of the pumping tests conducted on the plateau. A bimodal recovery curve is shown in which the recovered water levels appear to be leveling off, but then later show rapid recovery again, i.e., there is a prominent inflection point. This must be an air effect of some kind where compression of the air bubbles or dissolution of some of the air into the groundwater dampened the recovery rate temporarily. At any rate, as a result, the recovery data are not analyzable.

### C-8.4 Well R-61 Screen 1 Data Comparisons

Drawdown and recovery data from the 24-h pumping test are plotted on the same graph in Figure C-8.4-1 to compare the two curves. Theoretically, the plots should coincide at early and middle time, showing slight departure at late time. To the contrary, as shown in the figure, the two curves are entirely different. This confirms that the late-time drawdown increase was associated with changes in well efficiency rather than boundary conditions. If a boundary had been the cause, the recovery data would show a late-time effect having the same magnitude as that seen in the drawdown curve.

Further corroboration of this is supported by the early data. Note that the early recovery rate is sluggish compared with the early drawdown rate, i.e., there is less recovery than drawdown in the first minute or so. This implies a greater storage effect during recovery that, in turn, implies there was more air in the formation pores at the time of pump shutoff than when pumping started.

The drawdown data sets observed during the early stages of pumping were compared to identify any differences from one pumping event to another. The early pumping data for trials 1 and 2 and the 24-h test are shown in Figure C-8.4-2. Because the pumping rates were slightly different for each of the tests, all drawdown values were corrected mathematically for a discharge rate of 0.95 gpm (by multiplying the drawdown by 0.95 and dividing by the actual pumping rate).

In theory, the three plots should have coincided exactly. As indicated in the figure, however, the plots show that the drawdown increased from one test to another, implying a slight degradation of well efficiency each time the zone was pumped. This is consistent with the accumulation of additional air in the

formation pores during each pumping event, degrading the permeability of the sediments slightly over time.

### **C-8.5 Well R-61 Screen 1 Packer Deflation**

Following testing of screen 1, the packer was deflated to prepare for pulling the pump. Figure C-8.5-1 shows water level changes observed when the packer was deflated. The enormous rise in water level of 40 ft was caused by trapped water above the packer that had leaked into the annulus above the packer during the test period. Once the packer deflated, this trapped water flowed downward into the well screen causing the observed head buildup seen on the graph. Leakage of water into the well above the packer would have occurred through either the threaded coupling joints in the drop pipe or the O-ring seals at the pump-wire pass-through assembly on the top side of the inflatable packer.

### **C-8.6 Well R-61 Screen 1 Specific Capacity Data**

Specific capacity data were used along with well geometry to estimate a lower-bound hydraulic conductivity value for the permeable zone penetrated by R-61 screen 1. This was done to provide a frame of reference for evaluating the foregoing analyses. Data from trial 1 were used for the calculations because these data would have included the least possible permeability degradation associated with accumulation of air in the formation pores.

At the end of the 30-min trial 1 pumping test, the discharge rate was 1.02 gpm with a resulting drawdown of 6.58 ft for a short-term specific capacity of 0.155 gpm/ft. In addition to specific capacity and pumping time, other input values used in the calculations included a storage coefficient value of 0.05, a borehole radius of 0.65 ft (inferred from the volume of filter pack required to backfill the screened zone), a screen length of 10 ft, and an arbitrary saturated thickness of 200 ft.

Applying the Brons and Marting method to these inputs yields a lower-bound hydraulic conductivity value of 11.4 gpd/ft<sup>2</sup>, or 1.5 ft/d. The average hydraulic conductivity value from the foregoing pumping test was 2 ft/d or less, depending on the effective height of the cone of depression associated with the analyzed data. The lower-bound value determined from the specific capacity of screen 1 was reasonably consistent with the pumping test analysis.

## **C-9.0 WELL R-61 SCREEN 2 DATA ANALYSIS**

This section presents the data obtained from the R-61 screen 2 pumping tests and the results of the analytical interpretations. Data are presented for drawdown and recovery from trial 1, trial 2, and the 24-h variable-rate test.

### **C-9.1 Well R-61 Screen 2 Specific Capacity Data**

Specific capacity data were used along with well geometry to estimate a lower-bound hydraulic conductivity value for the permeable zone penetrated by R-61 screen 2. This was done before the pumping test analysis to provide a frame of reference for evaluating parameters computed from the test data.

Because of the variable rate applied to the pumping test, as a simplification, just the last step was used in estimating the lower-bound hydraulic conductivity. The final pumping step applied a discharge rate of 22.3 gpm for a period of 840 min. At the end of this period, the drawdown was 39.3 ft for a specific capacity of 0.57 gpm/ft. In addition to specific capacity and pumping time, other input values used in the

calculations include a leaky-confined storage coefficient value of 0.003, a borehole radius of 0.66 ft (inferred from the volume of filter pack required to backfill the screened zone), a screen length of 20.6 ft, and an arbitrary saturated thickness of 200 ft.

Applying the Brons and Marting method to these inputs yields a lower-bound hydraulic conductivity value of 23.6 gpd/ft<sup>2</sup>, or 3.2 ft/d.

### C-9.2 Well R-61 Screen 2 Trial 1

Figure C-9.2-1 shows a semilog plot of the screen 2 drawdown data collected from trial 1. The first few data points describe a flat slope transitioning to a steeper slope. This has the appearance of a storage effect, perhaps associated with expansion of air bubbles in the formation pores in response to pressure reduction (drawdown). The transmissivity determined from the prominent early slope is 360 gpd/ft. Assigning this transmissivity to the screen length of 20.6 ft produces a hydraulic conductivity of 17.5 gpd/ft<sup>2</sup>, or 2.3 ft/d. This is less than the known lower-bound conductivity of 3.2 ft/d, confirming that a subtle storage effect influenced the early data.

The late data show a computed transmissivity of 1780 gpd/ft. This would be the transmissivity of the unknown thickness of sediment penetrated by the cone of depression at that particular time.

Figure C-9.2-2 shows the recovery data collected following shutdown of the trial 1 pumping test. Again, the form of the early portion of the curve is consistent with storage-affected data. The transmissivity estimated from the early data is 250 gpd/ft, a clear underestimate of the true transmissivity of the screened interval, thus confirming the presence of storage effects on the data.

The balance of the recovery data are plotted on the expanded-scale graph shown in Figure C-9.2-3. The curve shows continuous flattening, which is the expected response in a partially penetrating well. However, based on the nearly complete, premature recovery (well before a  $t/t'$  value of 1.0), the data likely were also influenced by hysteretic effects, primarily associated with a gradually increasing storage coefficient caused by compression of air in the formation pores as the water level rose.

### C-9.3 Well R-61 Screen 2 Trial 2

Figure C-9.3-1 shows a semilog plot of the drawdown data collected from the trial 2 test. The first couple of data points show the effects of minor antecedent drainage of the drop pipe. The bulk of the early data show the general form of storage-affected drawdown data, as was observed in trial 1. Indeed, the transmissivity computed from the line of fit shown on the graph is an underestimate, similar to what was obtained from the trial 1 analysis, corroborating the idea of storage effects.

The late drawdown data shown on the expanded-scale plot in Figure C-9.3-2 show continual flattening of the drawdown curve associated with ongoing vertical expansion of the cone of depression (partial penetration effects). The late data support a transmissivity calculation of 3090 gpd/ft, which is reflective of the transmissivity of the interval of unknown thickness penetrated by the cone of depression at that particular time. Examination of the data shows continuing flattening of the curve to the end of the pumping period.

To account for partial penetration effects, the trial 2 data were analyzed using the Hantush equation. Figures C-9.3-3 through C-9.3-6 show Hantush curve matching results for anisotropy ratios of 0.1, 0.01, 0.001, and 0.0001, respectively. The poor fit of the earliest data to the type curve reinforces the conclusion that storage effects influenced the pumping response.

The storage coefficient values corresponding to severe anisotropy appear unrealistically low, tentatively suggesting that the results for moderate anisotropy are the most accurate. This suggests a hydraulic conductivity around 3 or 4 ft/d. Values in this range are consistent with the lower-bound hydraulic conductivity determined from the specific capacity of the zone. It should be noted, however, that because the data under analysis are from the pumped well, inefficiency also can bias the storage coefficient calculation. Thus, the severe anisotropy scenarios cannot be completely ruled out. The combined results bracketed the hydraulic conductivity between about 3 and 6 ft/d. It is also notable that the curve matching method can produce a biased (low) transmissivity result if the well is inefficient.

Figure C-9.3-7 shows the recovery data collected following shutdown of the trial 2 pumping test. The transmissivity estimated from the early data is 230 gpd/ft, again an underestimate consistent with storage effects.

The balance of the recovery data are plotted on the expanded-scale graph shown in Figure C-9.3-8. The continuous flattening of the recovery curve shows partial penetration and hysteretic effects, likely primarily associated with a gradually increasing storage coefficient caused by compression of air in the formation pores as the water level rose. The recovery data are thus not analyzable.

#### **C-9.4 Well R-61 Screen 2 24-H Test**

Figure C-9.4-1 shows a semilog plot of the drawdown data collected from the 24-h three-step pumping test conducted at discharge rates of 21.6, 12.7, and 22.3 gpm. The first couple of data points show the effects of minor antecedent drainage of the drop pipe. The bulk of the early data show the general form of storage-affected drawdown data, as was observed in trials 1 and 2. Indeed, the transmissivity computed from the line of fit shown on the graph is an underestimate, similar to what was obtained from the trial 1 and 2 analyses, supporting the idea of storage effects.

The drawdown data over the last half of the pumping test show a gradual rise in water level with a constant pumping rate. Over this period, the air content of the pumped water diminished noticeably. It was concluded that gradual removal of air from the formation pores improved the sediment permeability somewhat, resulting in slightly improved well efficiency as pumping went on.

The drawdown response observed in screen 1 while pumping screen 2 during the first pumping step was analyzed using the Hantush partial penetration equation. Figures C-9.4-2 through C-9.4-5 show Hantush curve matching results for anisotropy ratios of 0.1, 0.01, 0.001, and 0.0001, respectively.

The analyses show hydraulic conductivity values around 8 ft/d for the most reasonable range of storage coefficient values. Values obtained from pumped zones are in the range of 3 to 6 ft/d. This suggests that the pumped interval was slightly inefficient, yielding somewhat biased hydraulic conductivity results from the pumped well data set.

After an hour of pumping, the drawdown data show a flattening effect, deviating from the type curves implied by the early data. This may be an indication of delayed yield effects associated with downward movement of the phreatic surface at screen 1. It is also possible that it may be a response to slight leakage of water from the drop pipe into screen 1.

The application of varying pumping rates during testing of screen 2 did not provide any information or benefit because the nearby wells did not show any measurable response to pumping screen 2.

Figure C-9.4-6 shows the recovery data collected following shutdown of the 24-h pumping test. The transmissivity value of 210 gpd/ft estimated from the early data is an underestimate, consistent with storage effects.

The balance of the recovery data are plotted on the expanded-scale graph shown in Figure C-9.4-7. The continuous flattening of the recovery curve shows partial penetration and hysteretic effects, likely primarily associated with a gradually increasing storage coefficient caused by compression of air in the formation pores as the water level rose. The late recovery data are not analyzable.

## **C-10.0 SUMMARY**

Constant-rate pumping tests were conducted on R-61 screens 1 and 2. The tests were performed to gain an understanding of the hydraulic characteristics of the aquifer in the vicinity of the screened zones and the degree of interconnection between them. Numerous observations and conclusions were drawn from the tests as summarized below.

The static water levels observed in screens 1 and 2 were essentially identical at 1100.95 ft bgs.

A comparison of barometric pressure and R-61 water level data shows a high barometric efficiency for each zone. Screen 2 showed a small diurnal effect, probably a result of Earth tides. Screen 1 showed a small diurnal effect that may have been related to either Earth tides or barometric pressure effects.

Both screened zones produced aerated water. The air content in the formation water caused brief storage effects in the pumping and recovery data. In addition, temporal changes in well efficiency were noted as gas content apparently increased in the pores near screen 1 (reducing the efficiency) and decreased at screen 2 (increasing the efficiency).

Pumping screen 1 at about 1 gpm had no discernable effect on water levels in screen 2, whereas pumping screen 2 at 21.6 gpm for 300 min caused a drawdown response at screen 1 of 0.16 ft. Pumping either zone had no effect on nearby monitored regional wells R-15, R-42, R-43 screens 1 and 2, and R-50 screens 1 and 2.

Water leaked from the drop pipe during the tests, either through worn threaded coupling joints or O-ring seals where the submersible pump wires entered the drop pipe above the inflatable packer. The leakage affected water levels enough to impede portions of the analysis.

Test analysis suggests a hydraulic conductivity of 2 ft/d or less for the sediments opposite screen 1.

Pumping screen 1 at 1.02 gpm for 30 min produced a drawdown of 6.58 ft and a short-term specific capacity of 0.155 gpm/ft. The lower-bound hydraulic conductivity computed from this performance is 1.5 ft/d, consistent with the pumping test value. During extended pumping of screen 1, buildup of air in the formation pores increased the drawdown: screen 1 produced 0.95 gpm for 1440 min with a drawdown of 16.2 ft for a long-term specific capacity of just 0.059 gpm/ft.

Test analysis from screen 2 suggests a hydraulic conductivity of about 8 ft/d for the bulk of the saturated sediments.

Pumping screen 2 for 1440 min, including the final 840 min at a discharge rate of 22.3 gpm, produced 39.3 ft of drawdown for a specific capacity of 0.57 gpm/ft. The lower-bound hydraulic conductivity computed from this information is 3.2 ft/d, consistent with the pumping test results but suggesting a well efficiency on the order of 50%.

## C-11.0 REFERENCES

*The following list includes all documents cited in this appendix. Parenthetical information following each reference provides the author(s), publication date, and ER ID. This information is also included in text citations. ER IDs are assigned by the Environmental Programs Directorate's Records Processing Facility (RPF) and are used to locate the document at the RPF and, where applicable, in the master reference set.*

*Copies of the master reference set are maintained at the NMED Hazardous Waste Bureau and the Directorate. The set was developed to ensure that the administrative authority has all material needed to review this document, and it is updated with every document submitted to the administrative authority. Documents previously submitted to the administrative authority are not included.*

- Bevan, M.J., A.L. Endres, D.L. Rudolph, and G. Parkin, December 2005. "A Field Scale Study of Pumping-Induced Drainage and Recovery in an Unconfined Aquifer," *Journal of Hydrology*, Vol. 315, No. 1–4, pp. 52–70. (Bevan et al. 2005, 105186)
- Bradbury, K.R., and E.R. Rothschild, March-April 1985. "A Computerized Technique for Estimating the Hydraulic Conductivity of Aquifers from Specific Capacity Data," *Ground Water*, Vol. 23, No. 2, pp. 240-246. (Bradbury and Rothschild 1985, 098234)
- Brons, F., and V.E. Marting, 1961. "The Effect of Restricted Fluid Entry on Well Productivity," *Journal of Petroleum Technology*, Vol. 13, No. 2, pp. 172-174. (Brons and Marting 1961, 098235)
- Cooper, H.H., Jr., and C.E. Jacob, August 1946. "A Generalized Graphical Method for Evaluating Formation Constants and Summarizing Well-Field History," *American Geophysical Union Transactions*, Vol. 27, No. 4, pp. 526-534. (Cooper and Jacob 1946, 098236)
- Driscoll, F.G., 1986. Excerpted pages from *Groundwater and Wells*, 2nd Ed., Johnson Filtration Systems Inc., St. Paul, Minnesota. (Driscoll 1986, 104226)
- Hantush, M.S., July 1961. "Drawdown around a Partially Penetrating Well," *Journal of the Hydraulics Division, Proceedings of the American Society of Civil Engineers*, Vol. 87, No. HY 4, pp. 83-98. (Hantush 1961, 098237)
- Hantush, M.S., September 1961. "Aquifer Tests on Partially Penetrating Wells," *Journal of the Hydraulics Division, Proceedings of the American Society of Civil Engineers*, pp. 171–195. (Hantush 1961, 106003)
- Schafer, D.C., January-February 1978. "Casing Storage Can Affect Pumping Test Data," *The Johnson Drillers Journal*, pp. 1-6, Johnson Division, UOP, Inc., St. Paul, Minnesota. (Schafer 1978, 098240)
- Theis, C.V., 1934-1935. "The Relation Between the Lowering of the Piezometric Surface and the Rate and Duration of Discharge of a Well Using Ground-Water Storage," *American Geophysical Union Transactions*, Vol. 15-16, pp. 519-524. (Theis 1934-1935, 098241)





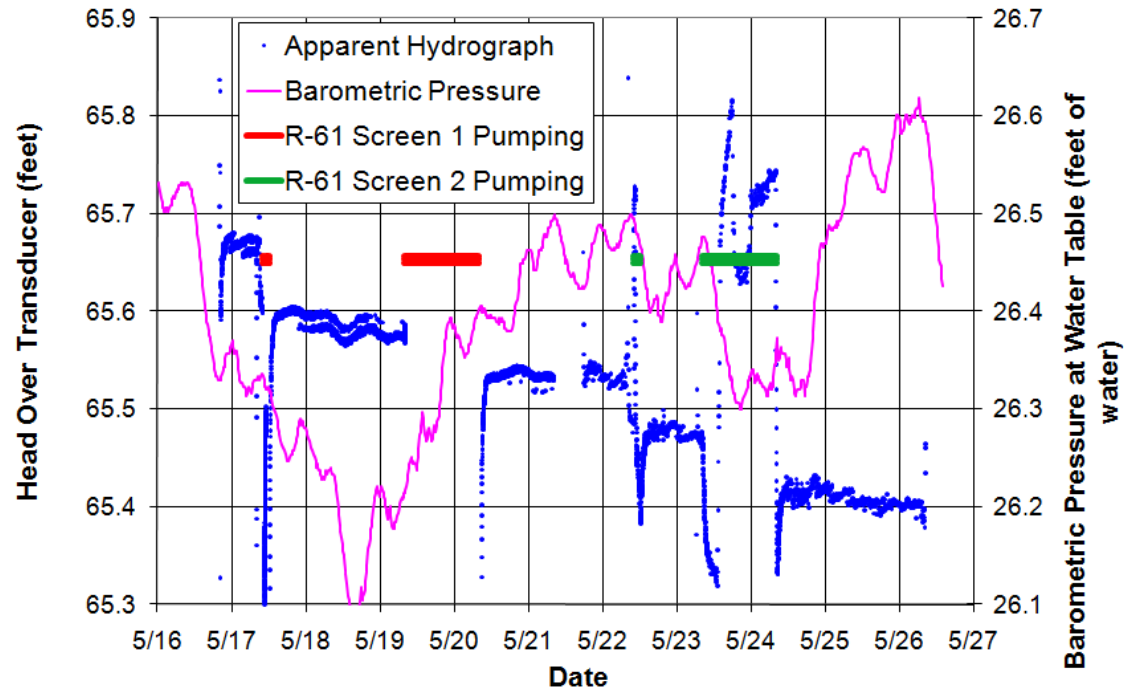


Figure C-7.0-1 Well R-61 screen 1 apparent hydrograph

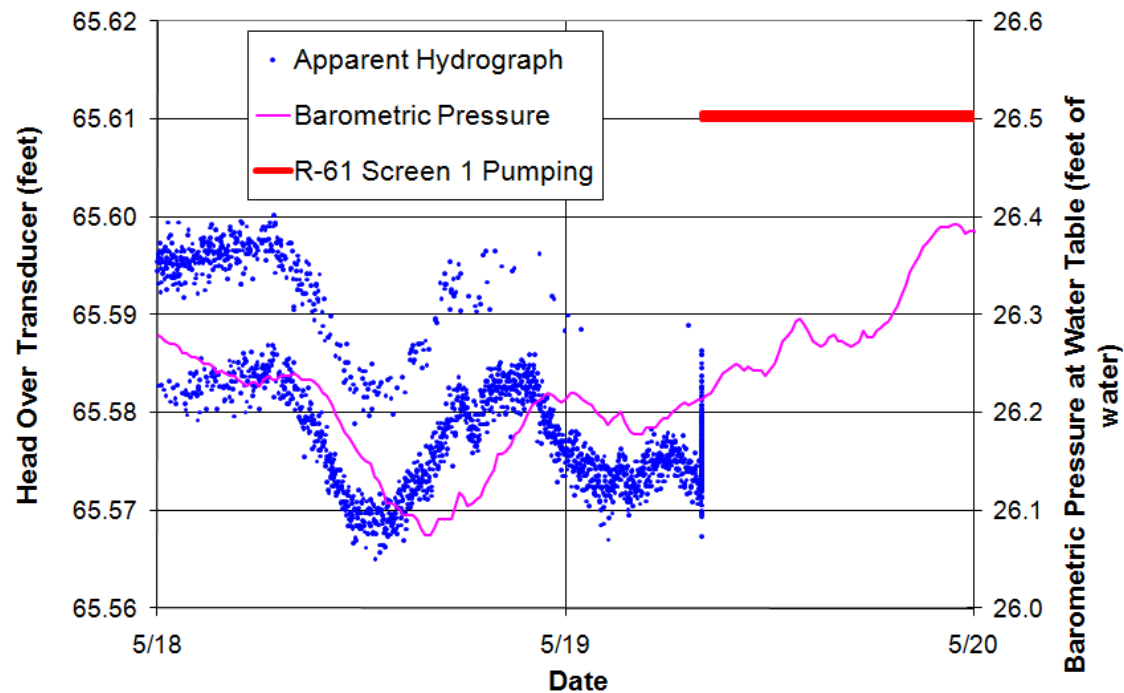


Figure C-7.0-2 Well R-61 screen 1 apparent hydrograph—expanded scale

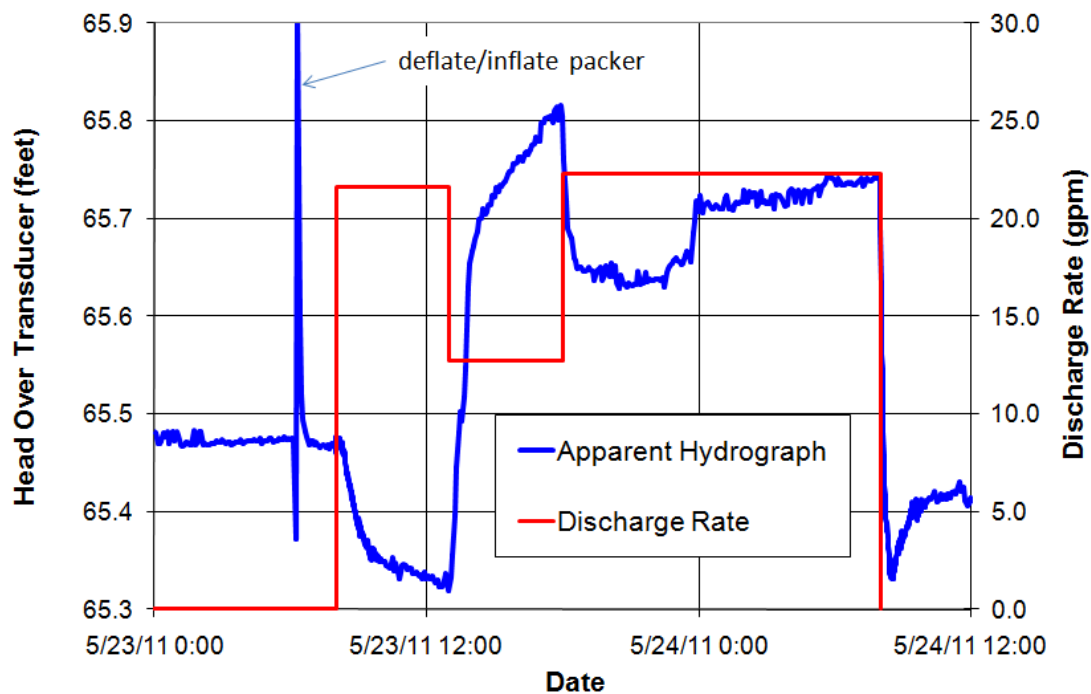


Figure C-7.0-3 Well R-61 screen 1 response to pumping screen 2—expanded

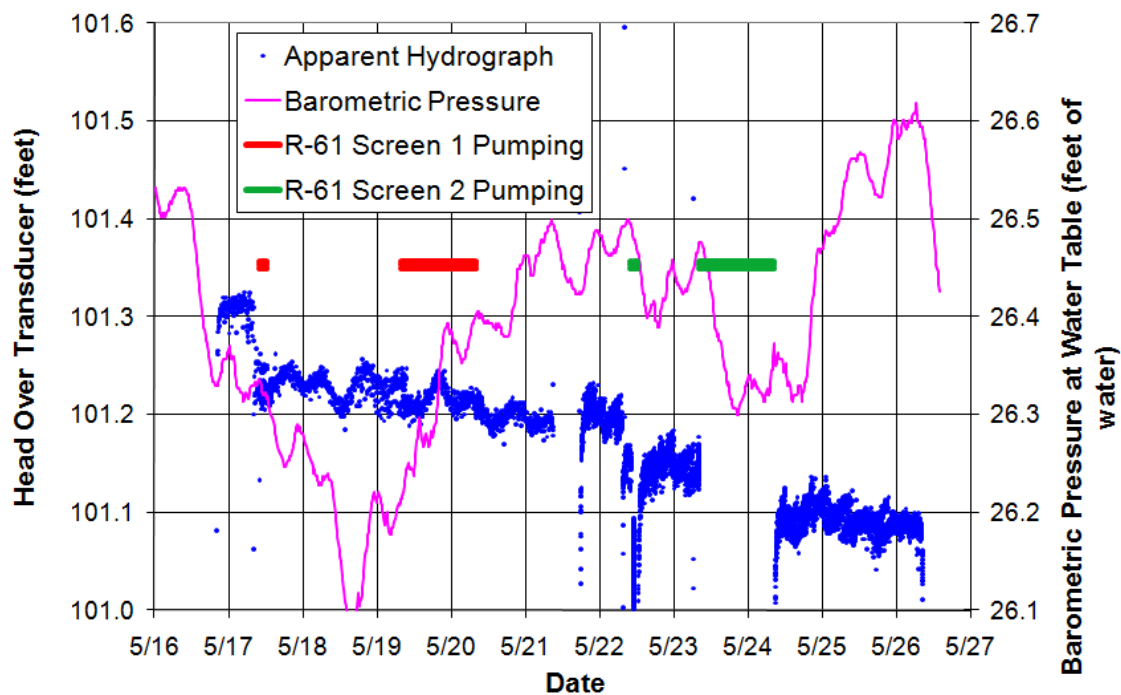


Figure C-7.0-4 Well R-61 screen 2 apparent hydrograph

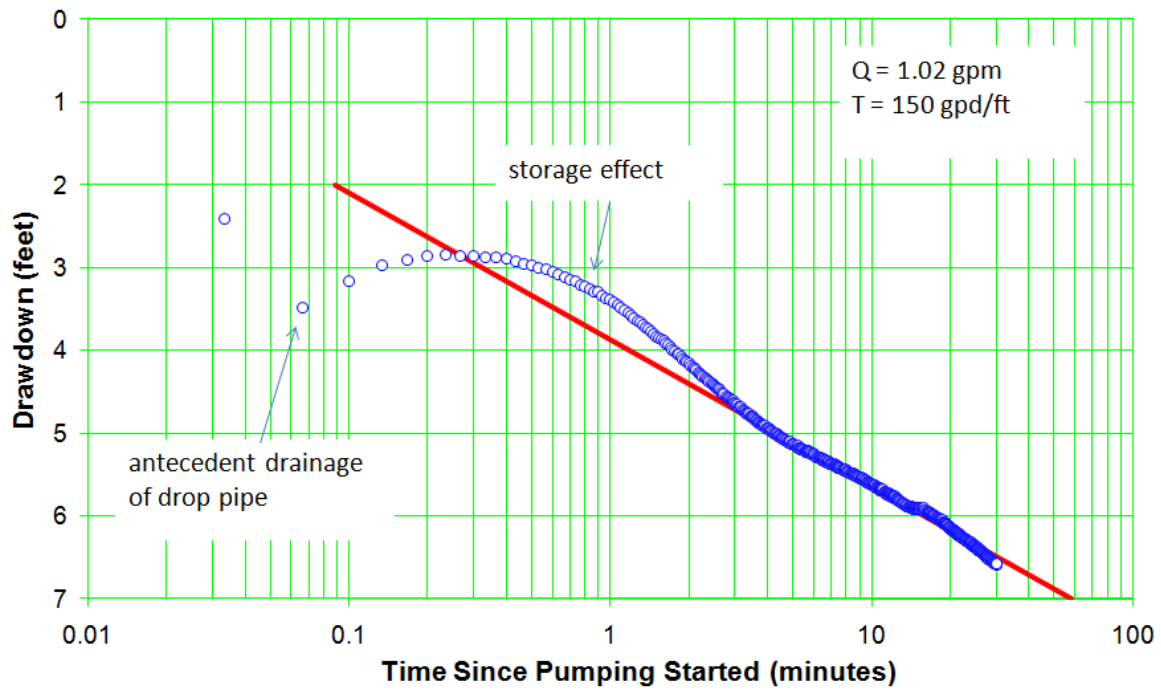


Figure C-8.1-1 Well R-61 screen 1 trial 1 drawdown

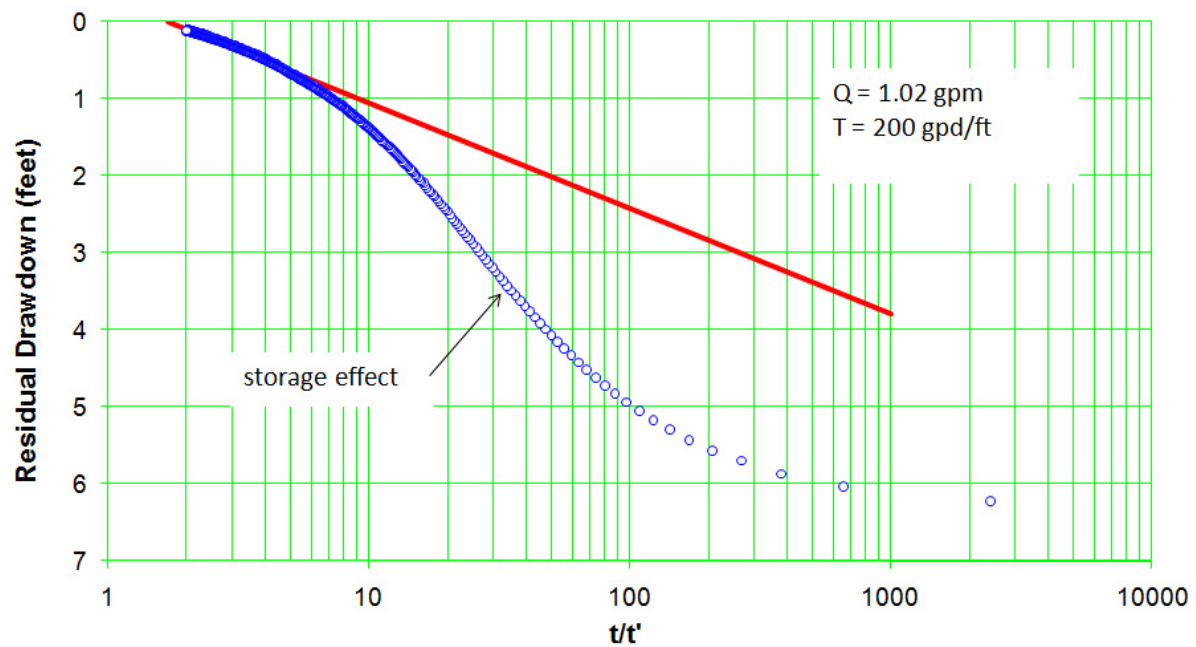


Figure C-8.1-2 Well R-61 screen 1 trial 1 recovery

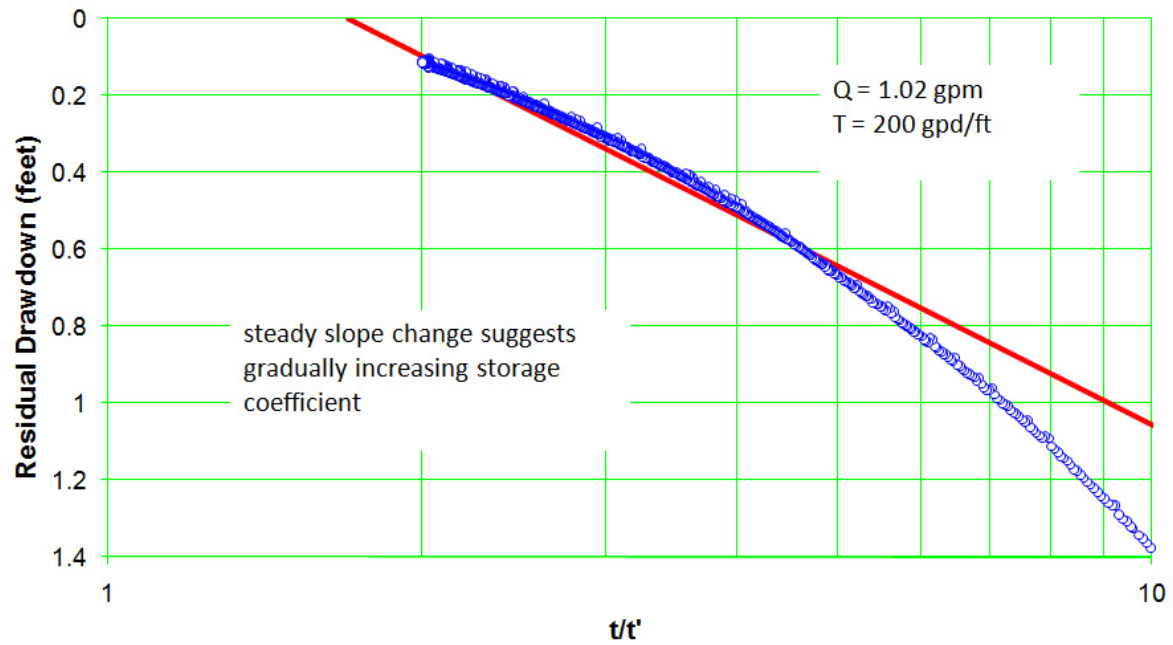


Figure C-8.1-3 Well R-61 screen 1 trial 1 recovery—expanded scale

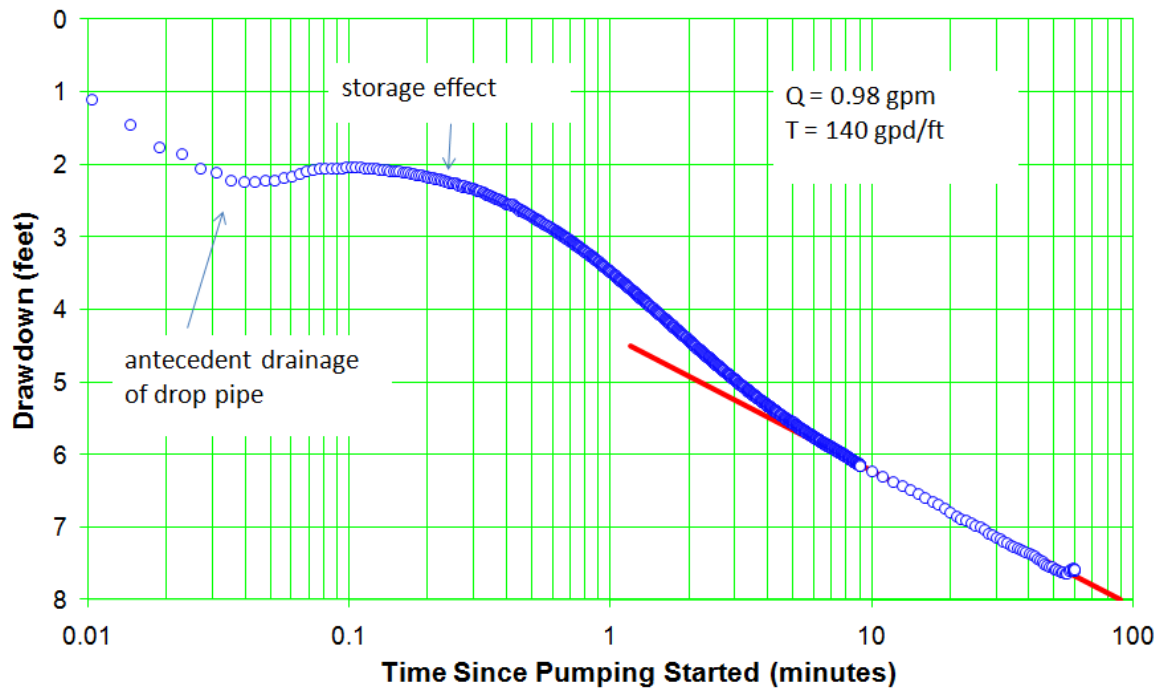


Figure C-8.2-1 Well R-61 screen 1 trial 2 drawdown

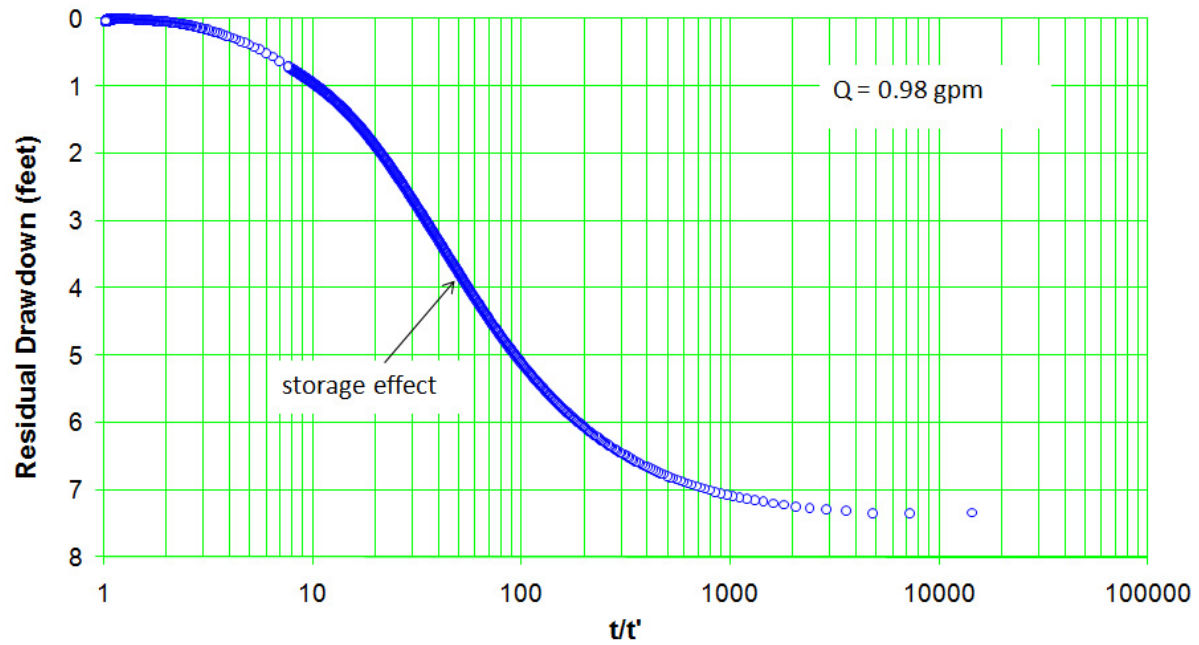


Figure C-8.2-2 Well R-61 screen 1 trial 2 recovery

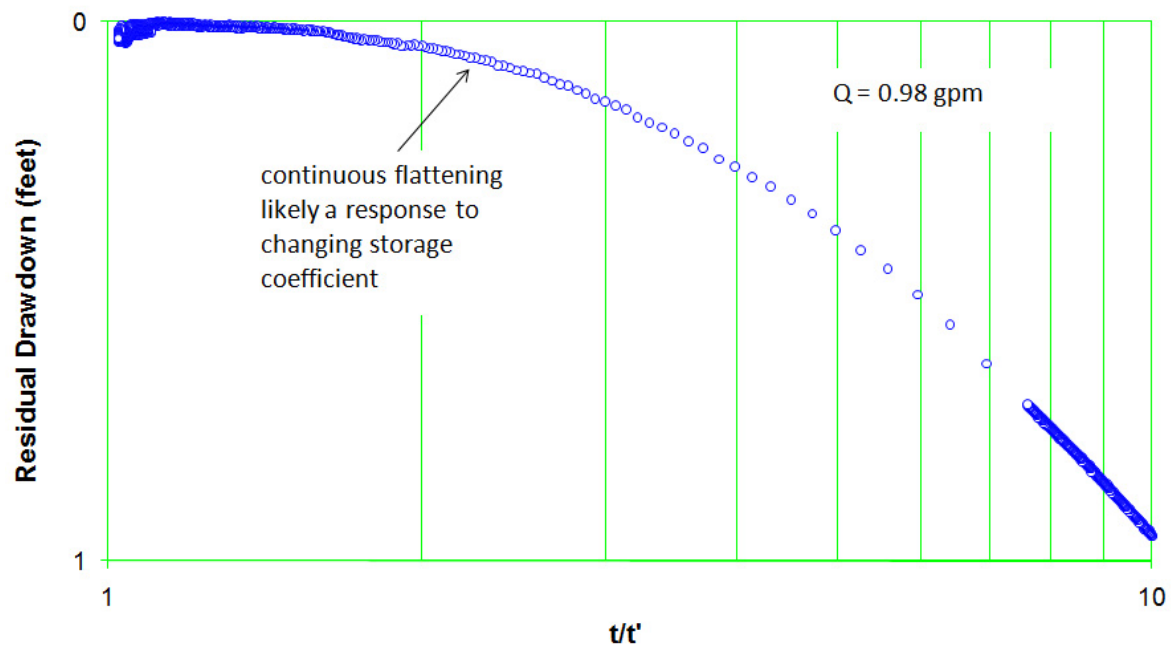


Figure C-8.2-3 Well R-61 screen 1 trial 2 recovery—expanded scale

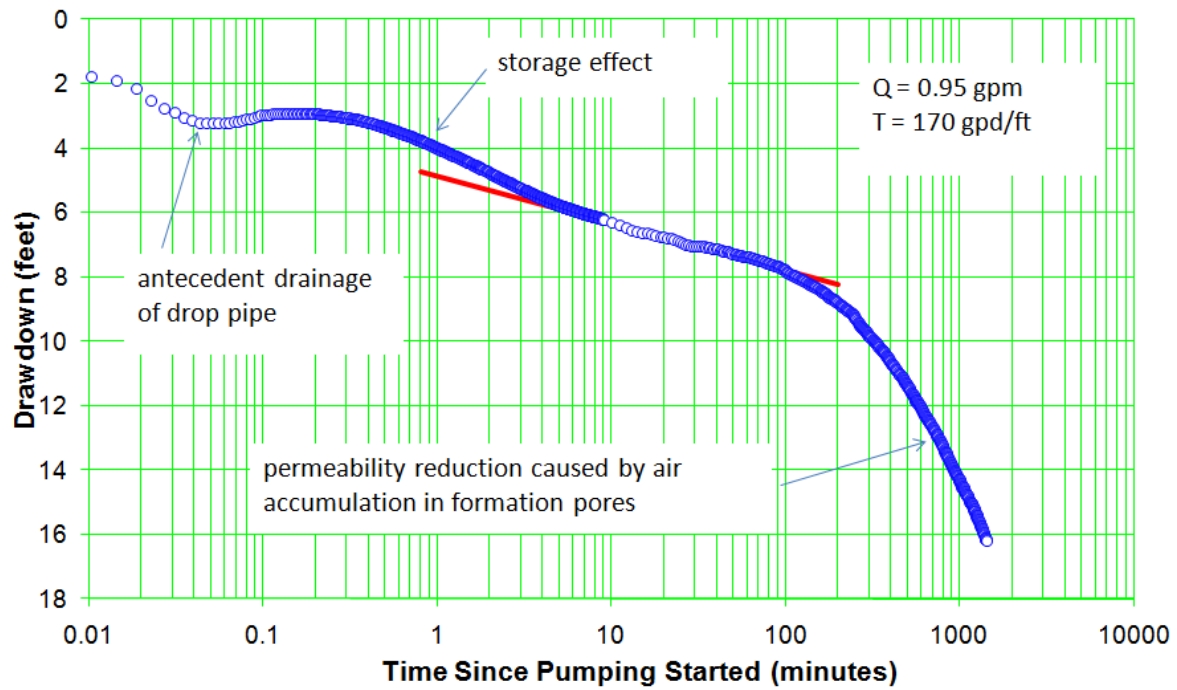


Figure C-8.3-1 Well R-61 screen 1 drawdown

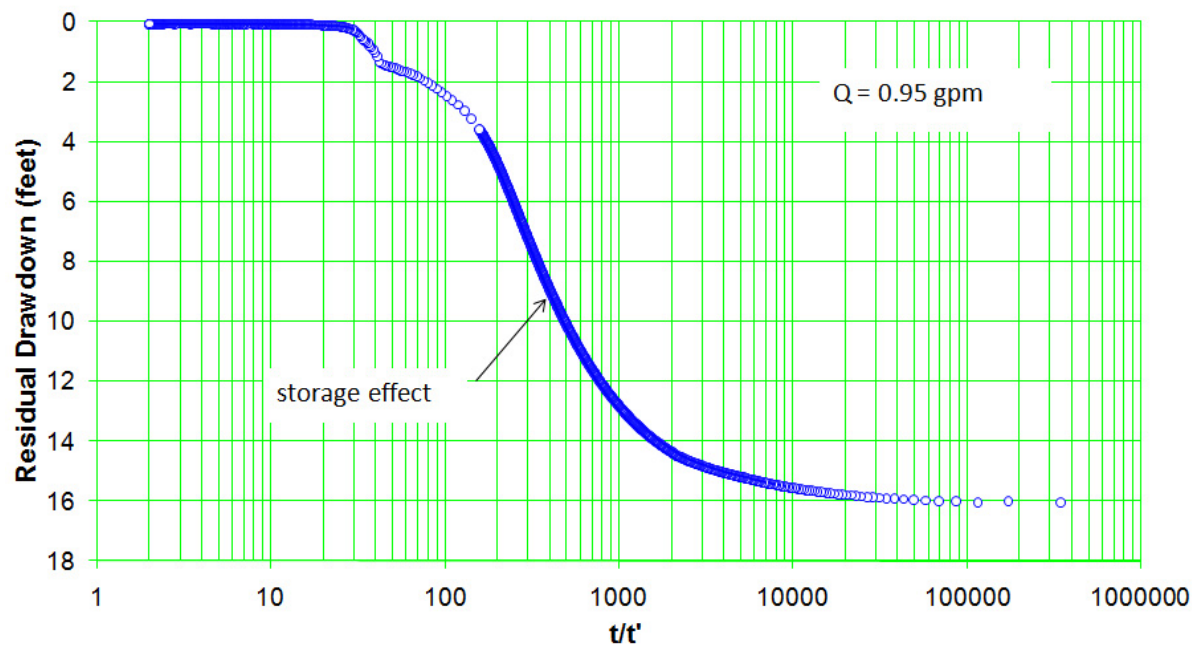


Figure C-8.3-2 Well R-61 screen 1 recovery

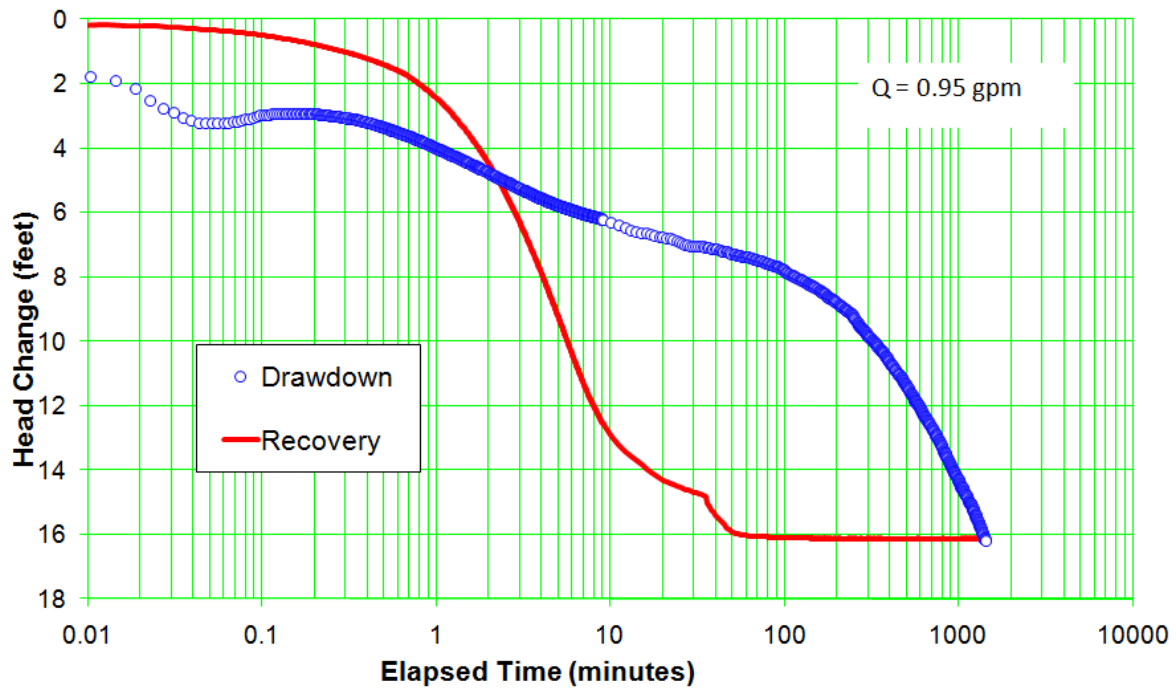


Figure C-8.4-1 Well R-61 screen 1 drawdown and recovery comparison

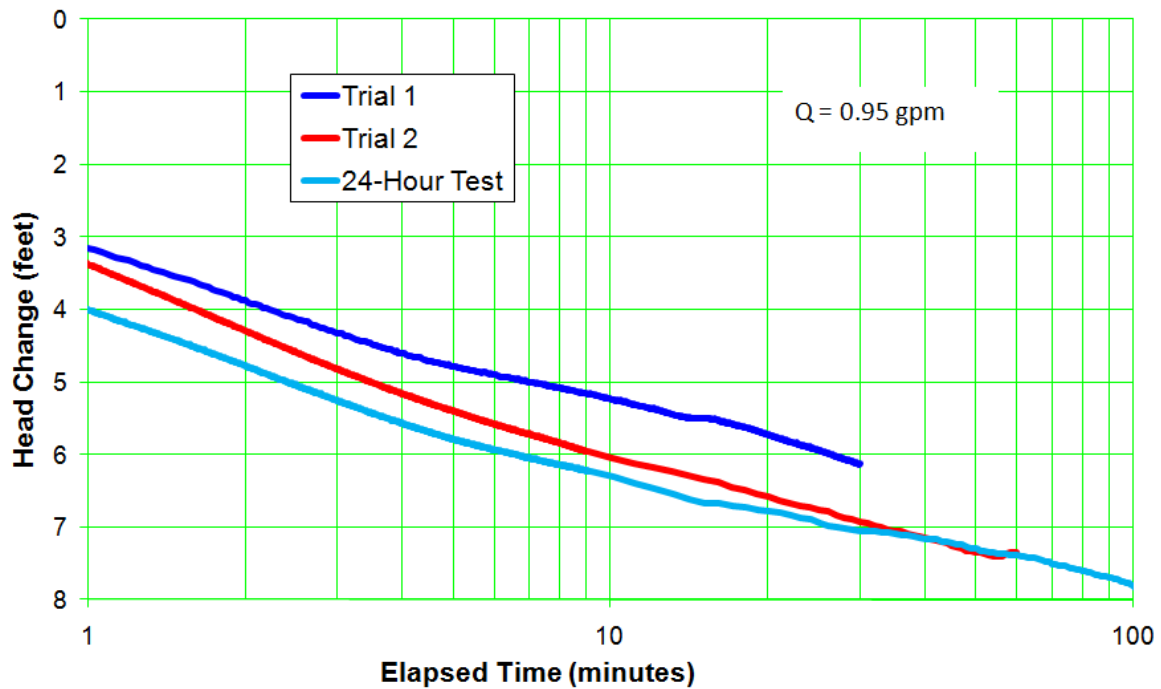


Figure C-8.4-2 Well R-61 screen 1 drawdown comparison for 0.95 gpm

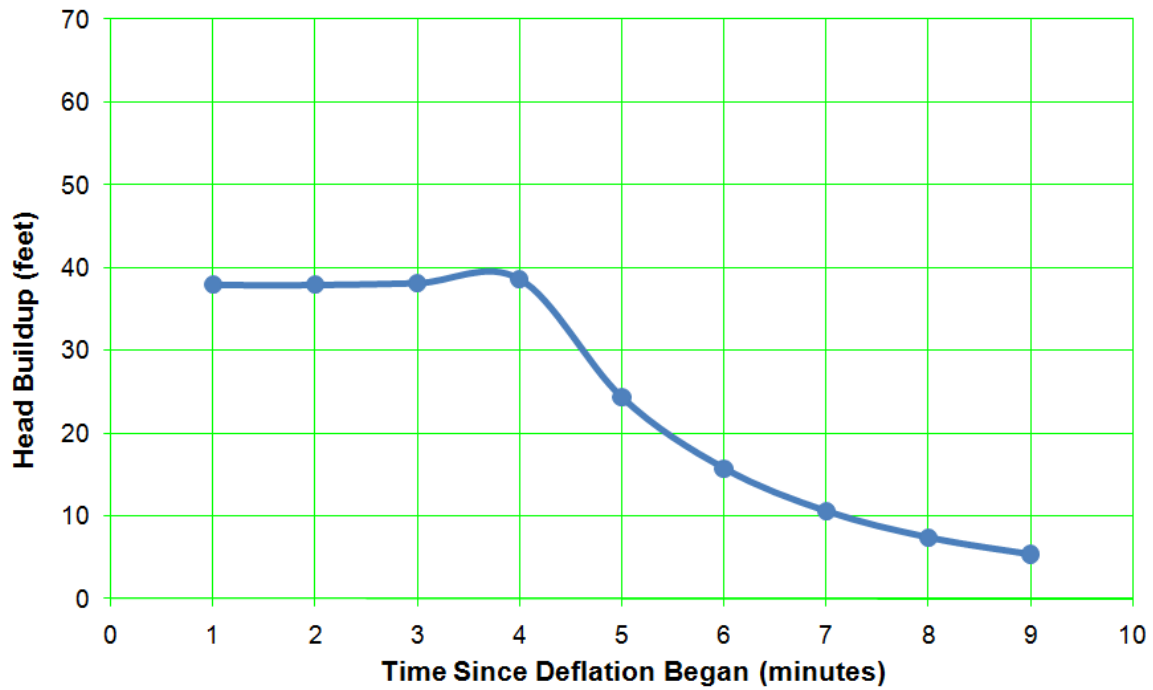


Figure C-8.5-1 Well R-61 screen 1 Packer deflation response

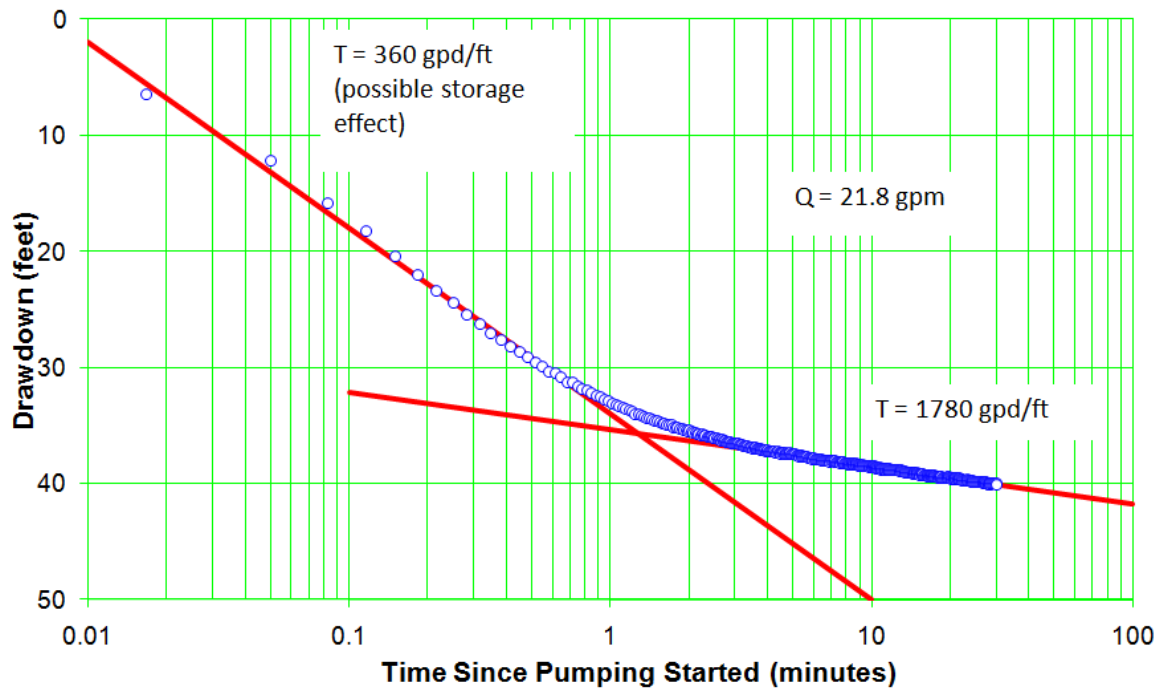


Figure C-9.2-1 Well R-61 screen 2 trial 1 drawdown



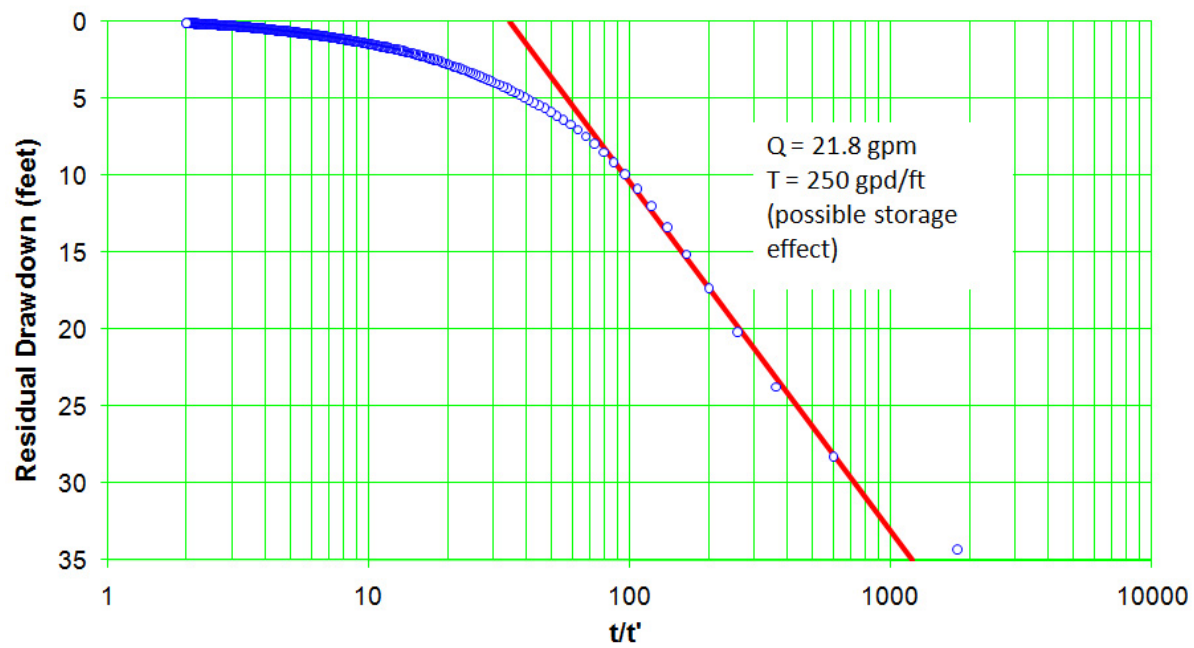


Figure C-9.2-2 Well R-61 screen 2 trial 1 recovery

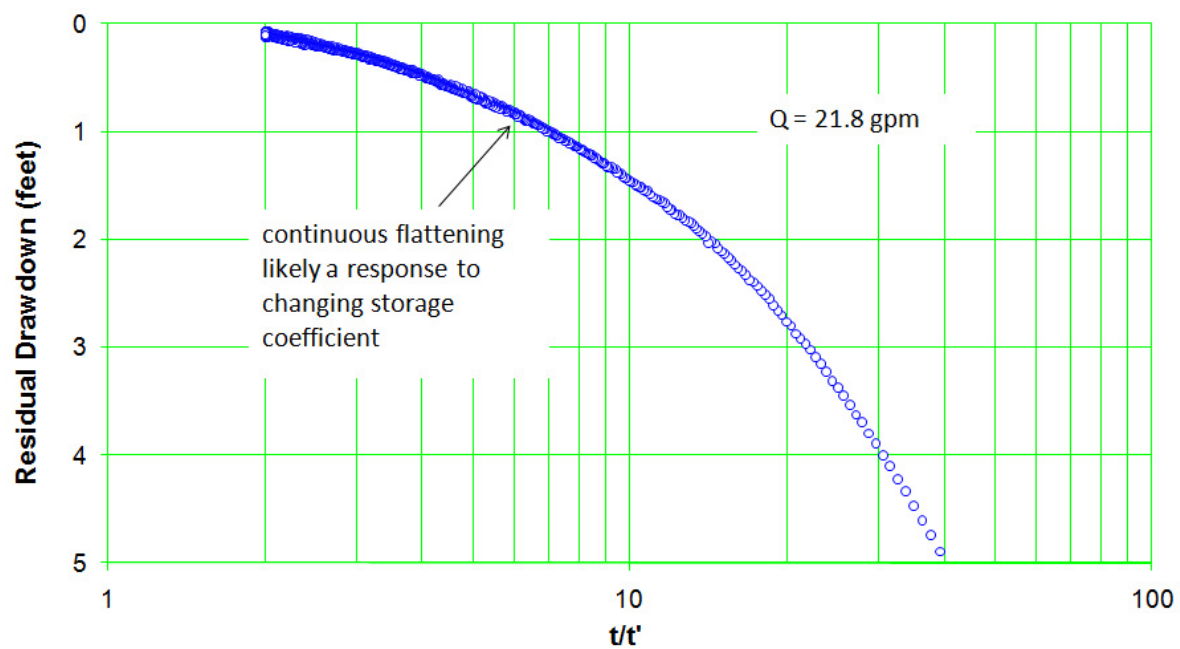


Figure C-9.2-3 Well R-61 screen 2 trial 1 recovery—expanded scale

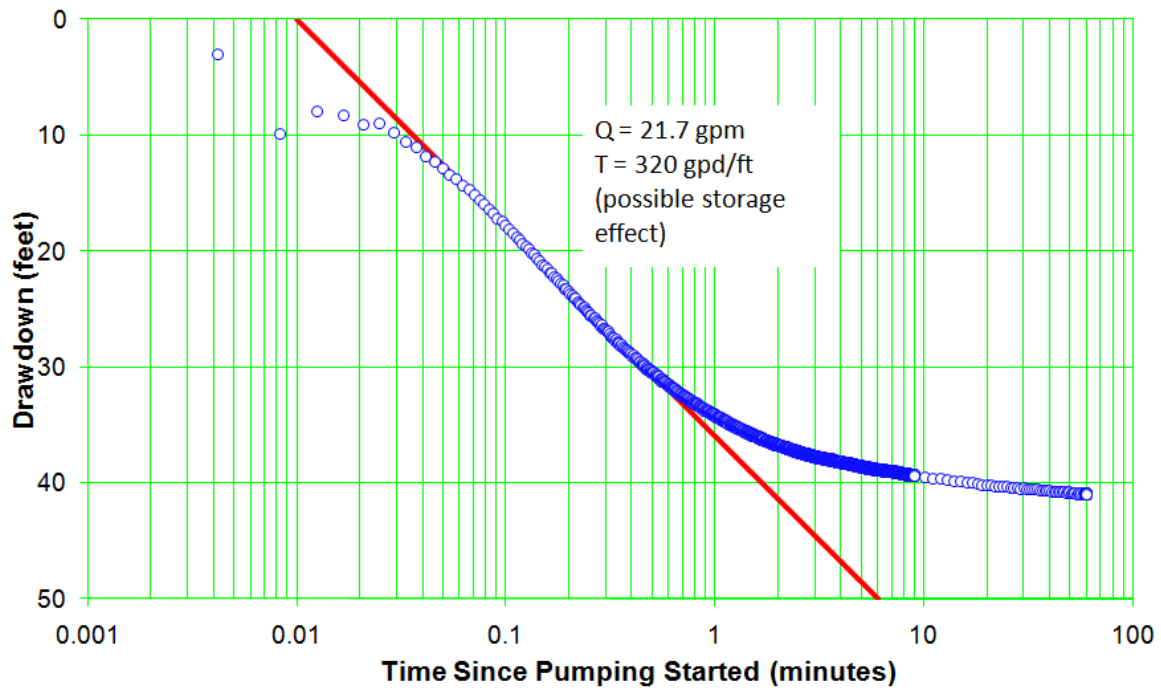


Figure C-9.3-1 Well R-61 screen 2 trial 2 drawdown

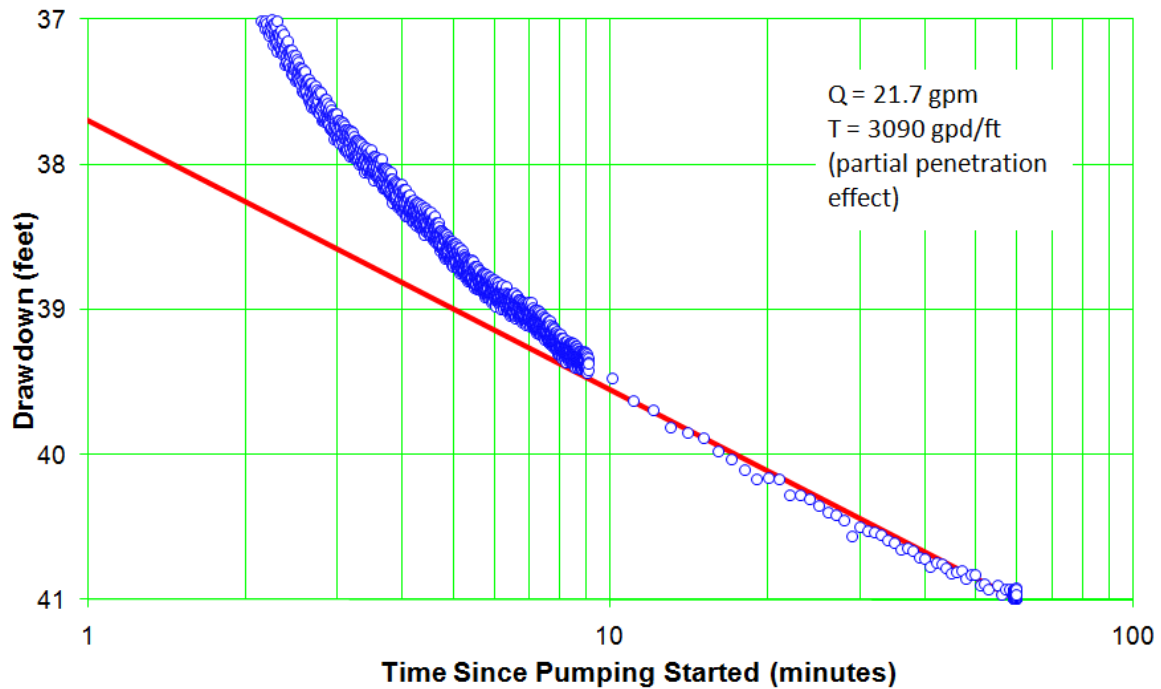


Figure C-9.3-2 Well R-61 screen 2 trial 2 drawdown—expanded scale

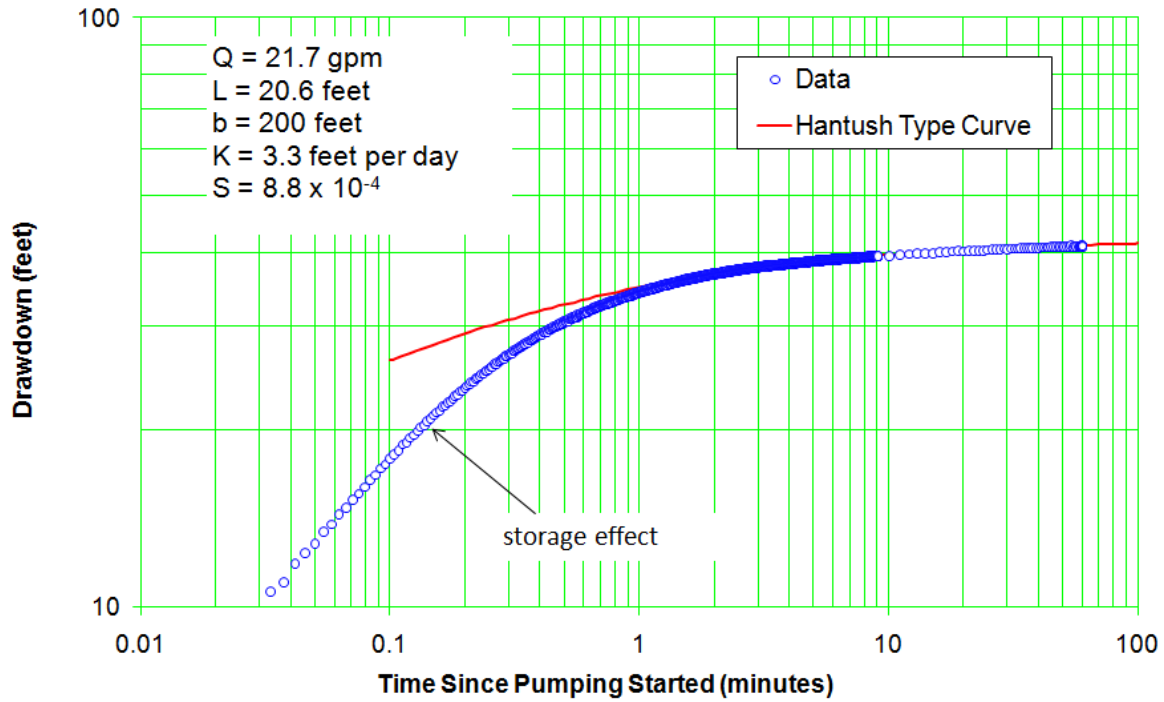


Figure C-9.3-3 Well R-61 screen 2 trial 2 drawdown—Hantush solution for anisotropy of 0.1

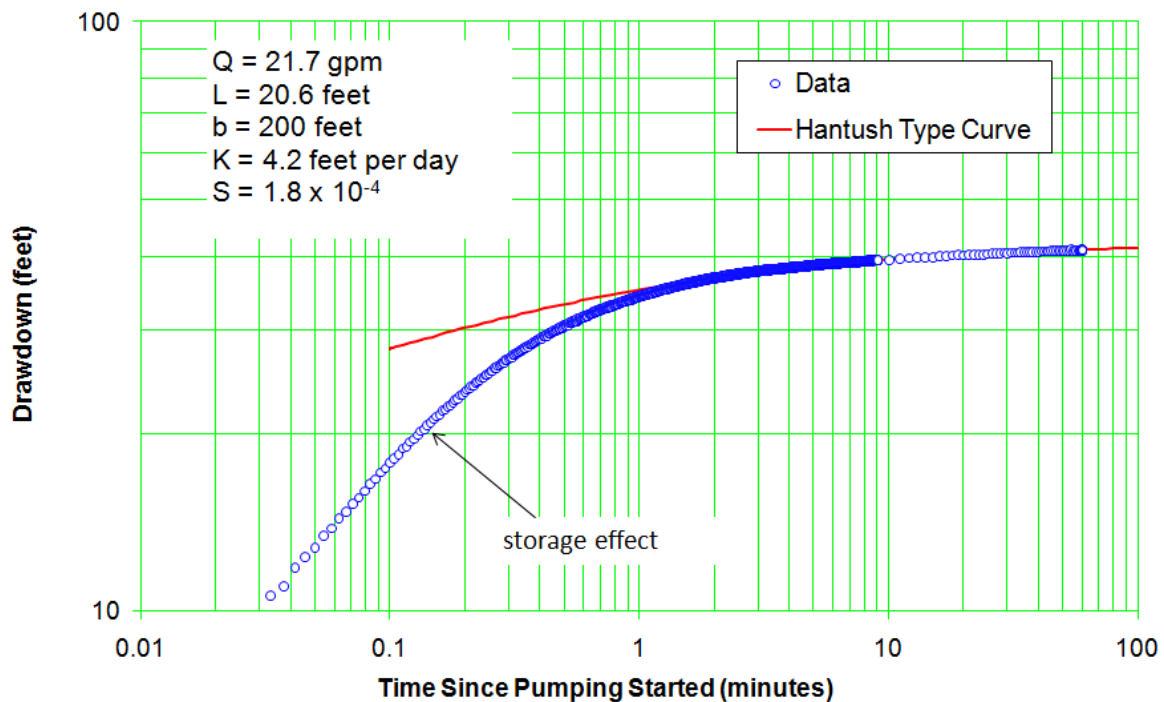


Figure C-9.3-4 Well R-61 screen 2 trial 2 drawdown—Hantush solution for anisotropy of 0.01

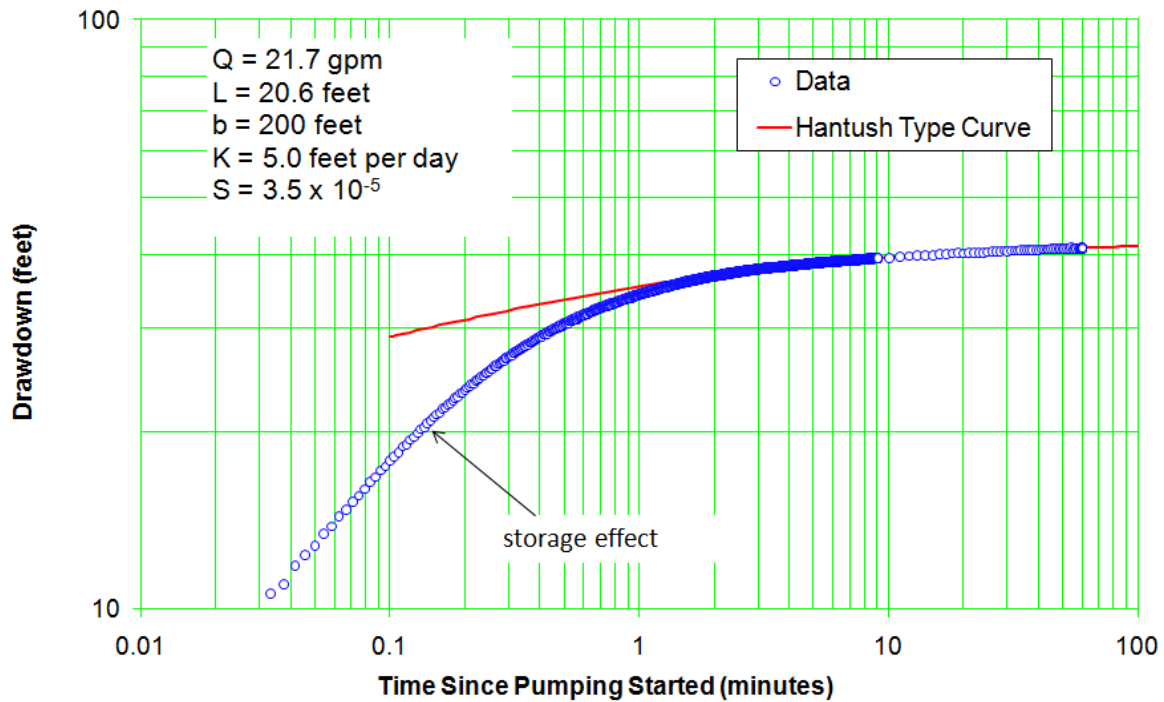


Figure C-9.3-5 Well R-61 screen 2 trial 2 drawdown—Hantush solution for anisotropy of 0.001

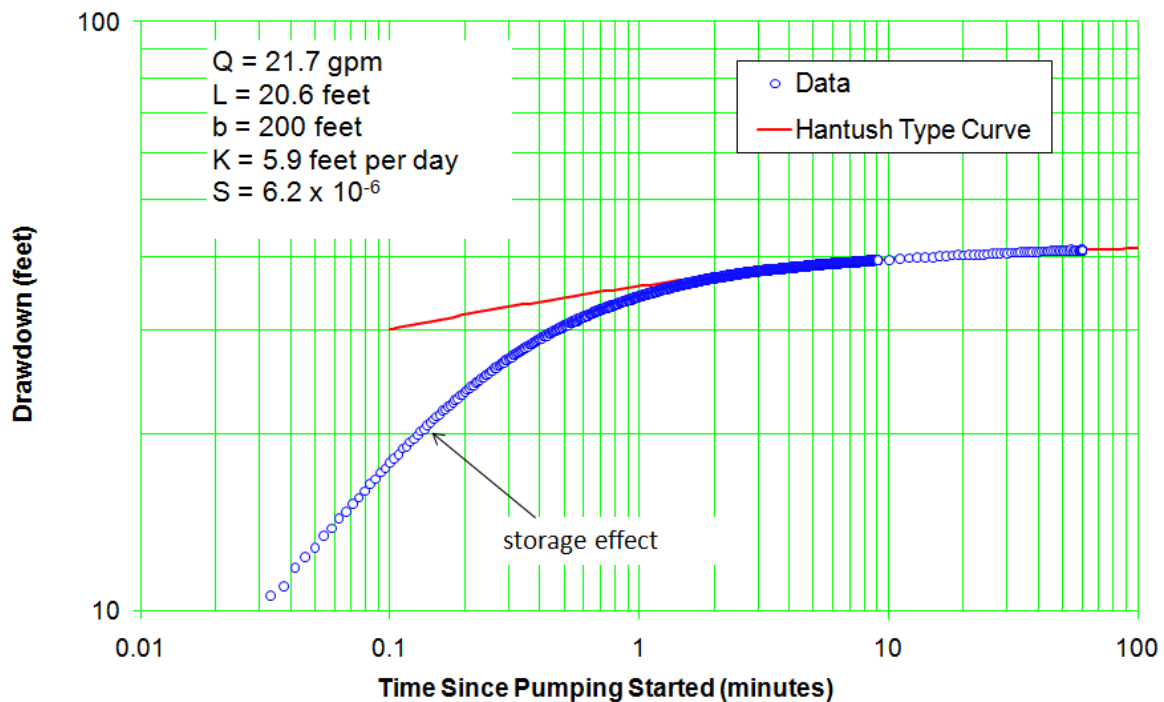


Figure C-9.3-6 Well R-61 screen 2 trial 2 drawdown—Hantush solution for anisotropy of 0.0001

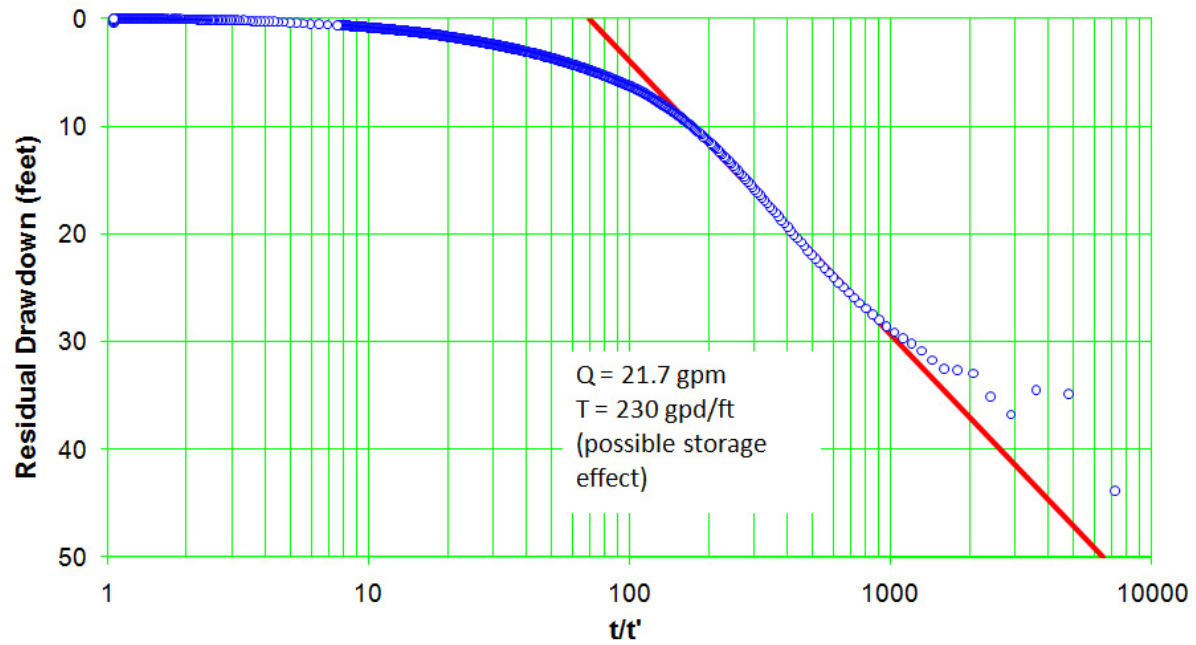


Figure C-9.3-7 Well R-61 screen 2 trial 2 recovery

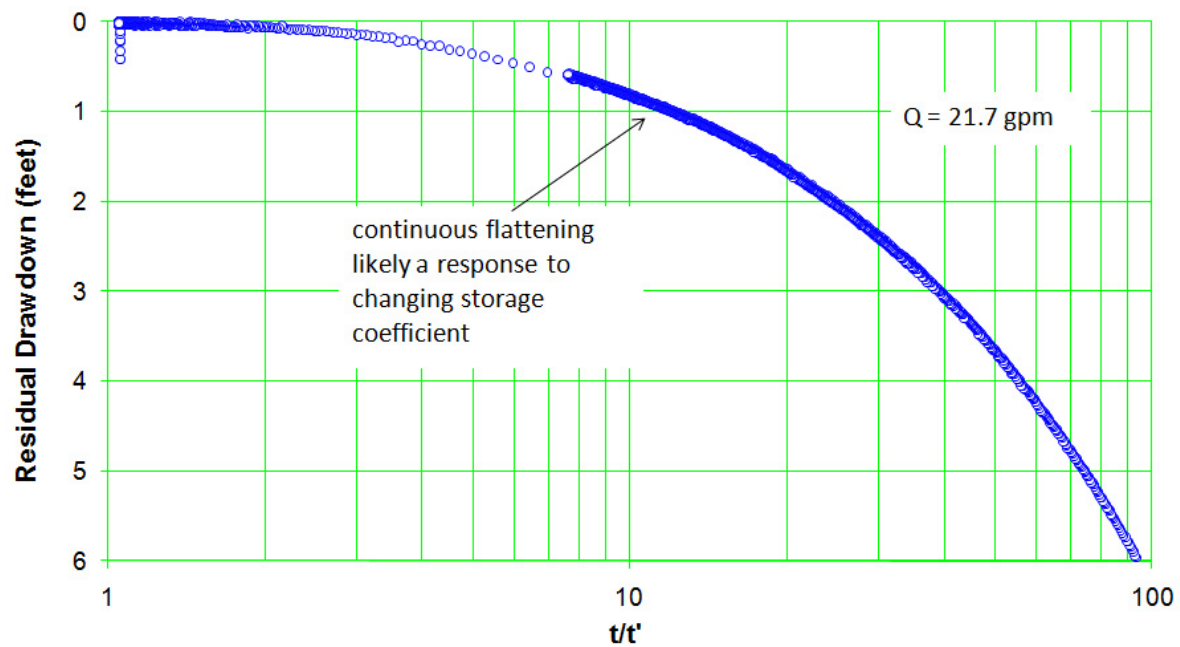


Figure C-9.3-8 Well R-61 screen 2 trial 2 recovery—expanded scale

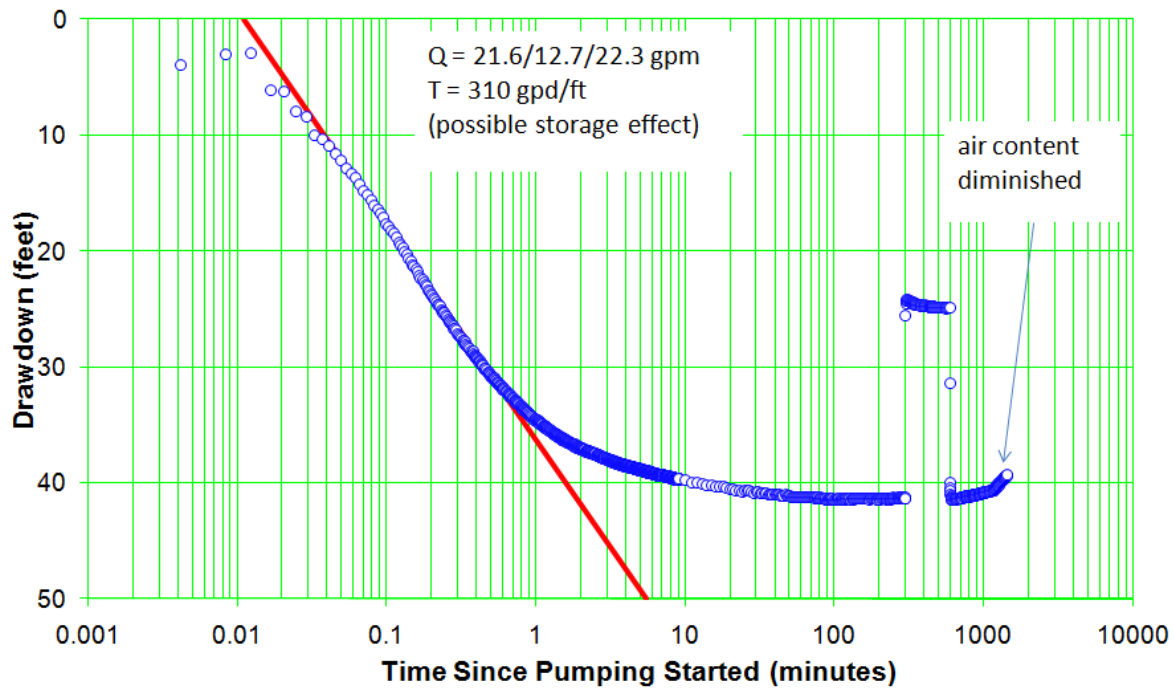


Figure C-9.4-1 Well R-61 screen 2 drawdown

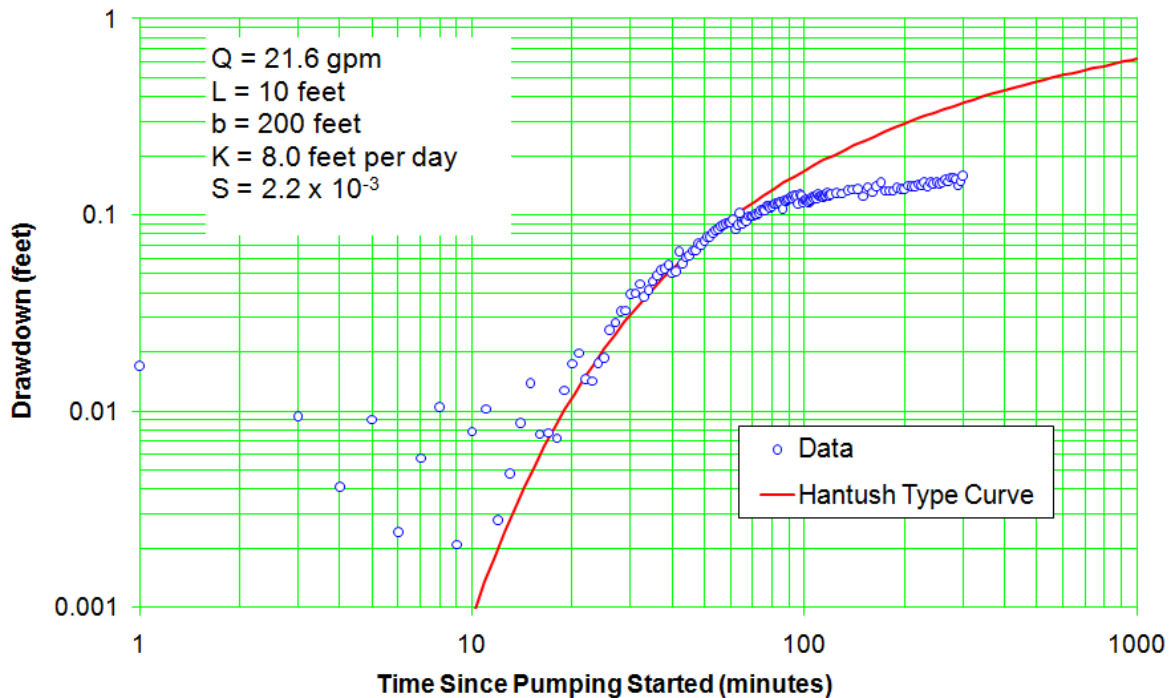


Figure C-9.4-2 Well R-61 screen 1 drawdown—Hantush solution for anisotropy of 0.1

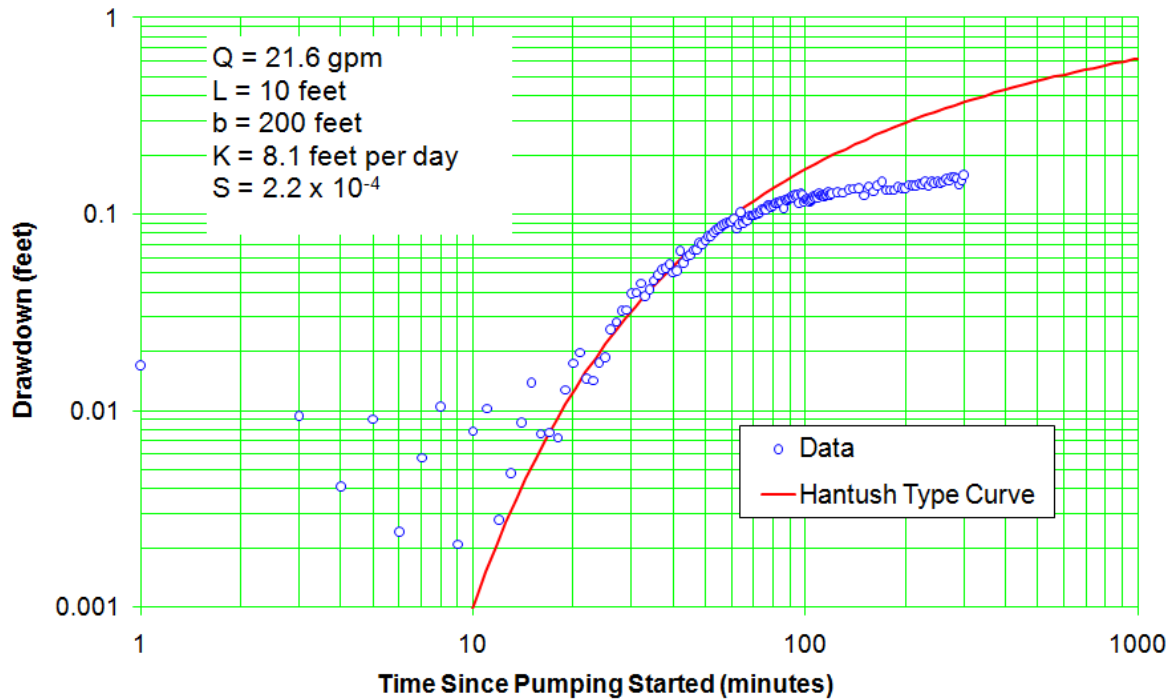


Figure C-9.4-3 Well R-61 screen 1 drawdown—Hantush solution for anisotropy of 0.01

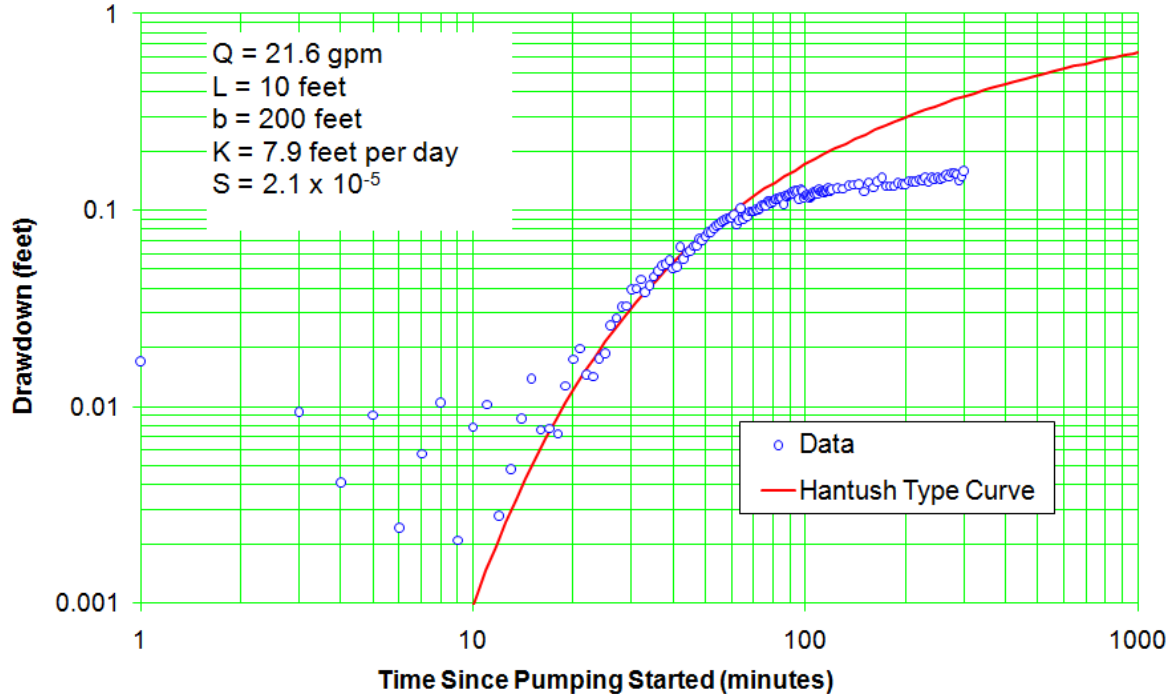


Figure C-9.4-4 Well R-61 screen 1 drawdown—Hantush solution for anisotropy of 0.001

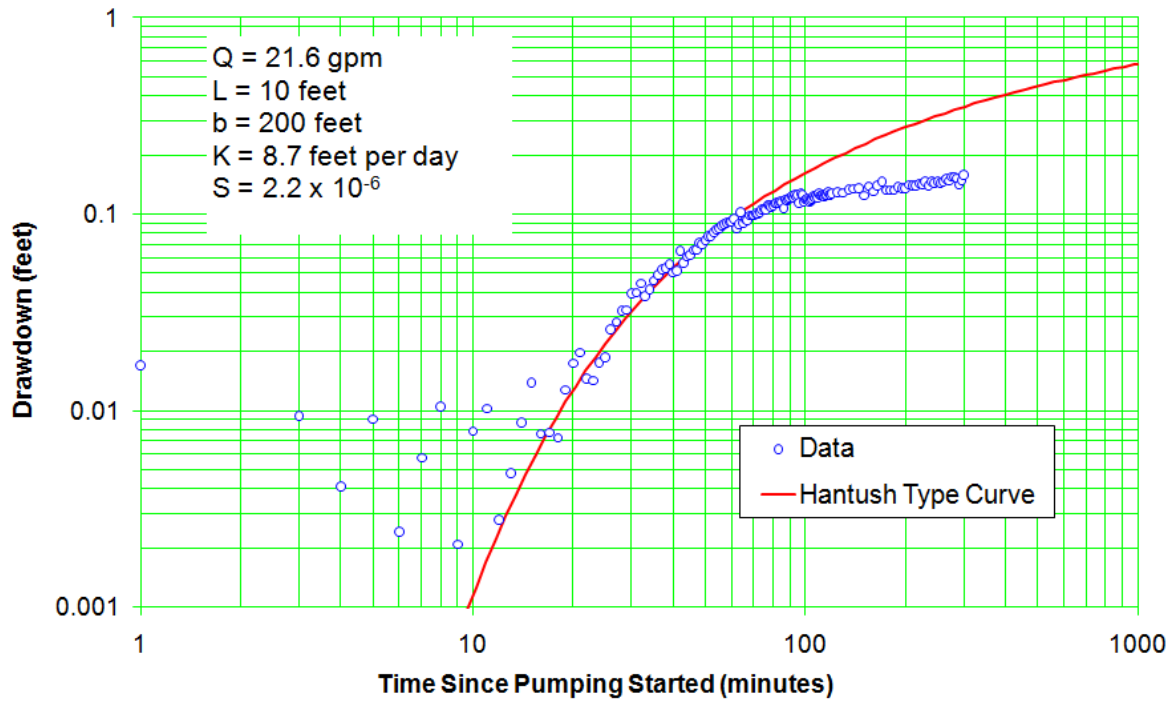


Figure C-9.4-5 Well R-61 screen 1 drawdown—Hantush solution for anisotropy of 0.0001

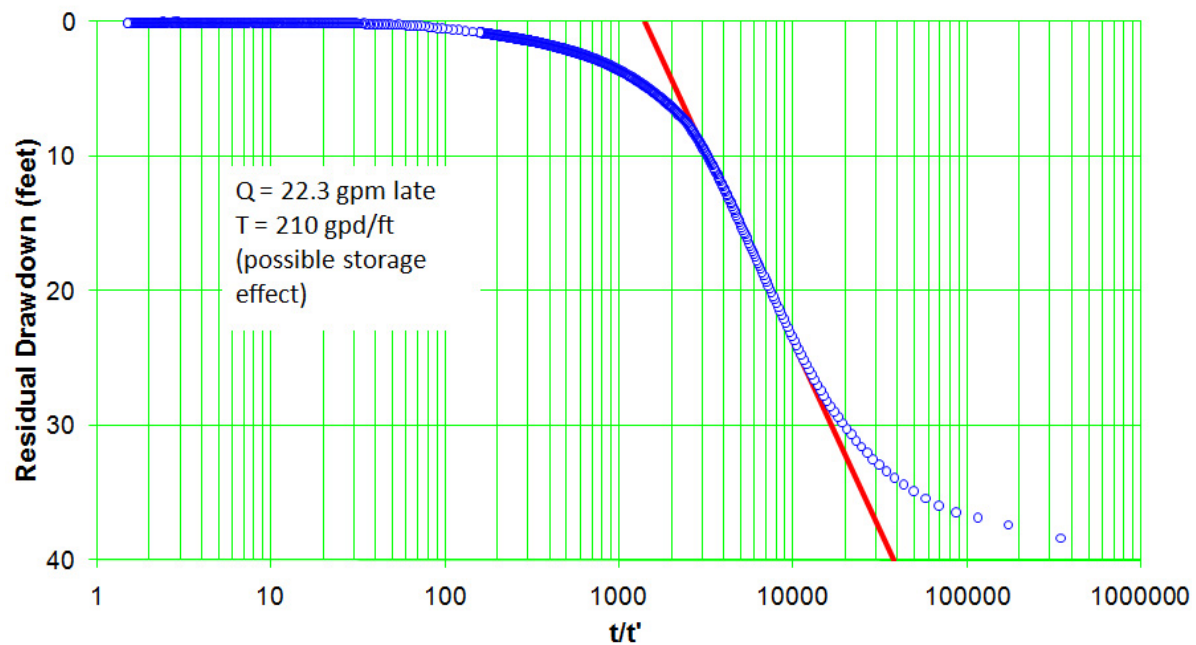


Figure C-9.4-6 Well R-61 screen 2 recovery



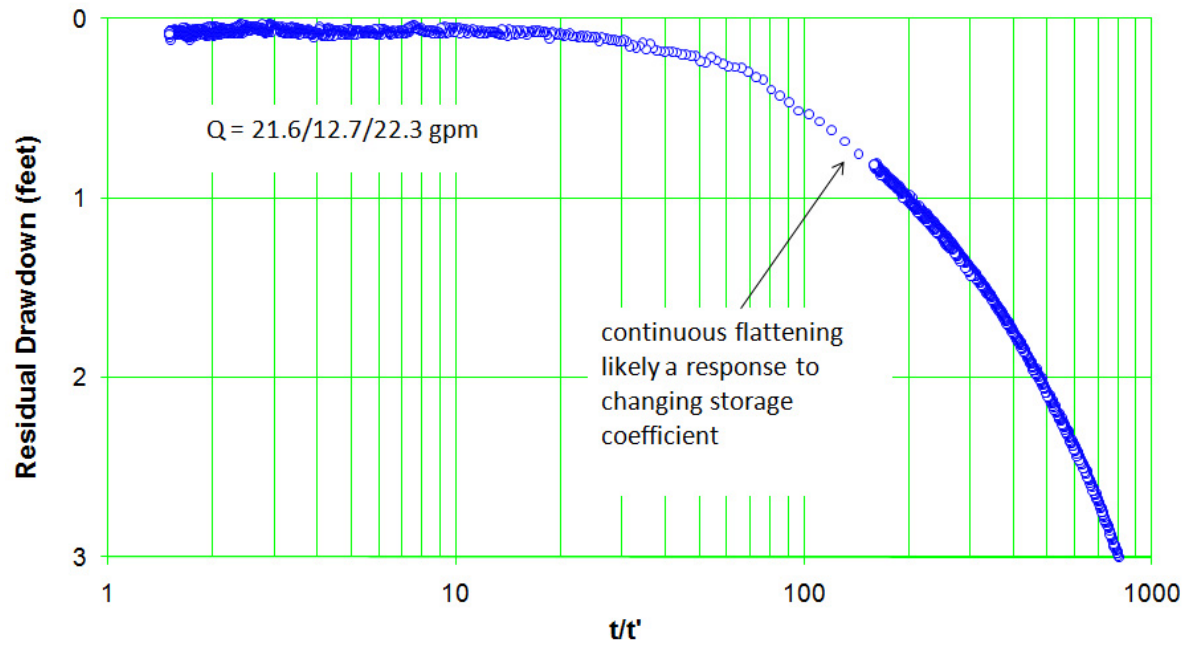


Figure C-9.4-7 Well R-61 screen 2 recovery—expanded scale



## **Appendix D**

---

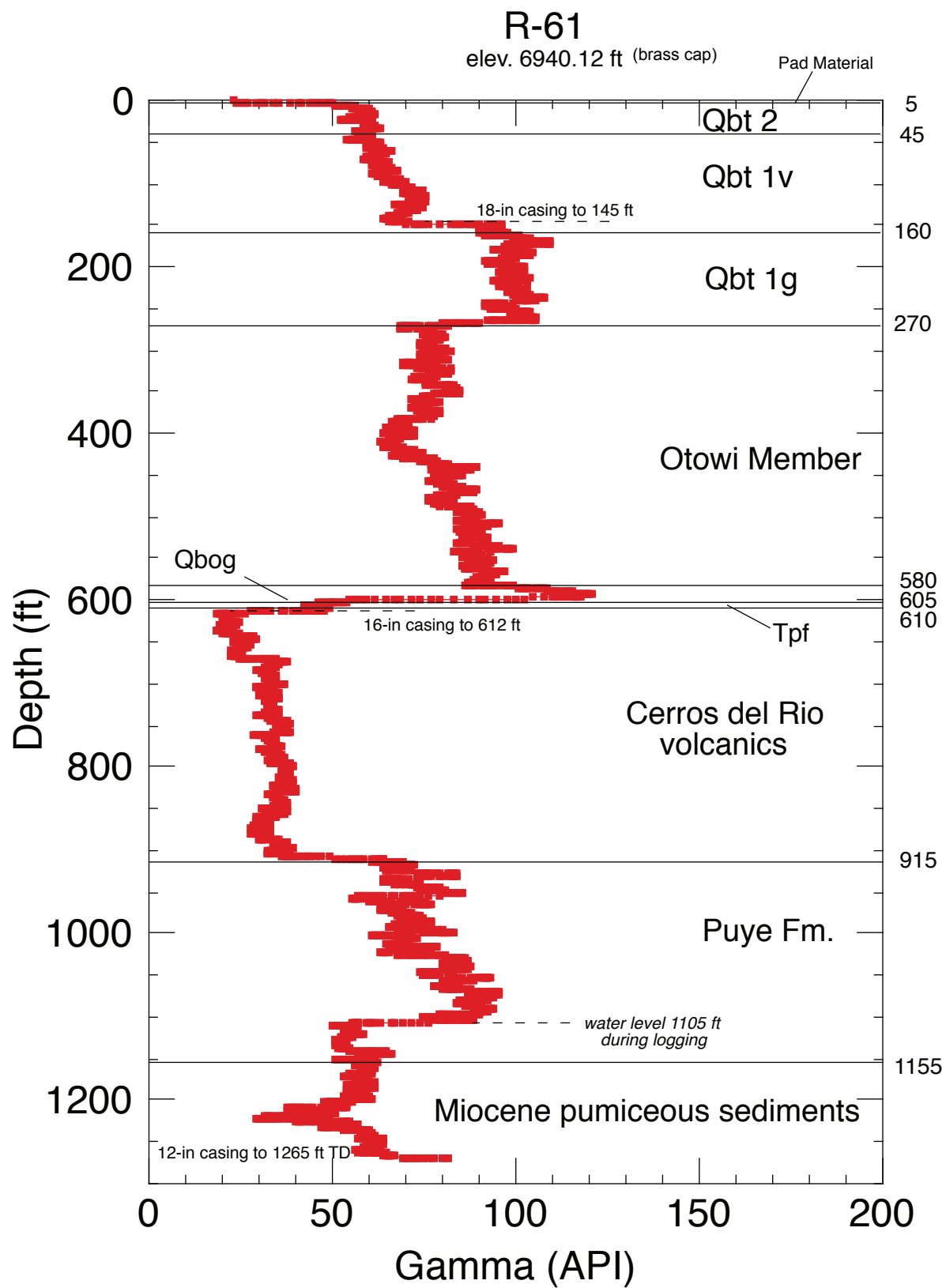
*Borehole Video Logging  
(on DVD included with this document)*

***TO VIEW THE VIDEO  
THAT ACCOMPANIES  
THIS DOCUMENT,  
PLEASE CALL THE  
HAZARDOUS WASTE  
BUREAU AT 505-476-6000  
TO MAKE AN  
APPOINTMENT***

## **Appendix E**

---

*Geophysical Logging*  
*(on CD included with this document)*



[illegible]

[illegible]





1	2	3	4	5	6	7	8	9	10	11	12	13	14	15	16	17	18	19	20	21	22	23	24	25	26	27	28	29	30	31	32	33	34	35	36	37	38	39	40	41	42	43	44	45	46	47	48	49	50	51	52	53	54	55	56	57	58	59	60	61	62	63	64	65	66	67	68	69	70	71	72	73	74	75	76	77	78	79	80	81	82	83	84	85	86	87	88	89	90	91	92	93	94	95	96	97	98	99	100
1	2	3	4	5	6	7	8	9	10	11	12	13	14	15	16	17	18	19	20	21	22	23	24	25	26	27	28	29	30	31	32	33	34	35	36	37	38	39	40	41	42	43	44	45	46	47	48	49	50	51	52	53	54	55	56	57	58	59	60	61	62	63	64	65	66	67	68	69	70	71	72	73	74	75	76	77	78	79	80	81	82	83	84	85	86	87	88	89	90	91	92	93	94	95	96	97	98	99	100
1	2	3	4	5	6	7	8	9	10	11	12	13	14	15	16	17	18	19	20	21	22	23	24	25	26	27	28	29	30	31	32	33	34	35	36	37	38	39	40	41	42	43	44	45	46	47	48	49	50	51	52	53	54	55	56	57	58	59	60	61	62	63	64	65	66	67	68	69	70	71	72	73	74	75	76	77	78	79	80	81	82	83	84	85	86	87	88	89	90	91	92	93	94	95	96	97	98	99	100
1	2	3	4	5	6	7	8	9	10	11	12	13	14	15	16	17	18	19	20	21	22	23	24	25	26	27	28	29	30	31	32	33	34	35	36	37	38	39	40	41	42	43	44	45	46	47	48	49	50	51	52	53	54	55	56	57	58	59	60	61	62	63	64	65	66	67	68	69	70	71	72	73	74	75	76	77	78	79	80	81	82	83	84	85	86	87	88	89	90	91	92	93	94	95	96	97	98	99	100
1	2	3	4	5	6	7	8	9	10	11	12	13	14	15	16	17	18	19	20	21	22	23	24	25	26	27	28	29	30	31	32	33	34	35	36	37	38	39	40	41	42	43	44	45	46	47	48	49	50	51	52	53	54	55	56	57	58	59	60	61	62	63	64	65	66	67	68	69	70	71	72	73	74	75	76	77	78	79	80	81	82	83	84	85	86	87	88	89	90	91	92	93	94	95	96	97	98	99	100
1	2	3	4	5	6	7	8	9	10	11	12	13	14	15	16	17	18	19	20	21	22	23	24	25	26	27	28	29	30	31	32	33	34	35	36	37	38	39	40	41	42	43	44	45	46	47	48	49	50	51	52	53	54	55	56	57	58	59	60	61	62	63	64	65	66	67	68	69	70	71	72	73	74	75	76	77	78	79	80	81	82	83	84	85	86	87	8												

Year	Country	Population (millions)	GDP (billion USD)	Life expectancy (years)	Infant mortality (per 1,000 live births)	Urban population (%)	Healthcare expenditure (billion USD)	Healthcare expenditure per capita (USD)
2010	USA	312	14,980	78.4	12.1	80.7	2,840	9,130
2011	USA	314	15,380	78.6	11.9	81.0	2,920	9,300
2012	USA	316	15,780	78.8	11.7	81.3	3,000	9,470
2013	USA	318	16,180	79.0	11.5	81.6	3,080	9,640
2014	USA	320	16,580	79.2	11.3	81.9	3,160	9,810
2015	USA	322	16,980	79.4	11.1	82.2	3,240	9,980
2016	USA	324	17,380	79.6	10.9	82.5	3,320	10,150
2017	USA	326	17,780	79.8	10.7	82.8	3,400	10,320
2018	USA	328	18,180	80.0	10.5	83.1	3,480	10,490
2019	USA	330	18,580	80.2	10.3	83.4	3,560	10,660
2020	USA	332	18,980	80.4	10.1	83.7	3,640	10,830
2010	China	1,370	5,880	74.8	30.1	49.6	1,120	820
2011	China	1,375	6,080	75.0	29.8	50.0	1,160	845
2012	China	1,380	6,280	75.2	29.5	50.4	1,200	870
2013	China	1,385	6,480	75.4	29.2	50.8	1,240	895
2014	China	1,390	6,680	75.6	28.9	51.2	1,280	920
2015	China	1,395	6,880	75.8	28.6	51.6	1,320	945
2016	China	1,400	7,080	76.0	28.3	52.0	1,360	970
2017	China	1,405	7,280	76.2	28.0	52.4	1,400	995
2018	China	1,410	7,480	76.4	27.7	52.8	1,440	1,020
2019	China	1,415	7,680	76.6	27.4	53.2	1,480	1,045
2020	China	1,420	7,880	76.8	27.1	53.6	1,520	1,070
2010	India	1,190	1,880	69.4	54.1	29.7	480	403
2011	India	1,200	1,980	69.6	53.8	30.1	500	417
2012	India	1,210	2,080	69.8	53.5	30.5	520	431
2013	India	1,220	2,180	70.0	53.2	30.9	540	445
2014	India	1,230	2,280	70.2	52.9	31.3	560	459
2015	India	1,240	2,380	70.4	52.6	31.7	580	473
2016	India	1,250	2,480	70.6	52.3	32.1	600	487
2017	India	1,260	2,580	70.8	52.0	32.5	620	501
2018	India	1,270	2,680	71.0	51.7	32.9	640	515
2019	India	1,280	2,780	71.2	51.4	33.3	660	529
2020	India	1,290	2,880	71.4	51.1	33.7	680	543
2010	Germany	82.0	3,780	80.6	7.1	91.3	1,120	13,660
2011	Germany	81.8	3,820	80.7	7.0	91.4	1,140	13,920
2012	Germany	81.6	3,860	80.8	6.9	91.5	1,160	14,180
2013	Germany	81.4	3,900	80.9	6.8	91.6	1,180	14,440
2014	Germany	81.2	3,940	81.0	6.7	91.7	1,200	14,700
2015	Germany	81.0	3,980	81.1	6.6	91.8	1,220	14,960
2016	Germany	80.8	4,020	81.2	6.5	91.9	1,240	15,220
2017	Germany	80.6	4,060	81.3	6.4	92.0	1,260	15,480
2018	Germany	80.4	4,100	81.4	6.3	92.1	1,280	15,740
2019	Germany	80.2	4,140	81.5	6.2	92.2	1,300	16,000
2020	Germany	80.0	4,180	81.6	6.1	92.3	1,320	16,260
2010	Japan	127.0	5,480	84.4	4.1	92.1	1,120	8,810
2011	Japan	126.8	5,520	84.5	4.0	92.2	1,140	9,070
2012	Japan	126.6	5,560	84.6	3.9	92.3</		

1  
2  
3  
4  
5  
6  
7  
8  
9  
10  
11  
12  
13  
14  
15  
16  
17  
18  
19  
20  
21  
22  
23  
24  
25  
26  
27  
28  
29  
30  
31  
32  
33  
34  
35  
36  
37  
38  
39  
40  
41  
42  
43  
44  
45  
46  
47  
48  
49  
50  
51  
52  
53  
54  
55  
56  
57  
58  
59  
60  
61  
62  
63  
64  
65  
66  
67  
68  
69  
70  
71  
72  
73  
74  
75  
76  
77  
78  
79  
80  
81  
82  
83  
84  
85  
86  
87  
88  
89  
90  
91  
92  
93  
94  
95  
96  
97  
98  
99  
100  
101  
102  
103  
104  
105  
106  
107  
108  
109  
110  
111  
112  
113  
114  
115  
116  
117  
118  
119  
120  
121  
122  
123  
124  
125  
126  
127  
128  
129  
130  
131  
132  
133  
134  
135  
136  
137  
138  
139  
140  
141  
142  
143  
144  
145  
146  
147  
148  
149  
150  
151  
152  
153  
154  
155  
156  
157  
158  
159  
160  
161  
162  
163  
164  
165  
166  
167  
168  
169  
170  
171  
172  
173  
174  
175  
176  
177  
178  
179  
180  
181  
182  
183  
184  
185  
186  
187  
188  
189  
190  
191  
192  
193  
194  
195  
196  
197  
198  
199  
200  
201  
202  
203  
204  
205  
206  
207  
208  
209  
210  
211  
212  
213  
214  
215  
216  
217  
218  
219  
220  
221  
222  
223  
224  
225  
226  
227  
228  
229  
230  
231  
232  
233  
234  
235  
236  
237  
238  
239  
240  
241  
242  
243  
244  
245  
246  
247  
248  
249  
250  
251  
252  
253  
254  
255  
256  
257  
258  
259  
260  
261  
262  
263  
264  
265  
266  
267  
268  
269  
270  
271  
272  
273  
274  
275  
276  
277  
278  
279  
280  
281  
282  
283  
284  
285  
286  
287  
288  
289  
290  
291  
292  
293  
294  
295  
296  
297  
298  
299  
300  
301  
302  
303  
304  
305  
306  
307  
308  
309  
310  
311  
312  
313  
314  
315  
316  
317  
318  
319  
320  
321  
322  
323  
324  
325  
326  
327  
328  
329  
330  
331  
332  
333  
334  
335  
336  
337  
338  
339  
340  
341  
342  
343  
344  
345  
346  
347  
348  
349  
350  
351  
352  
353  
354  
355  
356  
357  
358  
359  
360  
361  
362  
363  
364  
365  
366  
367  
368  
369  
370  
371  
372  
373  
374  
375  
376  
377  
378  
379  
380  
381  
382  
383  
384  
385  
386  
387  
388  
389  
390  
391  
392  
393  
394  
395  
396  
397  
398  
399  
400  
401  
402  
403  
404  
405  
406  
407  
408  
409  
410  
411  
412  
413  
414  
415  
416  
417  
418  
419  
420  
421  
422  
423  
424  
425  
426  
427  
428  
429  
430  
431  
432  
433  
434  
435  
436  
437  
438  
439  
440  
441  
442  
443  
444  
445  
446  
447  
448  
449  
450  
451  
452  
453  
454  
455  
456  
457  
458  
459  
460  
461  
462  
463  
464  
465  
466  
467  
468  
469  
470  
471  
472  
473  
474  
475  
476  
477  
478  
479  
480  
481  
482  
483  
484  
485  
486  
487  
488  
489  
490  
491  
492  
493  
494  
495  
496  
497  
498  
499  
500  
501  
502  
503  
504  
505  
506  
507  
508  
509  
510  
511  
512  
513  
514  
515  
516  
517  
518  
519  
520  
521  
522  
523  
524  
525  
526  
527  
528  
529  
530  
531  
532  
533  
534  
535  
536  
537  
538  
539  
540  
541  
542  
543  
544  
545  
546  
547  
548  
549  
550  
551  
552  
553  
554  
555  
556  
557  
558  
559  
560  
561  
562  
563  
564  
565  
566  
567  
568  
569  
570  
571  
572  
573  
574  
575  
576  
577  
578  
579  
580  
581  
582  
583  
584  
585  
586  
587  
588  
589  
590  
591  
592  
593  
594  
595  
596  
597  
598  
599  
600  
601  
602  
603  
604  
605  
606  
607  
608  
609  
610  
611  
612  
613  
614  
615  
616  
617  
618  
619  
620  
621  
622  
623  
624  
625  
626  
627  
628  
629  
630  
631  
632  
633  
634  
635  
636  
637  
638  
639  
640  
641  
642  
643  
644  
645  
646  
647  
648  
649  
650  
651  
652  
653  
654  
655  
656  
657  
658  
659  
660  
661  
662  
663  
664  
665  
666  
667  
668  
669  
670  
671  
672  
673  
674  
675  
676  
677  
678  
679  
680  
681  
682  
683  
684  
685  
686  
687  
688  
689  
690  
691  
692  
693  
694  
695  
696  
697  
698  
699  
700  
701  
702  
703  
704  
705  
706  
707  
708  
709  
710  
711  
712  
713  
714  
715  
716  
717  
718  
719  
720  
721  
722  
723  
724  
725  
726  
727  
728  
729  
730  
731  
732  
733  
734  
735  
736  
737  
738  
739  
740  
741  
742  
743  
744  
745  
746  
747  
748  
749  
750  
751  
752  
753  
754  
755  
756  
757  
758  
759  
760  
761  
762  
763  
764  
765  
766  
767  
768  
769  
770  
771  
772  
773  
774  
775  
776  
777  
778  
779  
780  
781  
782  
783  
784  
785  
786  
787  
788  
789  
790  
791  
792  
793  
794  
795  
796  
797  
798  
799  
800  
801  
802  
803  
804  
805  
806  
807  
808  
809  
810  
811  
812  
813  
814  
815  
816  
817  
818  
819  
820  
821  
822  
823  
824  
825  
826  
827  
828  
829  
830  
831  
832  
833  
834  
835  
836  
837  
838  
839  
840  
841  
842  
843  
844  
845  
846  
847  
848  
849  
850  
851  
852  
853  
854  
855  
856  
857  
858  
859  
860  
861  
862  
863  
864  
865  
866  
867  
868  
869  
870  
871  
872  
873  
874  
875  
876  
877  
878  
879  
880  
881  
882  
883  
884  
885  
886  
887  
888  
889  
890  
891  
892  
893  
894  
895  
896  
897  
898  
899  
900  
901  
902  
903  
904  
905  
906  
907  
908  
909  
910  
911  
912  
913  
914  
915  
916  
917  
918  
919  
920  
921  
922  
923  
924  
925  
926  
927  
928  
929  
930  
931  
932  
933  
934  
935  
936  
937  
938  
939  
940  
941  
942  
943  
944  
945  
946  
947  
948  
949  
950  
951  
952  
953  
954  
955  
956  
957  
958  
959  
960  
961  
962  
963  
964  
965  
966  
967  
968  
969  
970  
971  
972  
973  
974  
975  
976  
977  
978  
979  
980  
981  
982  
983  
984  
985  
986  
987  
988  
989  
990  
991  
992  
993  
994  
995  
996  
997  
998  
999  
1000

[illegible]

Year	Country	Population (millions)	GDP (billion USD)	Life expectancy (years)	Infant mortality (per 1,000 live births)	Urban population (%)	Healthcare expenditure (billion USD)	Healthcare expenditure per capita (USD)
1950	USA	150	200	72	26	65	10	66
1950	USSR	160	100	68	30	40	5	31
1950	China	550	50	45	100	15	1	18
1950	India	360	20	47	150	10	0.5	14
1950	Japan	90	100	75	20	70	10	111
1950	UK	55	100	72	20	85	10	182
1950	France	45	100	72	20	85	10	222
1950	Germany	50	100	72	20	85	10	200
1950	Italy	45	100	72	20	85	10	222
1950	Soviet Union	160	100	68	30	40	5	31
1950	USA	150	200	72	26	65	10	66
1950	USSR	160	100	68	30	40	5	31
1950	China	550	50	45	100	15	1	18
1950	India	360	20	47	150	10	0.5	14
1950	Japan	90	100	75	20	70	10	111
1950	UK	55	100	72	20	85	10	182
1950	France	45	100	72	20	85	10	222
1950	Germany	50	100	72	20	85	10	200
1950	Italy	45	100	72	20	85	10	222
1950	Soviet Union	160	100	68	30	40	5	31
1950	USA	150	200	72	26	65	10	66
1950	USSR	160	100	68	30	40	5	31
1950	China	550	50	45	100	15	1	18
1950	India	360	20	47	150	10	0.5	14
1950	Japan	90	100	75	20	70	10	111
1950	UK	55	100	72	20	85	10	182
1950	France	45	100	72	20	85	10	222
1950	Germany	50	100	72	20	85	10	200
1950	Italy	45	100	72	20	85	10	222
1950	Soviet Union	160	100	68	30	40	5	31
1950	USA	150	200	72	26	65	10	66
1950	USSR	160	100	68	30	40	5	31
1950	China	550	50	45	100	15	1	18
1950	India	360	20	47	150	10	0.5	14
1950	Japan	90	100	75	20	70	10	111
1950	UK	55	100	72	20	85	10	182
1950	France	45	100	72	20	85	10	222
1950	Germany	50	100	72	20	85	10	200
1950	Italy	45	100	72	20	85	10	222
1950	Soviet Union	160	100	68	30	40	5	31
1950	USA	150	200	72	26	65	10	66
1950	USSR	160	100	68	30	40	5	31
1950	China	550	50	45	100	15	1	18
1950	India	360	20	47	150	10	0.5	14
1950	Japan	90	100	75	20	70	10	111
1950	UK	55	100	72	20	85	10	182
1950	France	45	100	72	20	85	10	222
1950	Germany	50	100	72	20	85	10	200
1950	Italy	45	100	72	20	85	10	222
1950	Soviet Union	160	100	68	30	40	5	31
1950	USA	150	200	72	26	65	10	66
1950	USSR	160	100	68	30	40	5	31
1950	China	550	50	45	100	15	1	18
1950	India	360	20	47	150	10	0.5	14
1950	Japan	90	100	75	20	70	10	111
1950	UK	55	100	72	20	85	10	182

[illegible]

Year	Country	Population (millions)	GDP (billion USD)	Life expectancy (years)	Infant mortality (per 1,000 live births)	Urban population (%)	Renewable energy (%)	Forest cover (%)	CO2 emissions (million tons)	Water stress (%)	Land use change (ha)	Waste management (%)	Healthcare expenditure (%)	Education expenditure (%)	Gender inequality index	Corruption index	Trust index	Life satisfaction	Human development index	Quality of life index	Environmental quality index	Social quality index	Economic quality index	Political quality index	Overall quality index
2015	USA	321.0	16.5	78.5	10.0	80.0	12.0	23.0	5.0	15.0	1.0	65.0	10.0	2.5	0.75	0.85	0.90	7.5	0.85	8.5	7.0	8.0	7.5	8.0	7.5
2016	USA	323.0	16.8	78.8	9.5	81.0	13.0	24.0	5.5	16.0	1.0	66.0	10.5	2.6	0.76	0.86	0.91	7.6	0.86	8.6	7.1	8.1	7.6	8.1	7.6
2017	USA	325.0	17.1	79.0	9.0	82.0	14.0	25.0	6.0	17.0	1.0	67.0	11.0	2.7	0.77	0.87	0.92	7.7	0.87	8.7	7.2	8.2	7.7	8.2	7.7
2018	USA	327.0	17.4	79.2	8.5	83.0	15.0	26.0	6.5	18.0	1.0	68.0	11.5	2.8	0.78	0.88	0.93	7.8	0.88	8.8	7.3	8.3	7.8	8.3	7.8
2019	USA	329.0	17.7	79.5	8.0	84.0	16.0	27.0	7.0	19.0	1.0	69.0	12.0	2.9	0.79	0.89	0.94	7.9	0.89	8.9	7.4	8.4	7.9	8.4	7.9
2020	USA	331.0	18.0	79.8	7.5	85.0	17.0	28.0	7.5	20.0	1.0	70.0	12.5	3.0	0.80	0.90	0.95	8.0	0.90	9.0	7.5	8.5	8.0	8.5	8.0
2021	USA	333.0	18.3	80.0	7.0	86.0	18.0	29.0	8.0	21.0	1.0	71.0	13.0	3.1	0.81	0.91	0.96	8.1	0.91	9.1	7.6	8.6	8.1	8.6	8.1
2022	USA	335.0	18.6	80.2	6.5	87.0	19.0	30.0	8.5	22.0	1.0	72.0	13.5	3.2	0.82	0.92	0.97	8.2	0.92	9.2	7.7	8.7	8.2	8.7	8.2
2023	USA	337.0	18.9	80.5	6.0	88.0	20.0	31.0	9.0	23.0	1.0	73.0	14.0	3.3	0.83	0.93	0.98	8.3	0.93	9.3	7.8	8.8	8.3	8.8	8.3
2024	USA	339.0	19.2	80.8	5.5	89.0	21.0	32.0	9.5	24.0	1.0	74.0	14.5	3.4	0.84	0.94	0.99	8.4	0.94	9.4	7.9	8.9	8.4	8.9	8.4
2025	USA	341.0	19.5	81.0	5.0	90.0	22.0	33.0	10.0	25.0	1.0	75.0	15.0	3.5	0.85	0.95	1.00	8.5	0.95	9.5	8.0	9.0	8.5	9.0	8.5
2026	USA	343.0	19.8	81.2	4.5	91.0	23.0	34.0	10.5	26.0	1.0	76.0	15.5	3.6	0.86	0.96	1.00	8.6	0.96	9.6	8.1	9.1	8.6	9.1	8.6
2027	USA	345.0	20.1	81.5	4.0	92.0	24.0	35.0	11.0	27.0	1.0	77.0	16.0	3.7	0.87	0.97	1.00	8.7	0.97	9.7	8.2	9.2	8.7	9.2	8.7
2028	USA	347.0	20.4	81.8	3.5	93.0	25.0	36.0	11.5	28.0	1.0	78.0	16.5	3.8	0.88	0.98	1.00	8.8	0.98	9.8	8.3	9.3	8.8	9.3	8.8
2029	USA	349.0	20.7	82.0	3.0	94.0	26.0	37.0	12.0	29.0	1.0	79.0	17.0	3.9	0.89	0.99	1.00	8.9	0.99	9.9	8.4	9.4	8.9	9.4	8.9
2030	USA	351.0	21.0	82.2	2.5	95.0	27.0	38.0	12.5	30.0	1.0	80.0	17.5	4.0	0.90	1.00	1.00	9.0	1.00	10.0	8.5	9.5	9.0	9.5	9.0
2031	USA	353.0	21.3	82.5	2.0	96.0	28.0	39.0	13.0	31.0	1.0	81.0	18.0	4.1	0.91	1.00	1.00	9.1	1.00	10.1	8.6	9.6	9.1	9.6	9.1



Year	Country	Population (millions)	GDP (billion USD)	Life expectancy (years)	Infant mortality (per 1,000 live births)	Urban population (%)	Healthcare expenditure (billion USD)	Healthcare expenditure per capita (USD)
2010	USA	312	14,980	78.4	12.1	80.7	2,540	8,140
2011	USA	314	15,380	78.6	11.9	81.0	2,600	8,280
2012	USA	316	15,780	78.8	11.7	81.3	2,660	8,420
2013	USA	318	16,180	79.0	11.5	81.6	2,720	8,560
2014	USA	320	16,580	79.2	11.3	81.9	2,780	8,700
2015	USA	322	16,980	79.4	11.1	82.2	2,840	8,840
2016	USA	324	17,380	79.6	10.9	82.5	2,900	8,980
2017	USA	326	17,780	79.8	10.7	82.8	2,960	9,120
2018	USA	328	18,180	80.0	10.5	83.1	3,020	9,260
2019	USA	330	18,580	80.2	10.3	83.4	3,080	9,400
2020	USA	332	18,980	80.4	10.1	83.7	3,140	9,540
2021	USA	334	19,380	80.6	9.9	84.0	3,200	9,680
2022	USA	336	19,780	80.8	9.7	84.3	3,260	9,820
2023	USA	338	20,180	81.0	9.5	84.6	3,320	9,960
2024	USA	340	20,580	81.2	9.3	84.9	3,380	10,100
2025	USA	342	20,980	81.4	9.1	85.2	3,440	10,240
2026	USA	344	21,380	81.6	8.9	85.5	3,500	10,380
2027	USA	346	21,780	81.8	8.7	85.8	3,560	10,520
2028	USA	348	22,180	82.0	8.5	86.1	3,620	10,660
2029	USA	350	22,580	82.2	8.3	86.4	3,680	10,800
2030	USA	352	22,980	82.4	8.1	86.7	3,740	10,940
2031	USA	354	23,380	82.6	7.9	87.0	3,800	11,080
2032	USA	356	23,780	82.8	7.7	87.3	3,860	11,220
2033	USA	358	24,180	83.0	7.5	87.6	3,920	11,360
2034	USA	360	24,580	83.2	7.3	87.9	3,980	11,500
2035	USA	362	24,980	83.4	7.1	88.2	4,040	11,640
2036	USA	364	25,380	83.6	6.9	88.5	4,100	11,780
2037	USA	366	25,780	83.8	6.7	88.8	4,160	11,920
2038	USA	368	26,180	84.0	6.5	89.1	4,220	12,060
2039	USA	370	26,580	84.2	6.3	89.4	4,280	12,200
2040	USA	372	26,980	84.4	6.1	89.7	4,340	12,340
2041	USA	374	27,380	84.6	5.9	90.0	4,400	12,480
2042	USA	376	27,780	84.8	5.7	90.3	4,460	12,620
2043	USA	378	28,180	85.0	5.5	90.6	4,520	12,760
2044	USA	380	28,580	85.2	5.3	90.9	4,580	12,900
2045	USA	382	28,980	85.4	5.1	91.2	4,640	13,040
2046	USA	384	29,380	85.6	4.9	91.5	4,700	13,180
2047	USA	386	29,780	85.8	4.7	91.8	4,760	13,320
2048	USA	388	30,180	86.0	4.5	92.1	4,820	13,460
2049	USA	390	30,580	86.2	4.3	92.4	4,880	13,600
2050	USA	392	30,980	86.4	4.1	92.7	4,940	13,740
2051	USA	394	31,380	86.6	3.9	93.0	5,000	13,880
2052	USA	396	31,780	86.8	3.7	93.3	5,060	14,020
2053	USA	398	32,180	87.0	3.5	93.6	5,120	14,160
2054	USA	400	32,580	87.2	3.3	93.9	5,180	14,300
2055	USA	402	32,980	87.4	3.1	94.2	5,240	14,440
2056	USA	404	33,3					



Year	Country	Population (millions)	GDP (billion USD)	Life expectancy (years)	Infant mortality (per 1,000 live births)	Urban population (%)	Healthcare expenditure (billion USD)	Healthcare expenditure per capita (USD)
2010	USA	312	14,980	78.4	12.1	80.9	3,120	10,000
2011	USA	314	15,380	78.6	11.9	81.1	3,200	10,200
2012	USA	316	15,780	78.8	11.7	81.3	3,280	10,400
2013	USA	318	16,180	79.0	11.5	81.5	3,360	10,600
2014	USA	320	16,580	79.2	11.3	81.7	3,440	10,800
2015	USA	322	16,980	79.4	11.1	81.9	3,520	11,000
2016	USA	324	17,380	79.6	10.9	82.1	3,600	11,200
2017	USA	326	17,780	79.8	10.7	82.3	3,680	11,400
2018	USA	328	18,180	80.0	10.5	82.5	3,760	11,600
2019	USA	330	18,580	80.2	10.3	82.7	3,840	11,800
2020	USA	332	18,980	80.4	10.1	82.9	3,920	12,000
2010	China	1,370	5,880	74.8	21.5	51.2	1,370	10,000
2011	China	1,375	6,080	75.0	21.0	51.5	1,400	10,200
2012	China	1,380	6,280	75.2	20.5	51.8	1,430	10,400
2013	China	1,385	6,480	75.4	20.0	52.1	1,460	10,600
2014	China	1,390	6,680	75.6	19.5	52.4	1,490	10,800
2015	China	1,395	6,880	75.8	19.0	52.7	1,520	11,000
2016	China	1,400	7,080	76.0	18.5	53.0	1,550	11,200
2017	China	1,405	7,280	76.2	18.0	53.3	1,580	11,400
2018	China	1,410	7,480	76.4	17.5	53.6	1,610	11,600
2019	China	1,415	7,680	76.6	17.0	53.9	1,640	11,800
2020	China	1,420	7,880	76.8	16.5	54.2	1,670	12,000
2010	India	1,190	1,980	69.4	45.5	29.8	1,190	10,000
2011	India	1,200	2,080	69.6	44.5	30.1	1,200	10,200
2012	India	1,210	2,180	69.8	43.5	30.4	1,210	10,400
2013	India	1,220	2,280	70.0	42.5	30.7	1,220	10,600
2014	India	1,230	2,380	70.2	41.5	31.0	1,230	10,800
2015	India	1,240	2,480	70.4	40.5	31.3	1,240	11,000
2016	India	1,250	2,580	70.6	39.5	31.6	1,250	11,200
2017	India	1,260	2,680	70.8	38.5	31.9	1,260	11,400
2018	India	1,270	2,780	71.0	37.5	32.2	1,270	11,600
2019	India	1,280	2,880	71.2	36.5	32.5	1,280	11,800
2020	India	1,290	2,980	71.4	35.5	32.8	1,290	12,000
2010	Germany	82.0	3,580	80.8	7.5	73.5	3,580	43,800
2011	Germany	82.5	3,680	81.0	7.3	73.8	3,600	43,800
2012	Germany	83.0	3,780	81.2	7.1	74.1	3,620	43,800
2013	Germany	83.5	3,880	81.4	6.9	74.4	3,640	43,800
2014	Germany	84.0	3,980	81.6	6.7	74.7	3,660	43,800
2015	Germany	84.5	4,080	81.8	6.5	75.0	3,680	43,800
2016	Germany	85.0	4,180	82.0	6.3	75.3	3,700	43,800
2017	Germany	85.5	4,280	82.2	6.1	75.6	3,720	43,800
2018	Germany	86.0	4,380	82.4	5.9	75.9	3,740	43,800
2019	Germany	86.5	4,480	82.6	5.7	76.2	3,760	43,800
2020	Germany	87.0	4,580	82.8	5.5	76.5	3,780	43,800
2010	Japan	127.0	5,480	84.4	5.5	91.5	5,480	43,000
2011	Japan	127.5	5,580	84.6	5.3	91		

1  
2  
3  
4  
5  
6  
7  
8  
9  
10  
11  
12  
13  
14  
15  
16  
17  
18  
19  
20  
21  
22  
23  
24  
25  
26  
27  
28  
29  
30  
31  
32  
33  
34  
35  
36  
37  
38  
39  
40  
41  
42  
43  
44  
45  
46  
47  
48  
49  
50  
51  
52  
53  
54  
55  
56  
57  
58  
59  
60  
61  
62  
63  
64  
65  
66  
67  
68  
69  
70  
71  
72  
73  
74  
75  
76  
77  
78  
79  
80  
81  
82  
83  
84  
85  
86  
87  
88  
89  
90  
91  
92  
93  
94  
95  
96  
97  
98  
99  
100  
101  
102  
103  
104  
105  
106  
107  
108  
109  
110  
111  
112  
113  
114  
115  
116  
117  
118  
119  
120  
121  
122  
123  
124  
125  
126  
127  
128  
129  
130  
131  
132  
133  
134  
135  
136  
137  
138  
139  
140  
141  
142  
143  
144  
145  
146  
147  
148  
149  
150  
151  
152  
153  
154  
155  
156  
157  
158  
159  
160  
161  
162  
163  
164  
165  
166  
167  
168  
169  
170  
171  
172  
173  
174  
175  
176  
177  
178  
179  
180  
181  
182  
183  
184  
185  
186  
187  
188  
189  
190  
191  
192  
193  
194  
195  
196  
197  
198  
199  
200  
201  
202  
203  
204  
205  
206  
207  
208  
209  
210  
211  
212  
213  
214  
215  
216  
217  
218  
219  
220  
221  
222  
223  
224  
225  
226  
227  
228  
229  
230  
231  
232  
233  
234  
235  
236  
237  
238  
239  
240  
241  
242  
243  
244  
245  
246  
247  
248  
249  
250  
251  
252  
253  
254  
255  
256  
257  
258  
259  
260  
261  
262  
263  
264  
265  
266  
267  
268  
269  
270  
271  
272  
273  
274  
275  
276  
277  
278  
279  
280  
281  
282  
283  
284  
285  
286  
287  
288  
289  
290  
291  
292  
293  
294  
295  
296  
297  
298  
299  
300  
301  
302  
303  
304  
305  
306  
307  
308  
309  
310  
311  
312  
313  
314  
315  
316  
317  
318  
319  
320  
321  
322  
323  
324  
325  
326  
327  
328  
329  
330  
331  
332  
333  
334  
335  
336  
337  
338  
339  
340  
341  
342  
343  
344  
345  
346  
347  
348  
349  
350  
351  
352  
353  
354  
355  
356  
357  
358  
359  
360  
361  
362  
363  
364  
365  
366  
367  
368  
369  
370  
371  
372  
373  
374  
375  
376  
377  
378  
379  
380  
381  
382  
383  
384  
385  
386  
387  
388  
389  
390  
391  
392  
393  
394  
395  
396  
397  
398  
399  
400  
401  
402  
403  
404  
405  
406  
407  
408  
409  
410  
411  
412  
413  
414  
415  
416  
417  
418  
419  
420  
421  
422  
423  
424  
425  
426  
427  
428  
429  
430  
431  
432  
433  
434  
435  
436  
437  
438  
439  
440  
441  
442  
443  
444  
445  
446  
447  
448  
449  
450  
451  
452  
453  
454  
455  
456  
457  
458  
459  
460  
461  
462  
463  
464  
465  
466  
467  
468  
469  
470  
471  
472  
473  
474  
475  
476  
477  
478  
479  
480  
481  
482  
483  
484  
485  
486  
487  
488  
489  
490  
491  
492  
493  
494  
495  
496  
497  
498  
499  
500  
501  
502  
503  
504  
505  
506  
507  
508  
509  
510  
511  
512  
513  
514  
515  
516  
517  
518  
519  
520  
521  
522  
523  
524  
525  
526  
527  
528  
529  
530  
531  
532  
533  
534  
535  
536  
537  
538  
539  
540  
541  
542  
543  
544  
545  
546  
547  
548  
549  
550  
551  
552  
553  
554  
555  
556  
557  
558  
559  
560  
561  
562  
563  
564  
565  
566  
567  
568  
569  
570  
571  
572  
573  
574  
575  
576  
577  
578  
579  
580  
581  
582  
583  
584  
585  
586  
587  
588  
589  
590  
591  
592  
593  
594  
595  
596  
597  
598  
599  
600  
601  
602  
603  
604  
605  
606  
607  
608  
609  
610  
611  
612  
613  
614  
615  
616  
617  
618  
619  
620  
621  
622  
623  
624  
625  
626  
627  
628  
629  
630  
631  
632  
633  
634  
635  
636  
637  
638  
639  
640  
641  
642  
643  
644  
645  
646  
647  
648  
649  
650  
651  
652  
653  
654  
655  
656  
657  
658  
659  
660  
661  
662  
663  
664  
665  
666  
667  
668  
669  
670  
671  
672  
673  
674  
675  
676  
677  
678  
679  
680  
681  
682  
683  
684  
685  
686  
687  
688  
689  
690  
691  
692  
693  
694  
695  
696  
697  
698  
699  
700  
701  
702  
703  
704  
705  
706  
707  
708  
709  
710  
711  
712  
713  
714  
715  
716  
717  
718  
719  
720  
721  
722  
723  
724  
725  
726  
727  
728  
729  
730  
731  
732  
733  
734  
735  
736  
737  
738  
739  
740  
741  
742  
743  
744  
745  
746  
747  
748  
749  
750  
751  
752  
753  
754  
755  
756  
757  
758  
759  
760  
761  
762  
763  
764  
765  
766  
767  
768  
769  
770  
771  
772  
773  
774  
775  
776  
777  
778  
779  
780  
781  
782  
783  
784  
785  
786  
787  
788  
789  
790  
791  
792  
793  
794  
795  
796  
797  
798  
799  
800  
801  
802  
803  
804  
805  
806  
807  
808  
809  
810  
811  
812  
813  
814  
815  
816  
817  
818  
819  
820  
821  
822  
823  
824  
825  
826  
827  
828  
829  
830  
831  
832  
833  
834  
835  
836  
837  
838  
839  
840  
841  
842  
843  
844  
845  
846  
847  
848  
849  
850  
851  
852  
853  
854  
855  
856  
857  
858  
859  
860  
861  
862  
863  
864  
865  
866  
867  
868  
869  
870  
871  
872  
873  
874  
875  
876  
877  
878  
879  
880  
881  
882  
883  
884  
885  
886  
887  
888  
889  
890  
891  
892  
893  
894  
895  
896  
897  
898  
899  
900  
901  
902  
903  
904  
905  
906  
907  
908  
909  
910  
911  
912  
913  
914  
915  
916  
917  
918  
919  
920  
921  
922  
923  
924  
925  
926  
927  
928  
929  
930  
931  
932  
933  
934  
935  
936  
937  
938  
939  
940  
941  
942  
943  
944  
945  
946  
947  
948  
949  
950  
951  
952  
953  
954  
955  
956  
957  
958  
959  
960  
961  
962  
963  
964  
965  
966  
967  
968  
969  
970  
971  
972  
973  
974  
975  
976  
977  
978  
979  
980  
981  
982  
983  
984  
985  
986  
987  
988  
989  
990  
991  
992  
993  
994  
995  
996  
997  
998  
999  
1000

Year	1990	1991	1992	1993	1994	1995	1996	1997	1998	1999	2000	2001	2002	2003	2004	2005	2006	2007	2008	2009	2010	2011	2012	2013	2014	2015	2016	2017	2018	2019	2020	2021	2022	2023	2024	2025	2026	2027	2028	2029	2030	2031	2032	2033	2034	2035	2036	2037	2038	2039	2040	2041	2042	2043	2044	2045	2046	2047	2048	2049	2050	2051	2052	2053	2054	2055	2056	2057	2058	2059	2060	2061	2062	2063	2064	2065	2066	2067	2068	2069	2070	2071	2072	2073	2074	2075	2076	2077	2078	2079	2080	2081	2082	2083	2084	2085	2086	2087	2088	2089	2090	2091	2092	2093	2094	2095	2096	2097	2098	2099	2100
1990	1991	1992	1993	1994	1995	1996	1997	1998	1999	2000	2001	2002	2003	2004	2005	2006	2007	2008	2009	2010	2011	2012	2013	2014	2015	2016	2017	2018	2019	2020	2021	2022	2023	2024	2025	2026	2027	2028	2029	2030	2031	2032	2033	2034	2035	2036	2037	2038	2039	2040	2041	2042	2043	2044	2045	2046	2047	2048	2049	2050	2051	2052	2053	2054	2055	2056	2057	2058	2059	2060	2061	2062	2063	2064	2065	2066	2067	2068	2069	2070	2071	2072	2073	2074	2075	2076	2077	2078	2079	2080	2081	2082	2083	2084	2085	2086	2087	2088	2089	2090	2091	2092	2093	2094	2095	2096	2097	2098	2099	2100	

[illegible]

## **Appendix F**

---

*R-61 Final Well Design and  
New Mexico Environment Department Approval*

Note: The information in the final well design package was developed at the completion of borehole drilling and before development of the final lithologic log. The preliminary information in the well design summary may differ slightly from the final lithologic interpretations or data presented in the well completion report.



## R-61 Well Objectives

The R-61 well is intended to further define the southern extent of chromium contamination in the regional aquifer. R-61 is located to intersect potential pathways for chromium migration from the chromium source in the vicinity of R-42 and R-28 that may be more southerly than those sampled at R-44, R-45, and R-50 (Figure 1). Secondary objectives were to sample potential perched groundwater zones, if present, and refine the map of the water table in this area.

The drilling workplan for R-61 called for completion of a monitoring well with two screens in the regional aquifer. The R-61 borehole reached a total depth (TD) of 1266 ft with 12-in. casing. Repeated depth-to-water measurements of 1101 ft have been obtained within the casing.

## R-61 Recommended Well Design

It is recommended that R-61 be installed as a two-screen well with a 10-ft stainless-steel, 20 slot, wire-wrapped well screen extending from 1125 ft to 1135 ft bgs and a 20-ft stainless-steel, 20 slot, wire-wrapped well screen extending from 1220 ft to 1240 ft bgs. The depth to top of regional saturation is ~1101 feet (see discussion below). The primary filter packs for each screen will consist of 10/20 sand extending 5 ft above and 5 ft below the screen openings. A 2-ft secondary filter pack will be placed above each primary filter pack. The proposed well design is shown in Figure 2.

This well design is based on the objectives stated above and on the information summarized below.

## R-61 Well Design Considerations

Preliminary lithologic logs indicate that the geologic units encountered while drilling the R-61 borehole include the Tshirege Member of the Bandelier Tuff (surface to 270 ft), Otowi Member of the Bandelier Tuff (270-585 ft), Guaje Pumice Bed (580-605 ft), an upper interval of Puye Formation (605-615 ft), Cerros del Rio volcanic series (615-915 ft), a lower interval of Puye Formation (915-1155 ft), and Miocene pumiceous deposits (1155-1265 ft TD). The top of regional saturation is within the Puye Formation.

Perched water was not expected and there were no indications of perched water at R-61. When open borehole drilling was terminated at 896 ft bgs and before 12-inch casing was installed, water was observed standing in the borehole to 830 ft bgs. However, when this water was blown out and the borehole was interrogated over a period of ~6 hours it was observed to be completely dry, indicating that the water observed had been added during drilling. Over the next 40 ft of drilling with casing-advance methods, the borehole was repeatedly circulated and blown dry with no indication of formation water. Perched water does not occur at R-61, consistent with observations in surrounding boreholes (e.g., MCOI-10, MCOBT-8.5, R-50).

Examination of cuttings from the lower interval of the Puye Formation at R-61 indicates typical Tschicoma-derived intermediate volcanic lithologies. The lower 54 ft of the Puye formation is within the zone of regional saturation. There is no indication of clay-rich intervals within the Puye Formation. The upper screen is located at 1125-1135 ft to provide sufficient submergence beneath the top of regional saturation for well development. This places the upper screen at an elevation of ~5810-5820 ft, comparable to screen 1 at R-50 (5817-5827 ft elevation) and to the screen at R-42 (5806-5827 ft elevation).

The deeper screen is located at 1220-1240 ft depth to capture a stratigraphic position in the Miocene pumiceous strata at a depth where driller and site geologist observations suggested an increase in the rate of water produced from ~10 gpm to 20-30 gpm. The location of this deeper screen is at an elevation of 5705-5725 ft, comparable to screen 2 at R-50 (5698-5719 ft elevation).

At completion of drilling at R-61 the 12-inch casing extended to a TD of 1266 ft bgs. Water production from the regional aquifer was first detected in the range of 1108 to 1128 ft bgs. Initial water level measured on removal of tools from the borehole was 1101 ft bgs. Subsequent measurements of depth to water over a period of two days consistently reproduced this depth to water. The predicted top of regional saturation at this locality was 1103 ft bgs, consistent with observation. A natural gamma log collected after tools were removed from the borehole showed a decrease at 1102 ft bgs consistent with saturation below that depth. Constraints on the top of regional saturation fall within a range of 1101-1102 ft bgs, very consistent with the predicted depth of 1103 ft bgs.

### **Alternative Design Considerations**

Alternatives to the design presented above include screen placements and screen lengths. The upper screen could be moved a few feet higher but the placement shown in Figure 2 allows 17 ft of submergence to the top of the transition sand; raising the screen would decrease the submergence needed for adequate well development. This depth to the upper screen slots also insures full screen submergence as supply wells PM-4 and PM-5 are pumped. Moving the screen down would bring it closer to the transition between Puye Formation fanglomerates and Miocene pumiceous sediments. A 10 ft length for the upper screen allows discrete sampling near the top of the regional aquifer. The upper screen placement as proposed also puts it at an elevation comparable to the upper screen at R-50 (Figure 2).

The lower screen could also be adjusted several feet either up or down in elevation. The placement as shown here puts the screen slots at the top of this screen at the depth (1220 ft bgs) where significant increase in water production was first observed during drilling. The lower screen placement and length as shown also provide a sampling elevation comparable to that of the lower screen at R-50 (Figure 2).

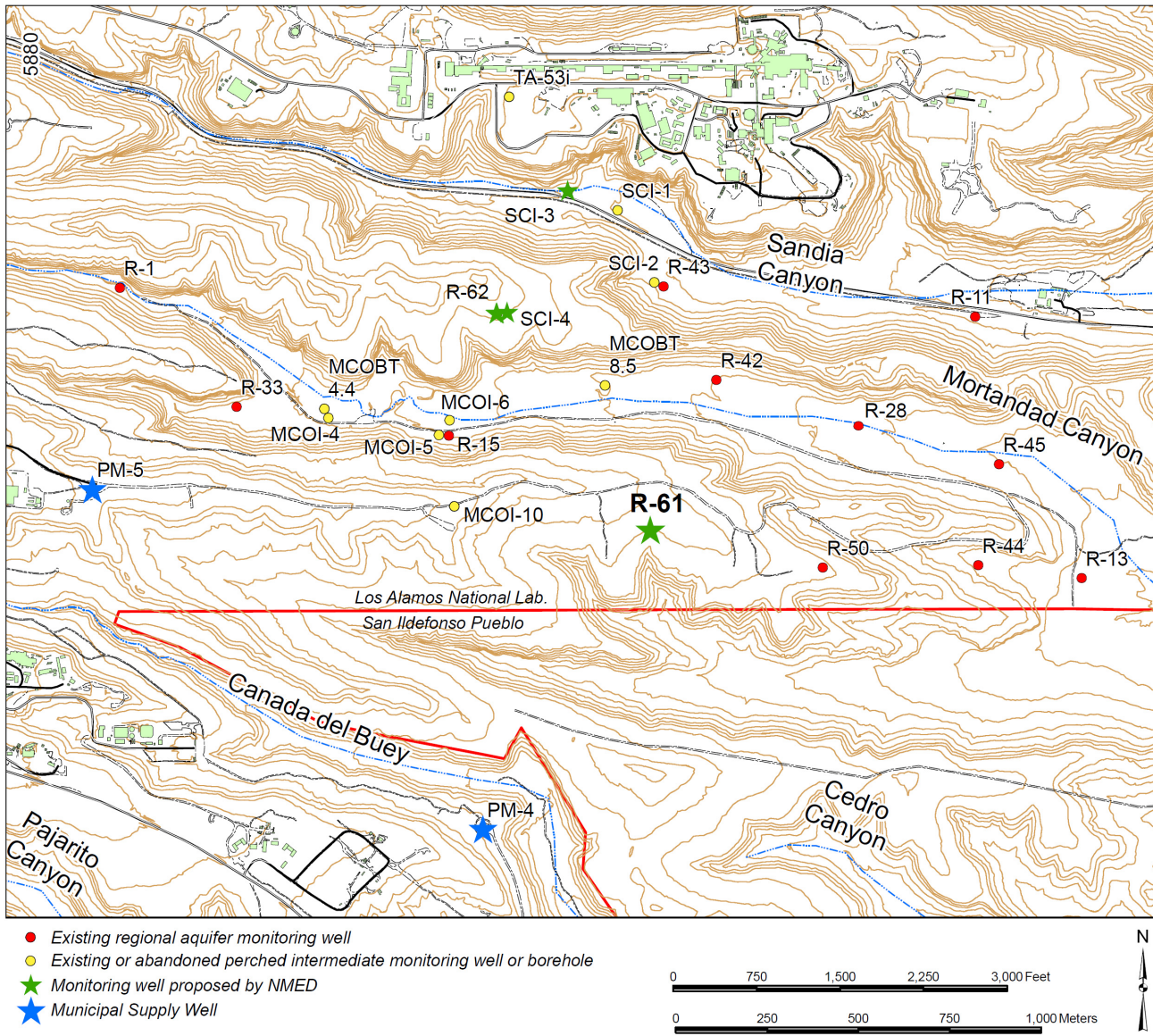


**Figure 1** Location map for R-61 relative to nearby regional and intermediate wells and boreholes.

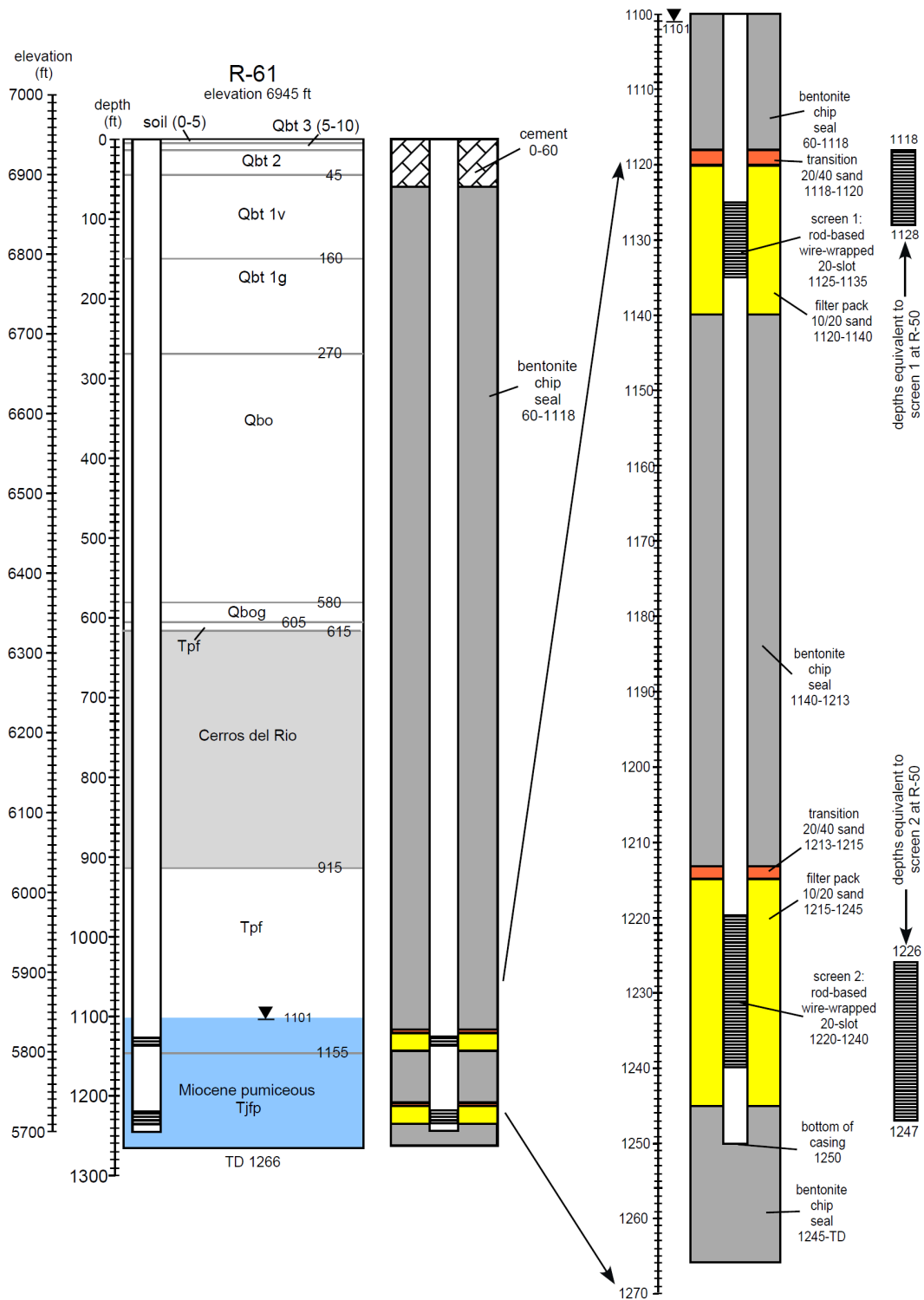


**Figure 2** Proposed well design, R-61 (Qbt 3, 2, 1v, 1g = subunits of the Tshirege Member of the Bandelier Tuff; Qbo = Otowi Member of Bandelier Tuff; Qbog = Guaje Pumice Bed, Tpf = Puye Formation; Tjfp = Miocene pumiceous unit beneath the Puye Formation)

From: "Kulis, Jerzy, NMENV" <[jerzy.kulis@state.nm.us](mailto:jerzy.kulis@state.nm.us)>  
To: "Everett, Mark C" <[meverett@lanl.gov](mailto:meverett@lanl.gov)>, "Cobrain, Dave, NMENV" <[dave.cobrain@state.nm.us](mailto:dave.cobrain@state.nm.us)>, "Dale, Michael, NMENV" <[Michael.Dale@state.nm.us](mailto:Michael.Dale@state.nm.us)>  
Date: Wed, 6 Apr 2011 16:54:00 -0600  
Subject: RE: R-61 proposed well design

Mark,

This e-mail serves as NMED approval for installation of regional aquifer well R-61 as proposed in the document attached to the original e-mail received by NMED on April 6, 2011 at 2:48 PM. This approval is based on the information available to NMED at the time of the approval. NMED understands that LANL will provide the results of preliminary water-quality sampling, any modifications to the proposed well design, and any additional information related to the installation of well R-61 as soon as such information becomes available. **LANL must notify NMED of well development and aquifer testing at R-61 at least three business days prior to commencing these activities.** LANL shall give notice of this installation to the New Mexico Office of the State Engineer as soon as possible.

Thanks,

Jerzy Kulis  
Environmental Scientist  
Hazardous Waste Bureau  
New Mexico Environment Department  
2905 Rodeo Park Drive East, Bldg 1  
Santa Fe, NM 87505-6303  
Phone: [505-476-6039](tel:505-476-6039)  
Fax: [505-476-6030](tel:505-476-6030)

---

**From:** Everett, Mark C [mailto:[meverett@lanl.gov](mailto:meverett@lanl.gov)]  
**Sent:** Wednesday, April 06, 2011 2:48 PM  
**To:** Kulis, Jerzy, NMENV; Cobrain, Dave, NMENV; Dale, Michael, NMENV  
**Cc:** Ball, Theodore T; Shen, Hai; Woodworth, Lance A; Lynnes, Kathryn D  
**Subject:** R-61 proposed well design

Jerzy,

Attached, please find our proposed design for well R-61. Well R-61 is on the mesa to the south of Mortandad canyon near existing well R-50. Please contact me with any questions or concerns. If the proposed design is acceptable, please respond to this e-mail with your concurrence.

Thanks,

Mark Everett, PG  
ADEP ET-EI  
Los Alamos National Laboratory  
[\(505\) 667-5931](tel:505-667-5931)

